

Synaptic vesicles dynamics in $\sigma 1B$ adaptin $-/-$ mouse model

PhD Thesis

Dissertation
for the award of the degree

“Doctor of Philosophy”
Division of Mathematics and Natural Sciences

of the Georg-August-Universität Göttingen

within the doctoral program *Molecular Biology of Cells*
of the Georg-August University School of Science (GAUSS)

submitted by
Ermes Candiello

born in Benevento, Italy

Göttingen 2015

Thesis Committee Members

First member (Supervisor):

Prof. Dr. Peter V. Schu

Cellular Biochemistry, University Medical Center Göttingen

Second member:

Prof. Dr. Mikael Simons

Cellular Neuroscience, Max Planck Institute for Experimental Medicine

Third Member:

Dieter Schmitt

Neurobiology, Max Planck Institute for Biophysical Chemistry

Members of the Examination Board

Referee: Prof. Dr. Peter V Schu

Cellular Biochemistry, University Medical Center Göttingen

2nd Referee: Prof. Dr. Mikael Simons

Cellular Neuroscience, Max Planck Institute for Experimental Medicine

Further members of the Examination Board

Prof. Dr. Blanche Schwappach

Molecular Biology, University Medical Center Göttingen

Dr. Camin Dean

Trans-Synaptic Signaling, European Neuroscience Institute Goettingen

Dr. Dr. Schlueter Oliver

Molecular Neurobiology, European Neuroscience Institute Goettingen

Date of oral examination: 08/06/2015

I hereby declare that I prepared the PhD thesis “Synaptic vesicles dynamics in $\sigma 1B$ adaptin $-/-$ mouse model” on my own and with no other sources and aids than quoted.

Göttingen, 30 March 2015

Ermes Candiello

Dedicato a Elisa, Emanuel, Omar e Roberta
Per essere sempre e ovunque la mia Forza

The most beautiful thing we can experience is the mysterious.

It is the source of all the true arts and science.

*He to whom the emotion is a stranger, who can no longer
pause to wonder and stand wrapped in awe, is as good as
dead-his eyes are closed.*

Albert Einstein, Living Philosophies

Table of contents

Abstract	IX
Abbreviations	X
Introduction	1
1.1 Coated vesicles.....	1
1.1.1 COPII vesicles shuttle the proteins from the ER to the Golgi complex.....	3
1.1.2 Retrograde transport from ER to the Golgi complex is mediated by COP-I vesicles	4
1.2 Clathrin-coated vesicles and Adaptor Complexes	5
1.2.1 AP-3, AP-4, AP-5 complexes	6
1.2.2 AP-2: Clathrin mediated endocytosis (CME)	7
1.2.3 AP-2 CCV in the synapse	14
1.2.4 AP-1 CCV: early-endosome mediated CCV biogenesis.....	15
1.3 AP-1/ σ 1B-adaptin mediates endosomal synaptic vesicle recycling, learning and memory.....	19
1.3.1 Early-endosomes cycle: accumulation in σ 1B $-/-$ synapses	23
1.4 Aim of the study.....	26
Material and Methods	27
2.1.1 Specific laboratory equipment	27
2.1.2 Buffers.....	27
2.2 Cell Culture methods	28
2.2.1 Mouse embryonic fibroblast's culture	29
2.2.2 Freezing and thawing of cells	29
2.3 Molecular Biology	30
2.3.1 Cloning procedures	30
2.4 Biochemical methods.....	32
2.4.1 Overexpression of recombinant proteins in E.coli.....	32
2.4.2 GST-tagged protein purification	33
2.4.3 6-His-tagged protein purification.....	33

2.4.4 Pull-down of proteins from brain cytosol by recombinant proteins	33
2.4.4.1 Pull-down experiments	34
2.4.5 Transient transfection.....	34
2.4.6 Protein extraction from MEF	35
2.4.7 Isolation fo synaptic Clathrin-Coated-Vesicles (CCV)	35
2.4.8 Immunoprecipitation	36
2.4.8.1 IP with 4G10® Platinum-Anti-Phosphotyrosine-Agarose Conjugated-beads	36
2.4.9 Protein concentration determination by Bradford assay	37
2.4.10 Semi-quantitative Western-blot analyses	37
2.4.11 Semi-dry Western-blot & immunostaining.....	39
2.4.12 Stripping of transfer membranes.....	40
2.4.13 Mass spectrometry	40
2.4.14 iTRAQ™ Mass spectrometry	42
2.4.15 Immunofluorescence microscopy	45
2.4.16 Proximity-Ligation-Assay.....	46
2.4.17 Primary antibody.....	47
2.4.18 Secondary antibody.....	49
Results	50
3.1.1 The synaptic AP-1 and AP-2 Clathrin-Coated-Vesicles (CCV).....	50
3.1.2 iTRAQ™ analyses	52
3.1.3 AP-1 CCV levels and AP-1 distribution in σ 1B -/- synapses	54
3.1.4 AP-2 CCV levels and AP-2 distribution in σ 1B -/- synapses	55
3.1.5 AP-2 CCV coat-protein composition and CCV stability	56
3.1.5.1 The clathrin cage	56
3.1.5.2 Association of clathrin cage disassembly proteins.....	57
3.1.6 AP-2 CCV co-adaptor protein composition.....	59
3.1.7 Dynamin recruitment to CCV	63
3.1.8 Stability of AP-2 CCV and μ 2-adaptin phosphorylation	65
3.1.9 Arf-GAP1 distribution in the synapse and synaptic CCV	66
3.2 AP-2 CME up-regulation and CCV stability	68
3.2.1 Hsc70 and co-chaperon distributions in the CCV pools	68
3.2.2 Clathrin cage proteins in the CCV pools.....	69
3.2.3 Ap-2 and μ 2 phosphorylation	70

3.2.4 “Accessory” coat proteins in the CCV pools	71
3.2.5 Arf-GAP1 protein distribution in the CCV pools	72
3.3 Analyses of the CCV Phosphoproteome.....	73
3.4 Membrane dynamics of early endosomes and AP-1 complexes.....	77
3.4.1 AP-1 adaptin binding of Rab5 effector proteins	77
3.4.2 Membrane distributions of Rab5-effectors and co-localization with AP-1	80
4 Discussion.....	83
4.1 AP-1 CCV reduction and AP-2 CCV accumulation in the σ 1B $-/-$ synapse.....	84
4.1.1 AP-2 CCV in ‘ko’ synapse have an altered coat composition	84
4.1.2 A new ‘stable’ AP-2 CCV pool in σ 1B $-/-$ synapses	87
4.2 Reorganization of the Rab5 cycle by AP-1/ σ 1B deficiency	88
4.3 Final model	90
Bibliography	92
Acknowledgments	
Curriculum Vitae	

Abstract

The adaptor protein 1 (AP-1) complex of clathrin-coated vesicles (CCVs) mediates protein transport between the trans-Golgi-network and endosomes. It consists of the two large adaptins γ 1 and β 1, both of which bind clathrin and accessory proteins, and the two smaller adaptins, μ 1 and σ 1, both of which bind cargo proteins. Three σ 1 adaptin isoforms, A, B, and C, are encoded by separate genes. σ 1B is the brain specific isoform and σ 1A is the ubiquitous isoform, this also explains the viability of the mice. σ 1B $-/-$ mice have impaired spatial memory and AP-1/ σ 1B deficient humans have a severe mental retardation. σ 1B $-/-$ mice have fewer synaptic vesicles (SV), reduced SV recycling, but more synaptic CCV and large endosomes. In this study I analyzed the CCV accumulation in 'ko' synapse in order to understand how and why they are formed due to the σ 1B-adaptin deficiency. First we found out that the accumulating CCV are endocytotic AP-2 CCV, although it was expected that this class of CCV is reduced, due to the reduction of SV recycling. Moreover, the coat composition of these AP-2 CCVs is altered, and thus, they represent a subpopulation of AP-2 CCVs. Based on these data we developed a model where the accumulation of the AP-2 CCV in 'ko' is due to an up-regulated CME or a slow uncoating, suggesting that there could be different sub-populations of AP-2 CCV. We were able to isolate a subpopulation, and it turned out to be a 'stable' AP-2 CCV pool, with higher coat stability and thus slower or delayed uncoating.

Furthermore, we found that the AP-1/ σ 1B deficiency leads to alterations in the endosomal Rab5 pathway. AP-1 σ 1A and σ 1B adaptins regulate the Rab5 cycle, by interacting with several Rab5 effector proteins. This interaction is altered in "ko" synapse, leading to enhanced Rab5 activation and thus enhanced early endosome to endolysosome protein transport and SV protein degradation.

These findings demonstrate that AP-1/ σ 1B deficiency strongly effects the AP-2 CCV endocytotic pathway and its functions indicating an interdependent regulation of AP-1 and AP-2 mediated synaptic vesicle recycling and that AP-1 complexes also regulate the endosomal sorting of SV proteins.

Abbreviations

ACAP1	Arf-GAP with coiled-coil, ANK repeat, and PH domains 1
AP	adaptor protein
ADP	adenosine diphosphate
ANTH	AP180 N-terminal homology
AP-1	“assembly polypeptide”, adaptor protein complex 1
Arf	ADP-ribosylation factor
ATP	adenosine triphosphate
BAR	Bin-Amphiphysin-Rvs
bp	basepair(s)
CCP	clathrin coated pits
CHC	clathrin-Heavy-Chain
CLASP	clathrin associated protein
CLC	clathrin-Light-Chain
CCV	clathrin-coated vesicle
CME	clathrin-mediated endocytosis
COP	coat protein complex
DMEM	Dulbecco’s modified Eagle medium
DMSO	dimethylsulfoxide
DNA	desoxyribonucleic acid
DTT	dithiothreitol
E. coli	Escherichia coli
EDTA	ethylene dinitrilotetraacetic acid
EM	electron microscopy
ENTH	epsin N-terminal homology
ER	endoplasmic reticulum
ES	cells embryonic stem cells
EST	expressed sequence tag
FACS	fluorescence-activated cell sorter
FCS	fetal calf serum
fig.	figure
FITC	fluoresceine-isothiocyanate
GAP	GTPase-activating protein
GEF	GTP-exchange factor
GGA	Golgi-localised, γ -ear-containing, ARF-binding
GDP	guanosine diphosphate
GTP	guanosine triphosphate
HEPES	N-2-hydroxyethylenepiperazine-N’-2-ethanesulfonic acid
HRP	horseradish peroxidase
HSC70	heat shock cognate 70
Hz	Hertz
IPTG	isopropyl- β -D-thiogalactopyranoside

kb	kilobasepairs
kDa/kD	kilodalton
ko	knock out
MEF	mouse embryonic fibroblasts
MPR	mannose 6-phosphate receptor
MVB	multivesicular bodies
OD	optical density
PBS	phosphate-buffered saline
PCR	polymerase chain reaction
PI4P	phosphatidylinositol-4-phosphate
PI(4,5)P ₂	phosphatidylinositol 4,5-biphosphate
PMSF	phenylmethylsulfonylfluoride
rev.	review
RNA	ribonucleic acid
RNAi	RNA interference
RT-PCR	real-time PCR
rpm	rounds per minute
SDS	sodium dodecylsulfate
SH3	SRC homology 3
siRNA	small interfering RNA
SNARE	soluble NSF attachment protein receptor
TBS	tris buffered saline
TD	terminal domain
TEMED	N, N, N', N'-tetramethyl-ethylene diamine
TGN	trans-Golgi-network
Tris	tris-(hydroxymethyl)-aminomethane
Vol	volume
wt	wild type
Y3H	yeast three-hybrid
Y2H	yeast two-hybrid

Introduction

The eukaryotic cell contains several membrane-enclosed compartments: the endoplasmic reticulum, the Golgi apparatus, lysosomes, peroxisomes, endosomes, secretory granula, nucleus and mitochondria. Newly synthesized proteins have to be transported to these organelles, because they are synthesized only in the cytoplasm or at the rough endoplasmic reticulum (ER). Proteins synthesized in the endoplasmic reticulum are targeted to the Golgi complex, where they are processed and glycosylated and afterwards processed, phosphorylated, sulfated etc. by Golgi and trans-Golgi network specific enzymes. These modifications are generally used to activate their biological functions and to target them to their final cellular compartment. Proteins, which have reached the cis-Golgi complex, will be either targeted to the medial and late Golgi complex or they will be sent back to the ER, if they are ER resident proteins or if they are not properly processed and non-functional. Once the proteins are correctly processed in the trans-Golgi-Network (TGN), they are sorted (Ferreira & Veldhoen, 2012) to organelles of the so-called 'late secretory pathway' and finally to either the plasma membrane or lysosomes. Proteins destined to regulated exocytotic release are transported to secretory granula, which are targeted to the plasma membrane. The trafficking is also retrograde, eg receptors that recycle between compartments. Exo- and endocytotic pathways are the connections of the cells with the environment. Plasma membrane and extracellular proteins enter the cells through a membrane-mediated process. The endocytotic membranes are targeted to the early endosomes, where recycling proteins are separated from those destined for degradation. All these steps are mediated by transport vesicles, able to target cargo proteins to all of the various compartments of the organelle network.

1.1 Coated vesicles

The transport vesicles are formed by a cytoplasmic protein coat and coated-vesicle biogenesis is orchestrated by those proteins. Coat complexes mediate two essential steps during coated vesicle formation: physical rearrangements of the membrane into highly curved areas that result in a membrane bud, and cargo protein recruitment. At the same time, they bind to membrane lipids, cargo protein and interact with co-

adaptor proteins and other components of the coated vesicles. Therefore, role cannot be simply reduced to the membrane budding and cargo protein recruitment. Once the coat polymerization is completed, the bud undergoes a scission event, separating it from the membrane and releasing the coated vesicle.

The trafficking among all the organelles is mediated by three categories of coated vesicles, distinguished by their different coats: COP, adaptin-complexes with clathrin-basket and adaptin-complexes without clathrin.

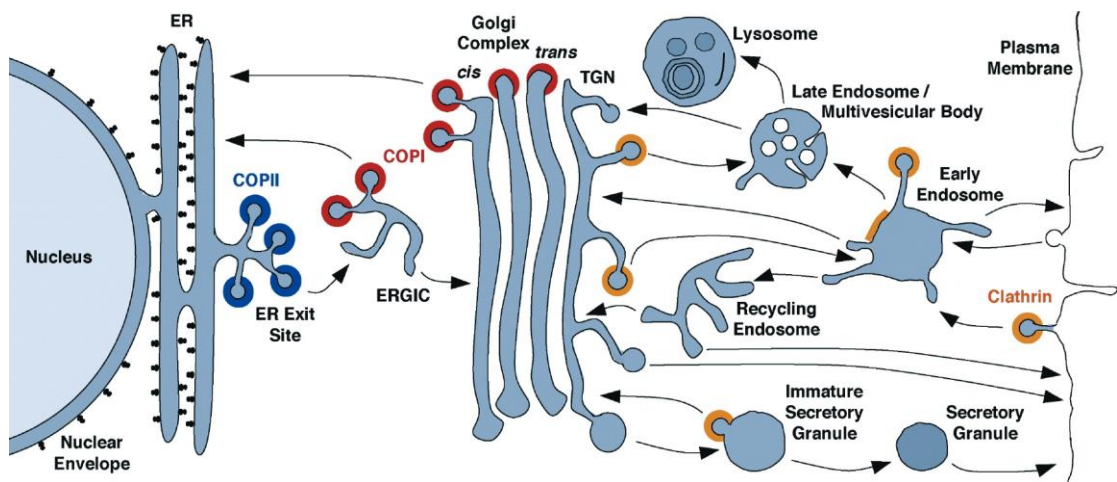


Fig. 1. Newly synthesized proteins are transported between the organelles of the biosynthetic/secretory pathway by different categories of coated vesicles: COPI, COPII, and CCV. (AP coats without clathrin are not indicated in this scheme) (taken from Bonifacino and Glick 2004).

The targeting of the proteins from the endoplasmic reticulum to the cis-Golgi compartment is mediated by COP-II vesicles, while COP-I vesicles shuttle the proteins from the Golgi complex compartments back to earlier organelles of the pathway. The last stage of this network is orchestrated by the clathrin-coated-vesicles (CCV), shuttling the proteins from the trans-Golgi network (TGN) to early endosomes and vice-versa. Furthermore, they mediate the endocytosis of plasma membrane proteins. Formation of all of these three vesicles categories has in common also the type of regulatory mechanisms acting in their formation. The timing is regulated by small GTP-binding proteins. The vesicle formation is initiated by activation of a small GTPase, which upon GTP-binding exposes an N-terminal amphipathic helix that anchors the protein to the outer leaflet of the membrane. The GTPase protein then supports the recruitment of coat protein complexes that in turn recruit the other coat protein components and the cargo proteins through a peptide-

motif specific interaction. In the clathrin-dependent endocytosis (explained in details further below) the GTP-binding protein is not necessary to support coat formation and complexes are recruited to the membrane solely by membrane lipids and cargo proteins.

1.1.1 COP-II vesicles shuttle the protein from the ER to the Golgi complex

The COP-II vesicles mediate the protein shuttling from the endoplasmic reticulum (ER) to the Golgi complex. The coat assembles sequentially; the GTP-binding protein is Sar1. As shown in Fig. 2, once that Sar1 is activated by the ER membrane glycoprotein Sec12, it recruits the adaptor heterodimeric complex Sec23-24 of about 200 kDa. Sec23-24 binds cargo proteins via several binding motifs distributed on its membrane-binding surface. Sec23-24 recruits the additional coat-protein Sec13-31 complex, recognizing its prolin-rich domain. Sec13-31 forms cage-like structures that impose membrane curvature and confer structural rigidity to the COP-II coat. The interaction between the two complexes activates the Sar-1 GAP activity of Sec23 and the GTP-GDP switch leads the membrane-associated coat to be rapidly disassembled. However the last step, the fission of the vesicle, is driven by the N-terminal helix of Sar1-GTP, inserted in the membrane, that induces surface asymmetry between the outer and inner membrane layers promoting curvature and subsequently the hemi-fusion of the lipid layers and then the fission of the membranes (Venditti, Wilson, and De Matteis 2014)

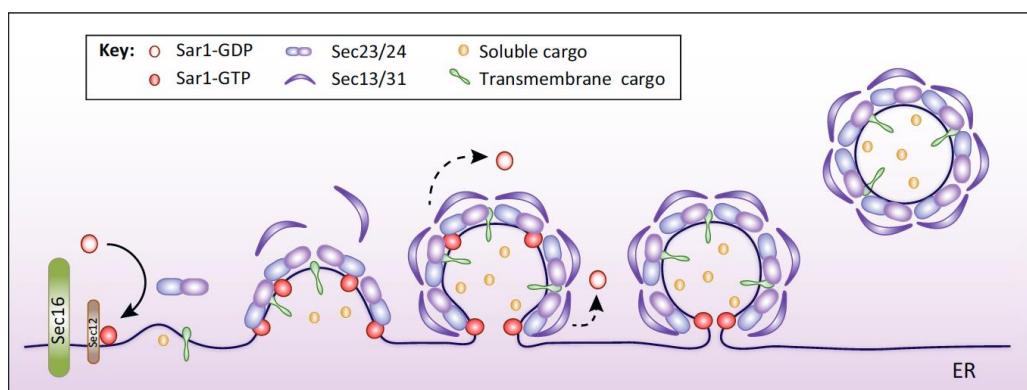


Fig. 2. COPII vesicle cycle is driven by the coat-complexes Sec23-24, Sec13-31 and the small GTP-binding protein Sar1 (taken from Venditti et al. Cell review 2014)

1.1.2 Retrograde transport from ER to the Golgi complex is mediated by COP-I vesicles.

The COP-I vesicles mediate the retrograde transport through the Golgi complex and back to the ER. The COP-I coat comprises a 600 kDa coatomer, composed of seven subunits (Kirchhausen et al., 2000). Unlike the COP-II and also the CCV coats, the COP-I coatomer is recruited 'en bloc' as a single complex. However, two subcomplexes can be distinguished: the adaptor subcomplex (γ - β - δ - ζ COPs), comparable to the Sec23-24, and the cage-like subcomplex (α - β' - ϵ COPs). The adaptor subcomplex (γ - ζ -COPs) interacts with the small GTP-binding protein Arf1, at a stoichiometric ratio of 1:2 Arf1:COPs. Arf1 binds the membrane through its myristoylated helix, which is free in the GTP-bound state; at the same time Arf1-GTP recruits and binds the COP-I coatomer leading to the membrane curvature (Fig. 3). The motif-specific (FFXXKKXX) for cargo recruitment competes with the Arf1 GTP-GDP switch (inactivation). This mechanism mediates the timing and regulation of the cycle.

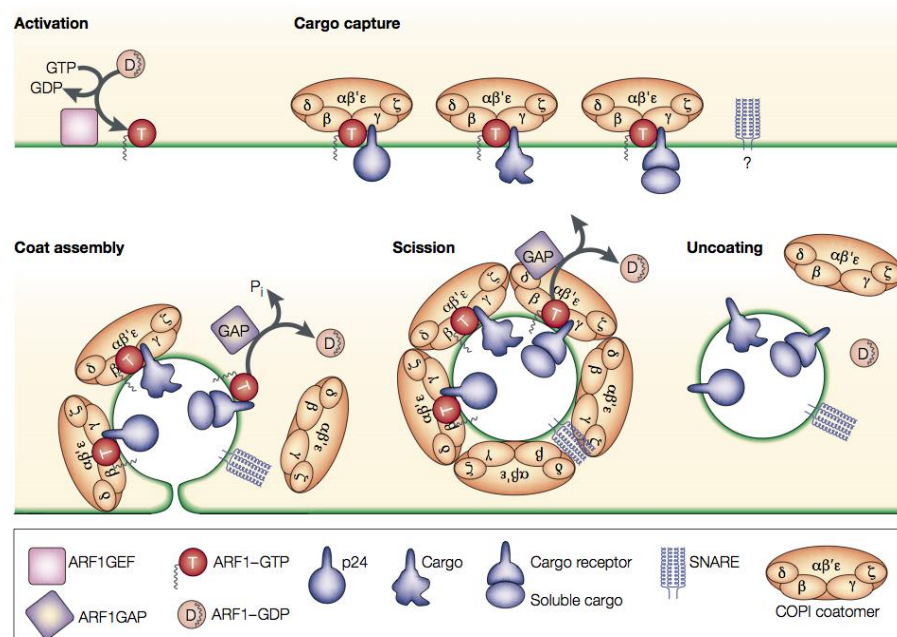


Fig. 3. COP-I coat is composed of only one heteroepitopic complex that with the Arf1-GTP drives the vesicle cycle (cargo recruitment, membrane curvature, vesicle release). The complex however can be subdivided in two subcomplexes: adaptor subcomplex (γ - ζ -COPs) and the cage-like subcomplex (α - β' - ϵ -COPs)(taken from Kirschhausen Nature Review 2000).

1.2 Clathrin-coated vesicles and Adaptor-Protein Complexes.

Clathrin-coated-vesicles (CCV) are the most prominent of the carrier vesicles. They mediate the transport between the TGN and the early endosomes, and the clathrin-mediated endocytosis (CME). CCV are mainly composed of two distinct complexes: the clathrin cage and the adaptor-protein complexes. There are 5 different, homologous adaptor-protein complexes (APs): AP-1, AP-2, AP-3, AP-4 and AP-5 differing in their localization and function. Of these only AP-1 and AP-2 form CCV, whereas clathrin-binding by the others could not be demonstrated. The CCV cycle is orchestrated by several different regulatory proteins: proteins sensing the membrane curvature, small GTP-binding proteins, kinases and phosphatases and CCV uncoating chaperons.

Although the five AP complexes have different localization and function, their main structure is the same (AP-1/AP4 showed in Fig. 4). They are all hetero-tetrameric complexes composed of two bigger subunits, whose N-terminal domains bind the medium and the small subunit, forming the core of the complex. The C-terminal domains of both large subunits, or adaptins, protrude out of the complex and are called appendage/ear domains. The cargo recruitment is mediated by the medium (μ) and the small adaptins (σ); the appendage domains are involved in the binding of co-adaptor proteins and the so called 'auxillary proteins' and the clathrin-heavy-chain, which in addition can be bound by the N-terminal core domains of the large adaptins of AP-1 and AP-2 (McMahon et al.)

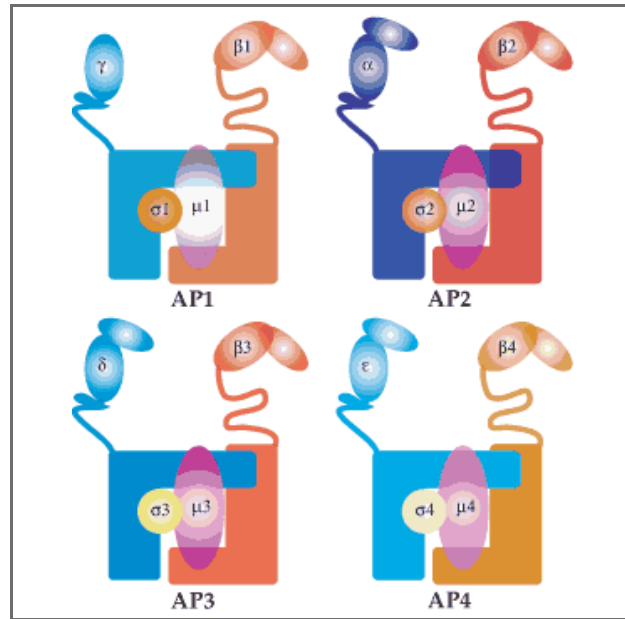


Fig. 4. APs complexes and their adaptor subunits have high structural homologies. The degree in homologies is indicated by the colors and their intensities (taken from McMahon, Endocytosis.org).

1.2.1 AP-3, AP-4, AP-5 complexes

The clathrin cage and the adaptor complexes have to interact directly and simultaneously with several of these regulatory proteins, with the cargoes and with the membrane. AP-1 and AP-2 depend on clathrin for vesicle formation, whereas AP-3, AP-4 and AP-5 appear to be clathrin-independent. While the roles of APs-1-3 are well established, less is known about AP-4 and AP-5. However mutant and patient phenotypes indicate that both are involved in a cargo-specific trafficking in the endosomal systems. Deficiency in one of these two complexes leads to spastic paraplegia, suggesting that AP-4 and AP-5 play a fundamental role in neuronal development and homeostasis (Hirst, Irving & Borner, 2013)

The AP-3 adaptor complex is implicated in the transport of lysosomal membrane proteins to lysosome-related organelles, like α -granules, melanosomes etc. Deficiencies in AP-3 subunits lead to the Hermansky-Pudlak syndrome, a disease characterized by impaired biogenesis of lysosome-related organelles (Dell'Angelica 2009)

The AP-2 adaptor localizes to the plasma membrane, where it mediates clathrin-dependent endocytosis. AP-2 has been studied in most detail and is the best characterized adaptor complex, because endocytosis is more readily measured than

intracellular vesicle modeling events. AP-1 mediates the shuttling between the TGN and early-endosomes (details in the next paragraphs).

1.2.2 AP-2: Clathrin-mediated endocytosis (CME)

The best-characterized sorting process by the endosomal system is the rapid internalization of selected trans-membrane proteins within clathrin-coated-vesicles (CCV). Endocytotic signals consist of linear motifs, conformational determinants, or covalent modifications in the cytosolic domains of trans-membrane cargo. These signals are interpreted by a diverse set of clathrin-associated sorting proteins (CLASPs) that translocate from the cytosol to the inner face of the plasma membrane (Traub & Bonifacino, 2013).

Selection of trans-membrane proteins (referred to as ‘cargo’) for internalization by CME involves recognition of endocytotic signals in the cytosolic domains of the proteins by adaptors located in the inner layer of clathrin coats. Signal-adaptor interactions lead to concentration of the trans-membrane proteins within clathrin-coated pits that eventually bud into the cytoplasm as CCV. The identification of endocytic signals requires extensive molecular dissection of the receptor sequences using a combination of mutational and functional analyses (Kirchhausen, Owen & Harrison, 2014). This effort led to the current understanding of endocytic signals as a highly diverse set of structural features in the cytosolic domains of trans-membrane proteins, which can be grouped into three functionally analogous but structurally distinct classes: (1) linear motifs, (2) conformational determinants, and (3) covalent modifications. Linear motifs are short arrays of invariant and variant amino acids, including ‘tyrosine-based’ YXXØ (Collawn et al., 1990; Jadot, Canfield, Gregory & Kornfeld, 1992), [FY]XNPX[YF] motifs (Chen, Goldstein & Brown, 1990; Collawn, Kuhn, Liu, Tainer & Trowbridge, 1991), and ‘dileucine-based’ [DE]XXXL[LI] motifs (Letourneur & Klausner, 1992; Pond et al., 1995). A variation of the dileucine motif is formed in the sortilin receptor, which is specifically bound by $\sigma 1B$ (Baltes et al., 2014). In this notation, amino acids are represented in single-letter code, X indicates any amino acid, Ø indicates an amino acid with a bulky hydrophobic side chain, and the brackets mean that either amino acid is allowed at that position. Not all signals, however, are linear sequences or fit a canonical motif. There are now

many examples of folded domains that contain information for endocytosis (Miller et al., 2011; Pryor et al., 2008; Yu, Xing, Harrison, & Kirchhausen, 2010). This information consists of conformational arrays of amino acids on the surface of the folded domains. Unlike linear motifs, which are common to many proteins, each conformational array described to date appears to be unique for a specific cargo. Finally, covalent modifications such as phosphorylation of hydroxyl amino acids (Di Fiore & von Zastrow, 2014; Ferguson et al., 1996) or poly-ubiquitination on the ϵ -amino group of lysine residues (Hicke & Riezman, 1996; Piper, Dikic, & Lukacs, 2014) in the cytosolic domains can also function as endocytic signals.

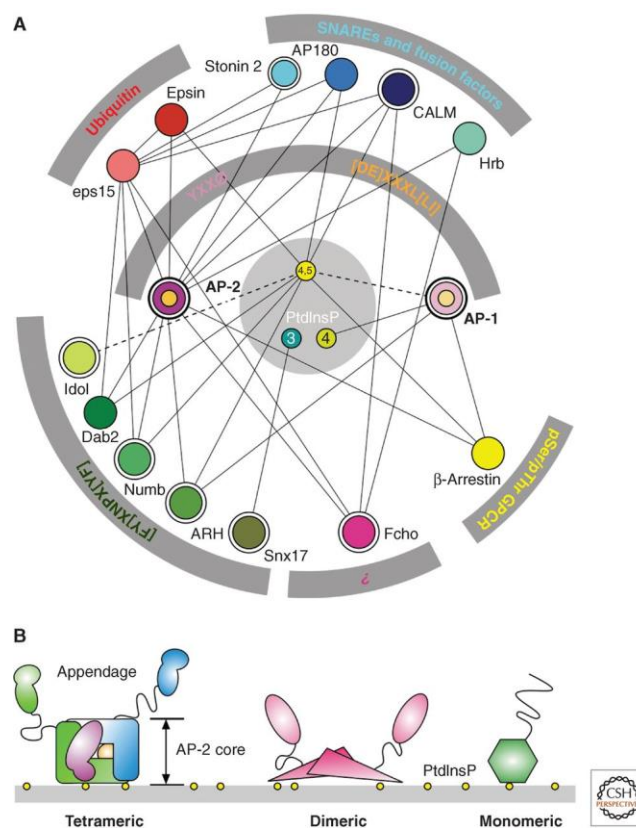


Fig. 5. The endocytic cargo–adaptor interaction network. (A) Schematic representation of selected sorting signal–recognition partner relationships for endocytic trafficking. Both protein–protein and protein–lipid (PtdInsP) interactions among the cargo–selective machinery are highlighted with connection lines. The solid lines indicate documented physical interactions, whereas dashed lines connote either interactions possible based on properties of other domain relatives (IDOL) or known (AP-1), but still of unclear functional necessity. Adaptors, CLASPs, and regulators (Idol) discussed explicitly are double circled. (B) Representative modular domain architecture classes of selected endocytic proteins. Heterotetrameric complex is AP-2; dimeric examples are Fcho1, Syp1p, and eps15; and monomeric CLASPs include ARH, Dab2, Numb, CALM, AP180, epsin, and β-arrestin. Tertiary-structured domains are indicated by geometric shapes, and intrinsically disordered protein segments by a line (taken from Traub & Bonifacio 2013).

The recognition of such a wide diversity of endocytic and intracellular sorting signals obviously necessitates the existence of multiple adaptors. Indeed, many proteins

located in the inner layer of protein coats, including proteins that were initially categorized as ‘accessory’, are now known to function as sorting adaptors (Fig. 5). Depending on the identity of the scaffolding protein that forms the outer layer, coats are classified as clathrin coats or non-clathrin coats. Coats involved in rapid internalization from the plasma membrane contain clathrin as their main constituent and a set of adaptors known as ‘clathrin-associated sorting proteins’ (CLASPs) (Fig. 5A). Clathrin coats containing different sets of CLASPs, as well as non-clathrin coats, mediate intracellular sorting events. CLASPs are recruited to membranes primarily via interactions with specific phosphoinositide lipids, small GTPases of the Arf family, and/or other CLASPs, or AP-1 and AP-2. Clathrin then binds to the CLASP armature and polymerizes into an overlying polyhedral scaffold. Concomitantly, CLASPs engage sorting signals in the cytosolic domains of transmembrane cargo, leading to cargo capture and stabilization of the coats. Both CLASP-clathrin (Dell'Angelica, Klumperman, Stoorvogel, & Bonifacino, 1998; Drake & Traub, 2001) and CLASP-CLASP interactions (Brett, Traub, & Fremont, 2002) involve linear motifs (analogous to, but distinct from, cargo sorting signals) binding to folded domains, highlighting the general role of this binding mode in the assembly and function of clathrin coats. Most interactions among components of clathrin coats are of moderate to low affinity (typically in the 1-100 μm range), making this mechanism of sorting a highly cooperative and dynamic process. From a structural standpoint, CLASPs can be categorized as (1) oligomeric (tetrameric or dimeric), and (2) monomeric (Fig. 5B) (Traub & Bonifacino 2013). The main endocytic adaptor is the clathrin-associated, heterotetrameric adaptor protein 2 (AP-2) complex. This complex is composed of two large ‘adaplin’ subunits (α and β 2), one medium-sized subunit (μ 2), and one small subunit (σ 2). AP-2 binds the cargoes, the PtdIns(4,5)P₂ on the membrane and the clathrin heavy chain. The binding module in the ‘ear’-domains overlap and bind several regulatory proteins, therefore in substoichiometric ratios. The cargo interaction and recruitment is mediated by the μ 2 and σ 2 adaptins. μ 2 binds to the Yxx ϕ motifs (ϕ – bulky hydrophobic) and σ 2 binds to the dileucine based [DE]XXXL[LI] motifs presented by the membrane bound cargo proteins. At this stage of the cycle there are different accessory adaptors, for the specific recruitment of several cargoes not bound by AP-2. For example Stonin2 recruits Synaptotagmin 1 and AP180 recruits SNARE proteins. All these co-adaptors

have a membrane binding domain (AP180 has an ANTH domain, epsin an ENTH domain, FCHO a F-BAR domain) that work also as membrane curvature effector. As the cargo is recruited (by AP-2 or co-adaptors), the clathrin coat assembly processes. Accumulating evidence suggests that the spatial and temporal regulation of clathrin and AP-2 assembly is coordinated by cycles of phosphorylation and dephosphorylation. In fact AP-2 recruitment to the plasma membrane appears to be modulated, negatively and positively, by phosphorylation. Phosphorylation of the $\beta 2$ subunit prevents AP-2 recruitment to clathrin cages in vitro. On the other side, $\mu 2$ phosphorylation, mediated by the specific serine/threonine-kinase AAK1 increases the binding affinity of AP-2 for tyrosine-based-internalization motifs (Conner, Schroter, & Schmid, 2003). Furthermore, this phosphorylation is crucial for the AP-2 complex-membrane binding. In fact when $\mu 2$ is not-phosphorylated, the adaptor complex is in the closed conformation, exhibiting only the one membrane binding site for PI-4,5-P₂ in the α -adaplin. The phosphorylation of Thr156 of $\mu 2$ stabilizes the open conformation of the complex, in which the second PIP₂ binding site is able to reach the membrane. In addition, the steric block of the YxxØ-binding site is released (Collins, McCoy, Kent, Evans, & Owen, 2002). This strongly increases the stability of the coat.

The AP-2 complex recruits the clathrin triskelia, the structural subunits of the clathrin-cage, directly from the cytosol. 'Knock down' of AP-2 does not block the nucleation of the membrane, but blocks the clathrin coat assembly (Boucrot, Saffarian, Zhang, & Kirchhausen, 2010). As shown in Fig. 6, the clathrin triskelion is composed by 2 sub-domains: clathrin light chain (CLC) and clathrin heavy chain (CHC). CHC of 180 kDa is the major component of clathrin-coated vesicles, and there are two CLC classes, CLCa and CLCb with a 1:1 stoichiometric ratio (Ungewickell & Ungewickell, 1991).

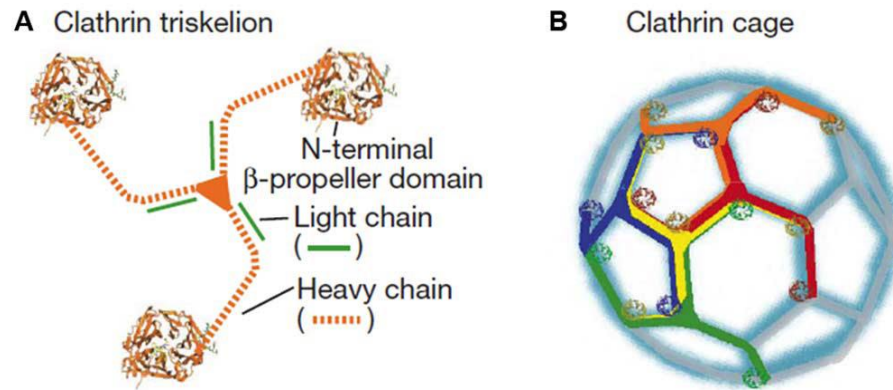


Fig. 6. The protein structure of clathrin and its assembly into clathrin coats. (A) Scheme of a clathrin triskelion comprised of three heavy chains and three light chains. (taken from Poupon et al. 2008). Schematic representation of a clathrin cage. Individual triskelia are highlighted in different colors.

The CLCb phosphorylation-dephosphorylation cycle orchestrates the regulation of different mechanisms in the clathrin-mediated endocytosis and CCVs cycle. Protease treatment, removing the CLCs and parts of the CHC, revealed that the core of CHC is still capable of self-assembly into baskets. Adding back CLCs to isolated CLC-free CHC triskelia impaired self-assembly, leading to the notion that CLCs are important negative regulators of assembly. Furthermore the CLC:CHC ratio is 1:1 only in the brain, in the liver it is 1:5 and is also low in all other organs tested. This altered ratio suggests a brain specific role of CLC in the regulation of coat-assembly. This hypothesis is supported by a CLC role in actin assembly regulation. CLC binds directly huntingtin-interacting protein 1-related protein (HIP1R) (Ferreira & Veldhoen, 2012), which is required for productive interactions of CCVs with the actin cytoskeleton (Poupon et al., 2008). Furthermore, it has been shown that the endocytosis of GPCR, a G protein-coupled receptor, is regulated by differential phosphorylation of CLCb. CLC phosphorylation at S204 is required for efficient uncoating. Mutation of this site effects the interactions between clathrin and uncoating effectors (Ferreira & Veldhoen, 2012). The complete formation of the clathrin coat results in stabilization of the curvature and the displacement of some accessory proteins as EPS15 and epsins.

The scission and the release of the vesicles depend on the mechanochemical GTP-enzyme dynamin, recruited by BAR domain-containing proteins, which have a preference for the high membrane curvature present at the vesicle neck (Fig. 7).

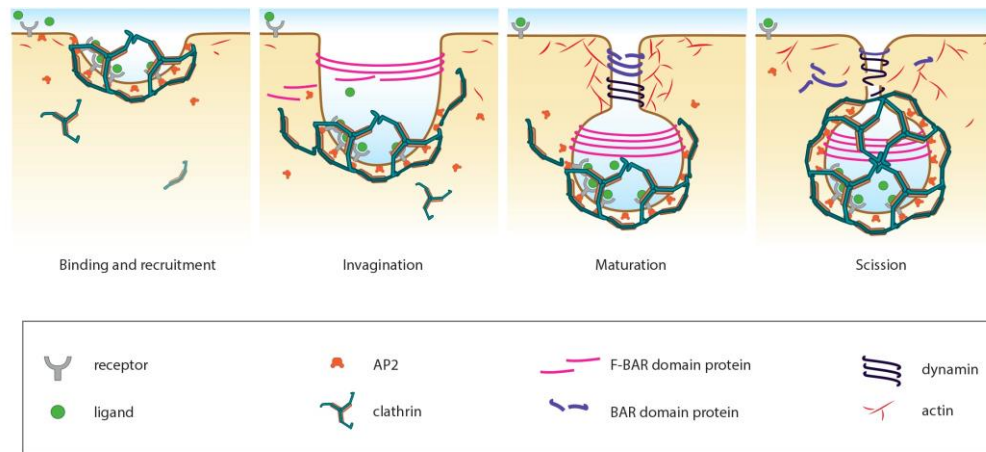


Fig. 7. the narrowing of the vesicle is mediated by the GTPase dynamin, that is recruited by the BAR proteins endophilin and amphiphysin and sorting nexin 9 (SNX9) (taken from MBInfo Wiki, Retrieved).

The BAR-domain proteins amphiphysin, endophilin and SNX9 have SRC homology 3 (SH3) domains able to recognize the Pro-rich domain of dynamin. Polymerization around the neck of the nascent vesicle favors GTP hydrolysis, dynamin conformational changes and, as consequence, the membrane fission (Neumann et al., 2013). The precise steps of the GTP hydrolysis-dependent conformational change are not clear. Once detached from the donor membrane, the vesicle has to fuse with the acceptor membrane, but before the clathrin coat has to disassemble. After uncoating the newborn vesicle is able to fuse with the acceptor compartment. The clathrin subunits; adaptor proteins are released in the cytosol and are thus available for a new cycle of transport vesicle formation. The uncoating reaction is mediated by the Hsc70 chaperone and its cochaperones auxilin 1 and auxilin 2 (or G-associated kinase GAK). As already mentioned above, the CHC is ‘constitutively’ able to make empty clathrin-baskets in the cytoplasm and in fact the primary function of the Hsc70 chaperone system is to ensure the availability of clathrin subunits for CCV formation.

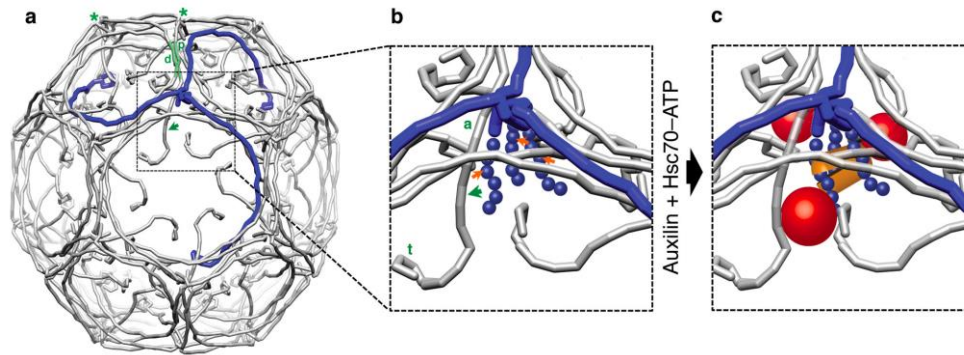


Fig. 8. The uncoating is mediated by the ATPase Chaperon Hsc70 and its cochaperonin Auxilin. The clathrin triskelion is highlighted in blue. Auxilin (in red) binds the clathrin triskelion, leading displacements of ankle segments; then Auxilin recruits Hsc70 (in orange) that through ATP hydrolysis changes its conformation pushing against the C-terminal domain of the triskelion. This process destabilizing the lattice and leads the shedding off the clathrin coat (taken from Böcking et al., Nature 2011).

Auxilin 1 is recruited after CCV formation, by binding to the terminal domains and ankles of clathrin triskelia, and it localizes under the ‘hub’ of a neighboring triskelium. Auxilin1 binding, which brings up to three J-domains into the neighborhood of each vertex, favors local displacements of the ankle segments, leading to expansion of the tunnel and allowing Hsc70 to access its target segment. Hsc70–ATP binds the peptide in a groove on its substrate-binding domain where it recognizes the QLMLT motif at the C-terminus domain of CHC (Fig. 8). ATP hydrolysis, stimulated by encounter with the target and the J-domain of Auxilin, clamps the groove in the closed state and releases the J-domain contact.

Exchange of ATP for ADP reopens the groove, liberates the substrate and resets the cycle (Bocking, Aguet, Harrison, & Kirchhausen, 2011). It is important to specify that, when CCV scission takes place, it is unlikely that the clathrin cage is completed across the zone where the neck was attached, thus leaving a defect in the clathrin cage, that allows the uncoating apparatus to start the uncoating process with ease. Synaptojanin 1, a PIP₂-specific 5-phosphatase, is recruited by endophilin A1. Through dephosphorylation of PIP₂ to PI-4-P, synaptojanin 1 promotes the dissociation of the AP-2 complex from the vesicle membrane. Genetic disruption of synaptojanin 1, or of endophilin, produces a striking accumulation of CCV in nerve terminals and delayed protein recycling (Cremona et al., 1999; Dickman et al., 2005; Hayashi et al., 2008; Milosevic et al., 2011; Schuske et al., 2003; Verstreken et al., 2003)

1.2.3 AP-2 CCV in the synapse

At synapses the number of synaptic vesicles that undergo exocytosis over a given time period greatly exceeds the supply of synaptic vesicle precursors delivered from the cell body. Thus, nerve terminals have developed efficient endocytic mechanisms to recapture and reuse membranes that have fused with the plasma membrane to release neurotransmitters. Although the exocytosis and endocytosis that occur at rest or during modest activity does not involve major structural perturbations of nerve terminals, intense activity induces major and reversible structural changes that vary dependent on the type of stimulation. There are numerous studies demonstrating the importance of CME in the internalization of synaptic vesicle proteins and there is also strong evidence for the hypothesis that synaptic vesicles can derive directly from the uncoating of AP-2 CCV (Saheki & De Camilli, 2012). However, clathrin may not be absolutely essential for synaptic vesicle reformation in lower eukaryotes, as a recent study in *Caenorhabditis elegans* has suggested (Sato et al., 2009). There are at least three different mechanisms through which endocytosis occurs. In response to a very strong exocytotic burst, a different endocytotic mechanism, called bulk endocytosis, comes into play. Bulk endocytosis leads to the generation of endocytotic vacuoles that are subsequently converted into synaptic vesicles that involve AP-2. A third form of ‘endocytosis’, the rapid closure of a vesicles fusion pore without a collapse of the vesicle membrane into the plasma membrane, termed ‘kiss and run’, remains an attractive model to explain electrophysiological and dynamic imaging data that are difficult to reconcile with full vesicle cycles and endocytotic mechanisms. Large organelles were observed after the intense induction of SV cycling in large neuromuscular synapses and thus CCV after their uncoating are thought to fuse with early endosomes. However as explained above, the direct reformation of SV from the uncoating CCV is also a plausible pathway in SV recycling (Fig. 9).

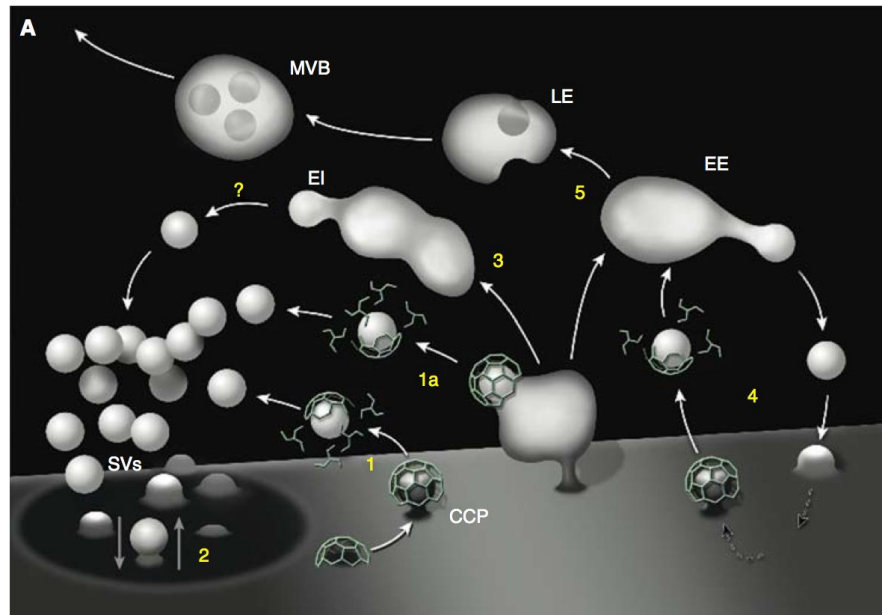


Fig. 9. There are different pathways of synaptic vesicles recycling. The schematic picture of membrane traffic in axon terminals illustrating endocytosis of synaptic vesicle (SV) membranes via clathrin-coated pits (CCP) (1), “kiss and run” (2) and bulk endocytosis (3) that leads to vesicle formation via unknown mechanisms from endocytic intermediates. This recycling traffic is interconnected with housekeeping membrane recycling (4) involving clathrin-mediated endocytosis and canonical early endosomes (EE) as well as with traffic to the cell body (5) via late endosomes (LE) and multivesicular bodies (MVBs) (taken from Saheki & De Camilli 2012).

1.2.4 AP-1 CCV: early-endosomes and CCV biogenesis

Adaptor protein complex AP-1 mediates protein sorting between the trans-Golgi network (TGN) and early-endosomes (EE) (Meyer et al., 2000, Ghosh & Kornfeld 2003). It consists of four adaptins: $\gamma 1$ and $\beta 1$ of 100 kDa and 90 kDa respectively, which interact with the clathrin cage. $\gamma 1$ binds the membrane via PI4P binding, and $\mu 1$ and $\sigma 1$, 45 kDa and 20 kDa respectively, that recruit the cargoes through motif specific interaction via motifs conserved in AP-2 and AP-1 adaptins. Thus $\mu 1$ is essential for high affinity membrane binding, but it does not contain, unlike $\mu 2$, a PIP-binding motif, PI4P indifferent cases (Di Paolo & De Camilli, 2006; Medigeschi et al., 2008; Ricotta, Hansen, Preiss, Teichert, & Honing, 2008; Rohde, Wenzel, & Haucke, 2002). In addition, $\mu 1$ is involved in the regulation of AP-1 membrane dissociation and binds the cytoplasmic protein PREPL (prolyl-oligopeptidase-like protein), which stimulates AP-1 membrane release (Pepperkok et al., 2000; Malsam et al., 1999; Lanoix et al., 1999; Nickel et al., 1998). The AP-1 core has a phosphoinositide-binding site for phosphatidylinositol-4-phosphate [PI-4-P] on its $\gamma 1$

adaptin, at a similar location to the PI-4,5-P₂-binding site on AP-2 α adaptin (Heldwein et al., 2004; Wang et al., 2003). PI-4-P is enriched within domains of the TGN and endosomes, and PI4II β -kinase is recruited by μ 1-binding to the site of vesicle formation, supporting rapid recruitment of AP-1 to the site of CCV formation (Wieffer et al., 2013).

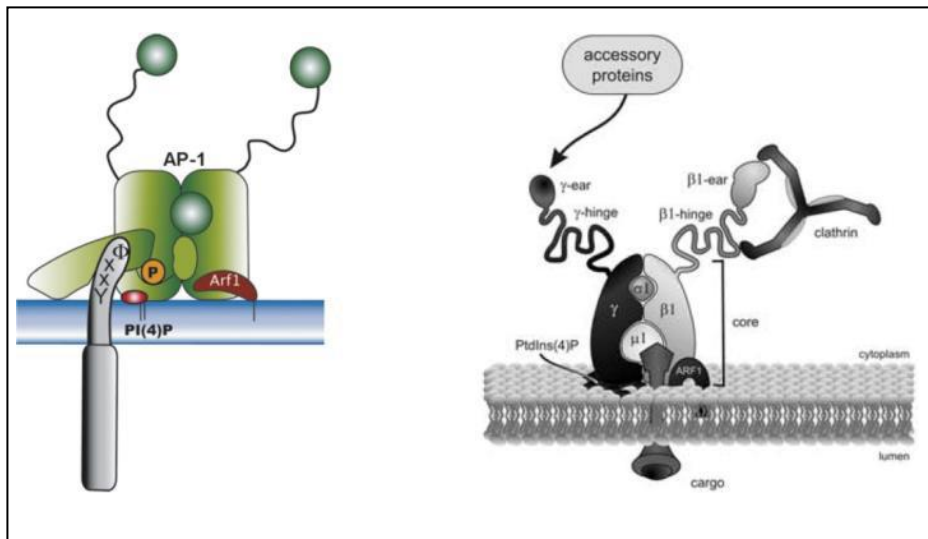


Fig. 10. Left: mediated Arf 1 and tyrosinbased, sorting signal bearing (YXX Φ), binding of the AP-1 complex to the membrane. The recognition of YXX Φ signals by AP-1 is only possible with a simultaneous PI-4-P binding (Krauss & Haucke, 2007). Right: the interaction of AP-1 hinge and ear domains associated with accessory proteins and clathrin (taken from McPherson and Knight, 2005).

In contrast to AP-2 membrane recruitment, phosphoinositides and cargo alone are insufficient to recruit AP-1 to its sites of action. AP-1 targeting to membranes also requires its interaction with a member of the ADP ribosylation factor (Arf) family of small GTPases, Arf1 (Fig. 10). Arf1 binds the β 1 subunit through its domains called Switch I and Switch II while the “back” of the Arf1 protein binds the γ 1 subunit, the stoichiometric ratio AP-1:Arf1 is 2:2 (Ren et al., 2013) (Fig. 11). Conversion to the GTP-bound form requires a guanine nucleotide exchange factor (GEF) (BIG1/BIG2), whereas conversion to the GDP-bound form is catalyzed by a GTPase activating protein Arf-GAP1. Loading with GTP causes Arfs to undergo a conformational change, exposing a myristoylated N-terminal amphipathic helix that inserts into the membrane while reconfiguring its switch I-II and interswitch regions to allow the binding of effector proteins (Donaldson & Jackson, 2011). Arf-GAP1 activates the GTP hydrolysis and thus contributes to AP-1 CCV uncoating (Lanoix et al., 1999; Malsam, Gommel, Wieland, & Nickel, 1999; Nickel et al., 1998; Pepperkok,

Whitney, Gomez, & Kreis, 2000). The GTP hydrolysis mediated by Arf-GAP1 promotes the release of the AP-1 from its CCV. Arf-GAP1 is in turn regulated and inhibited by the phosphorylation of the serine/threonine kinase LRRK2, that phosphorylates Arf-GAP1 in S155, S246, S284 T189, T216, T292. Mutations of any of these amino acids enhanced dramatically the Arf1 GTP hydrolysis mediated by Arf-GAP1, confirming that the phosphorylation inhibits its GAP activity. In turn Arf-GAP1 regulates the activity of LRRK2, which also contains a GTPase domain. Arf-GAP1 inhibits auto-phosphorylation and then activation of LRRK2. LRRK2 phosphorylates the BAR domain of endophilin 1A preventing its membrane binding and thus is able to inhibit CCV uncoating. (Xiong, Yuan, Chen, Dawson, & Dawson, 2012).

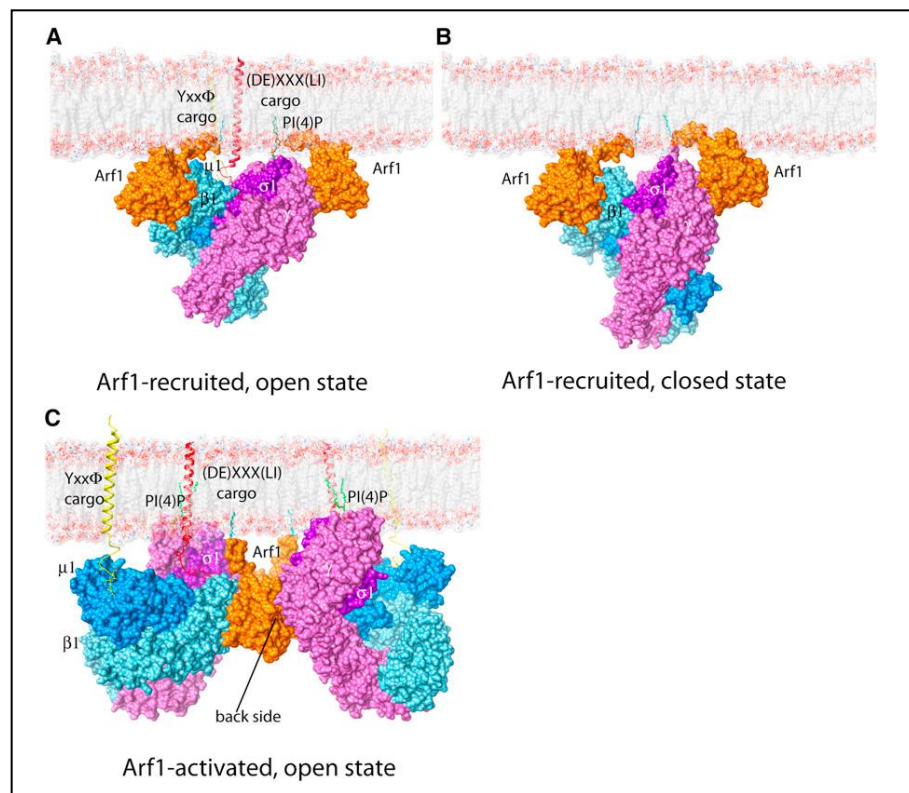


Fig. 11 (A) A model of AP-1 recruited by two myristoylated Arf1-GTP molecules in cooperation with PI(4)P on a membrane. The M- and LL-bearing cargos further bind and stabilize AP-1. (B) The closed conformation of AP-1 is sterically compatible with the simultaneous binding of Arf1 to $\beta 1$ and to the recruitment site on γ . Therefore, the docking of AP-1 to a membrane via the simultaneous binding to these two Arf1 molecules does not, by itself, appear to be sufficient for activation. (C) The crystallized AP-1:Arf1 dimer can be docked onto a cargo-bearing membrane such that the Arf1 myristate moieties, the ends of transmembrane helices of cargo proteins, and PI(4)P all lie in the plane of the membrane surface (taken from Ren et al., 2013).

However the regulation of the AP-1 CCV release is also modulated by the phosphorylation/dephosphorylation cycle of the complex. AP-1 is selectively phosphorylated on the hinge of its $\beta 1$ subunit, which impairs its binding to clathrin.

When AP-1 is recruited from Arf1-GTP to the TGN, the $\beta 1$ subunit is dephosphorylated by PP2A phosphatase, whereas in contrast the $\mu 1$ subunit is phosphorylated by AAK1 (Wilde & Brodsky, 1996). When AP-1 is on the membrane, it recruits the clathrin and facilitates clathrin assembly, which proceeds to the formation of a CCV. However AP-1 and AP-2 CCV differ in their set of co-adaptor and auxiliary proteins with which they interact. As mentioned above the AP-1 CCVs release is promoted by GTP hydrolysis of Arf1-GTP mediated by Arf-GAP1 (Fig. 12). It has been found that AP-1 activates the Arf-GAP1 induced GTP hydrolysis on Arf1. The interaction observed *in vitro* between the appendage domain of $\gamma 1$ adaptin and the C-terminal catalytic domain of Arf-GAP1 (Hirst, Motley, Harasaki, Peak Chew, & Robinson, 2003) is not responsible for GAP stimulation by AP-1. It means that there should be a second activating interaction residing in the catalytic part of Arf-GAP1 that is activated by AP-1/cargo oligomers. This activation is weaker in order to provide more time to complete coat formation. It has recently been shown that positive membrane curvature as at the neck of the budding vesicle strongly stimulates Arf-GAP1 recruitment to the membrane and most importantly its GAP-activity (Bigay, Gounon, Robineau, & Antony, 2003).

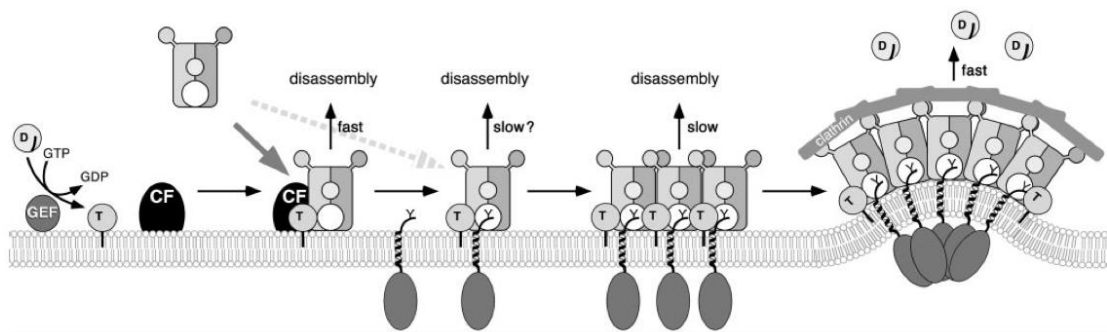


Fig. 12. A model for AP-1/clathrin coat recruitment and the role of GTP hydrolysis. Gray arrows indicate recruitment of AP-1 to the membrane via Arf1-GTP and either a cytosolic factor (CF) or directly to cargo proteins with tyrosine motifs (M). On interaction with cargo, AP-1 oligomerizes. GTP hydrolysis induced by ArfGAP1 (not drawn for simplicity) causes AP-1 dissociation unless the clathrin layer has been assembled. Arf1-GTP hydrolysis by ArfGAP1 is differentially stimulated by the AP-1/CF complex, the AP-1/cargo oligomers, and by membrane curvature limiting the time available for the next step in productive coat formation and preparing the adaptor layer for subsequent disassembly, respectively (taken from Bigay et al., 2003).

The disassembly of the clathrin coat of AP-1 CCV is not different from the already described AP-2 CCV disassembly. AP-1 coat release is promoted by PP2A phosphatase that dephosphorylates the $\mu 1$ subunit. An AP-1 role in the SV cycle has

been demonstrated by the analysis of our mouse model deficient in the small adaptin σ 1B (Glyvuk et al., 2010).

1.3 AP-1/ σ 1B-adaptin mediates endosomal synaptic vesicle recycling, learning and memory

As already explained above, the AP-1 complex consists of four adaptins: γ 1 and β 1, which interact with membrane and clathrin, the μ 1 and the σ 1 involved in the motif-specific-cargo recruitment. In vertebrates, three genes encode the σ 1-adaptins: A, B and C. One characterized function of σ 1-adaptins and their homologous of the other AP-complexes is cargo binding (Doray et al., 2007; Janvier et al., 2003)

However, σ 1-adaptins differ from σ 2 and σ 3 in a C-terminal extension, indicating that σ 1-adaptins might have additional functions specific for AP-1 mediated protein sorting and CCV formation.



Fig. 13. Comparison of σ 1A (gold) and σ 2 adaptin (yellow) structures as determined by Heldwein et al. 2004 PNAS and Collins et al. 2002 Cell; demonstrating the extended C-terminal helix in σ 1A-adaptin. Amino acids 150-158 of σ 1A are unstructured and are not shown (taken from Glyvuk et al., 2010)

Several mouse AP-1-adaptin mouse ‘ko’ models have been established by our group, which demonstrated that AP-1 is essential for in-utero development. The γ 1-deficient embryos cease development at embryonic day 3.5 pc, whereas μ 1A-deficient embryos cease development at mid-organogenesis (day 13.5 pc). The observation that μ 1A-deficient embryos reach organogenesis is probably due to the homologous μ 1B isoform, expressed exclusively in polarized epithelial cells (Meyer et al, 2000). **We generated a targeted mouse ‘knock-out’ of the X-chromosomal σ 1B-adaptin** (Glyvuk et al. 2010). We found that σ 1B-adaptin deficient mice are viable and fertile, but they were hypoactive. Analysis of hippocampal SV recycling revealed impaired SV recycling and the accumulation of endocytotic membranes, indicating for the first

time, AP-1 dependent SV recycling through endosomal intermediates in small hippocampal boutons. Clathrin-dependent protein sorting has been demonstrated to mediate in general basolateral protein sorting, but the pre-synapse corresponds to the apical domain (Deborde et al., 2008). Thus, this was the first demonstration of an apical function of AP-1 and also a new function of AP-1 in protein sorting. It demonstrates SV recycling in small synapses through endosomes that might originate from bulk endocytosis. These data also revealed the molecular mechanism for a severe human X-chromosome-linked mental retardation. Patients with premature STOP-codons in the $\sigma 1B$ gene have a severe mental retardation (Tarpey et al., 2006). Tissue-specific mRNA expression of $\sigma 1$ isoforms was analyzed by northern blot analysis and RT-PCR. The $\sigma 1A$ mRNA is ubiquitously expressed and is readily detected in all tissues analyzed, but expression is significantly higher in the brain. Expression levels of $\sigma 1B$ and $\sigma 1C$ are highly variable and tissue specific, with most tissues expressing $\sigma 1A$ and only one of the other isoforms. A genomic fragment of the X-chromosomal $\sigma 1B$ locus was isolated, mutated, and introduced into the 129SV/J mouse line and crossed with C57/B16 animals. The $\sigma 1B$ -deficient mice are viable, growth and development is normal, but they are hypoactive, have impaired motor coordination and a severely impaired spatial memory. The mice phenotypes match the disease in humans. Patients learn to walk only at 4-6 years and they do not develop any intelligible language capabilities and require lifelong comprehensive care (Tarpey et al 2006). The viability of the $\sigma 1B$ -deficient mice and the tissue-dependent $\sigma 1B$ expression pattern demonstrate that $\sigma 1B$ is not required for ubiquitous, 'house-keeping' AP-1 functions, but is expected to mediate tissue-specific (brain-specific) AP-1 functions. Through 4Pi microscopy it has been revealed that AP-1 has a pre-synaptic localization indeed, in line with the mice phenotypes in the pre-synaptic membrane organization (Glyvuk et al., 2010).

In hippocampal synapses number and distribution of SV were determined at resting conditions and after stimulation by 900 AP/10 Hz. Although resting synapses from controls contained ~ 230 SVs per μm^2 , $\sigma 1B$ $-/-$ synapses contained only ~ 135 SVs per μm^2 . After stimulation, the SV density was reduced to ~ 105 SVs per μm^2 in wt synapse, whereas in $\sigma 1B$ the reduction was to 47 SVs per μm^2 . This could be caused by defects in SV recycling or by defect in SV biogenesis, generating vesicles with impaired recycling rates. In addition, SV from $\sigma 1B$ deficient neurons were enlarged,

at rest, with diameters of ~ 41 nm compared with ~ 38 nm in controls and were more heterogenous (Fig. 14 right panel). This indicates that $\sigma 1B$ deficiency reduces the fidelity of SV formation already at resting conditions.

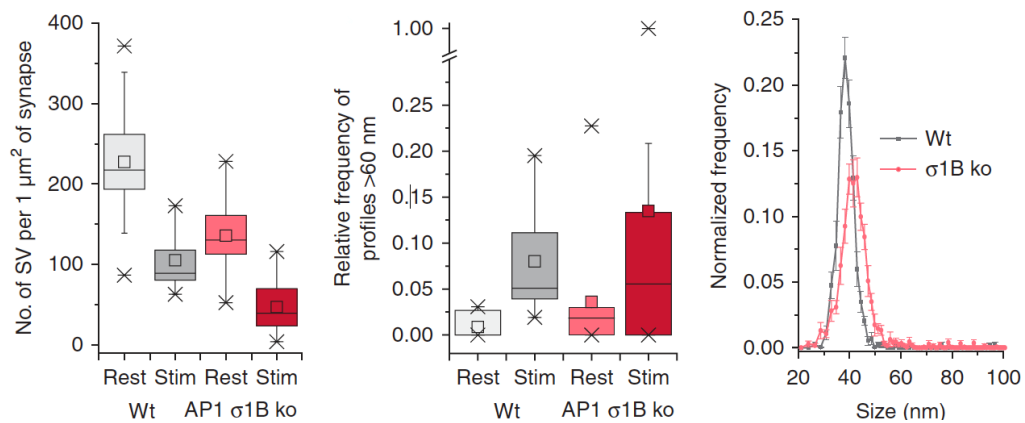


Fig. 14. Quantification of synaptic vesicles (SV) number (left panel) and of the accumulation of membranous structures with diameters larger than 60 nm (Central panel). Distribution of SV diameters at resting condition in the synapse (Right panel) (taken from Glyvuk et al 2010)

Subsequently the targeting of SV to the active zone and their docking to the plasma membrane was analyzed and it turned out to be very efficient in $\sigma 1B$ $-/-$ synapses, able to partially compensate for the reduced SV numbers.

On the other side, stimulation of SV recycling increased the number and size of organelles (Fig. 15, 3D reconstruction) with a diameter larger than 60 nm (central panel Fig. 14). These organelles were isolated and have been biochemically characterized as classic, PI-3-P and Rab5-positive early-endosomes (Kratzke et al. 2014).

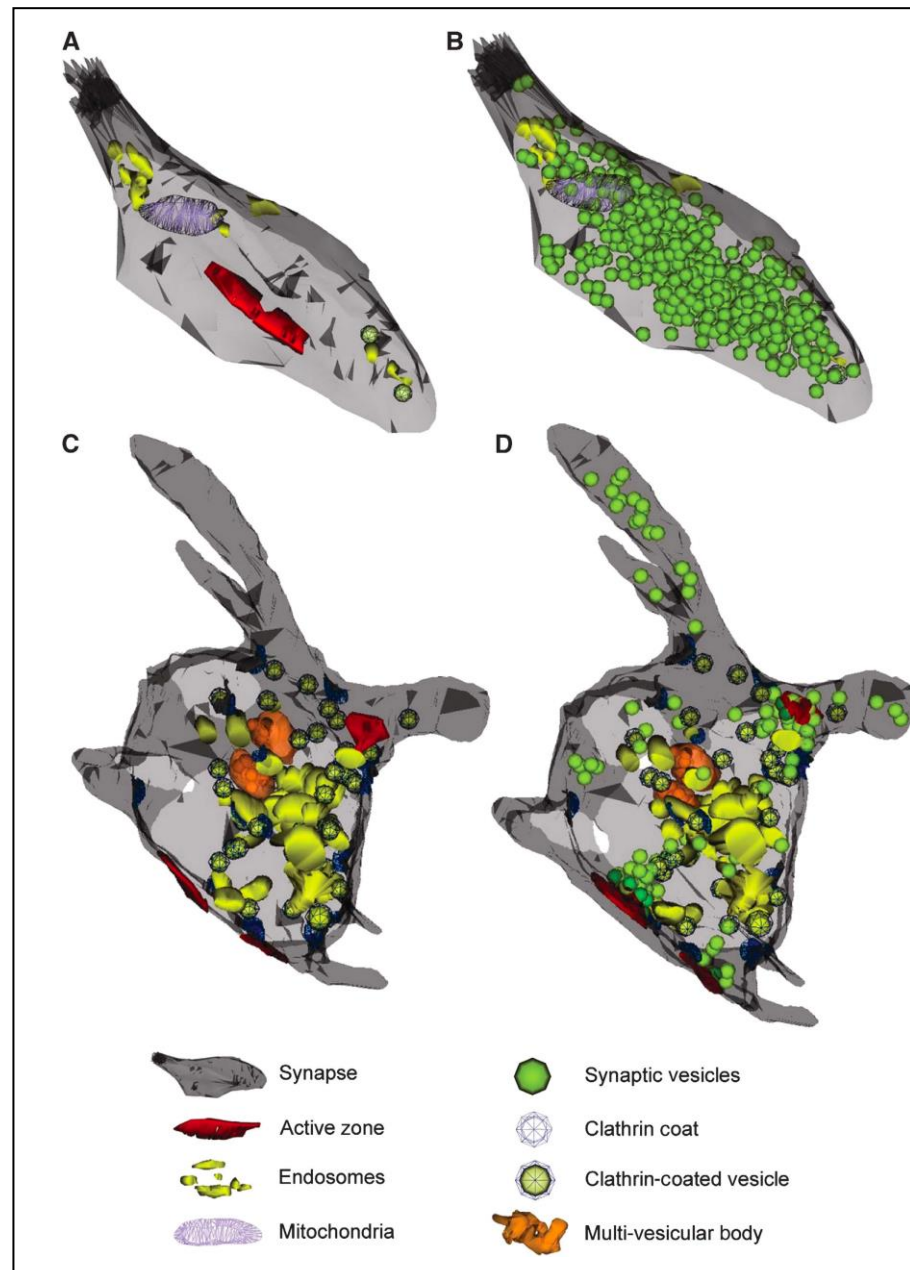


Fig. 15. 3D reconstruction of synapses from wt (A,B) and “ko” (C,D). In (A) and (C) synaptic vesicles are excluded for a clear view of the other organelles. “ko” synapse shows an accumulation of large membrane enclosed organelles, characterized as Early-Endosomes (taken from Glyvuk et al., 2010).

These data suggest an AP-1/ σ 1B dependence of SV recycling through early endosomes, where most of the AP-1 complexes have been detected. Thus, AP-1/ σ 1B mediated SV formation from endosomal intermediates could contribute to SV recycling at high SV turnover rates. However, despite the absence of the AP-1/ σ 1B and the reduced SV recycling, EM images also showed an increase in CCV. The

most likely explanation for their existence would be the formation of functionally impaired AP-1/ σ 1A CCV, due to the absence of the second AP-1 complex.

1.3.1 Early-endosome functions in SV protein recycling.

Early endosomes are the first and major sorting compartment for endocytosed proteins. Proteins can recycle back to the plasma membrane, but can also be transported to late, recycling endosomes or even back to the TGN, where the proteins would join again the late biosynthetic pathway. Alternatively proteins are sorted to late endosomes/lysosomes for their degradation. Association of proteins from the cytosol to the cytosolic surface of the EE membrane indicate their major function in endosomal protein sorting. Proteins mediating protein sorting in those various pathways bind to PI-3-P, enriched in the early endosome membrane. This PI-3-P pool is largely generated from PI by the phosphatidylinositol 3- kinase Vps34p (Schu et al., 1993). Vps34p forms on the membrane a complex with the Ser/Thr kinase Vps15p (p150), this complex and the PI3-kinase activity is stimulated by Rab5, the marker protein of early endosomes (Stack et al., 1993). Rab5 regulates endocytotic vesicle to early endosome as well as homotypic early endosome fusion (Fig. 16).

Analysis of the SV protein content of the endosome/SV pool revealed that about one third of the SV proteins are degraded in σ 1B $-/-$ synapses. This degradation is mediated by their sorting into the multi-vesicular-body late endosome pathway, which requires Rab5 and PI-3-P formed by Vps34p (Glyvuk et al., 2010, Kratzke et al., 2014).

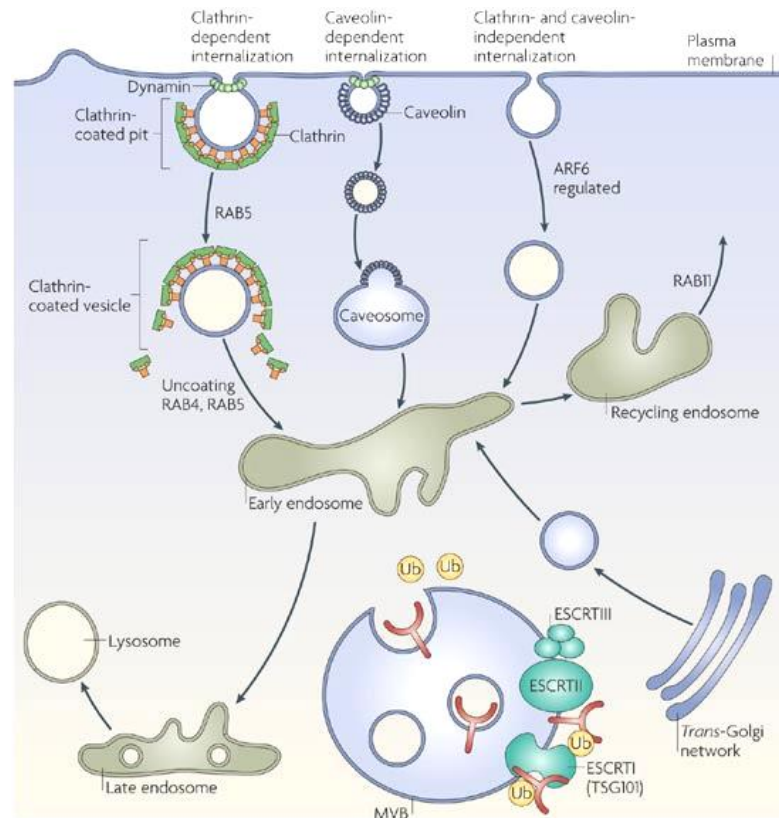


Fig. 16. Rab proteins are members of the Ras superfamily of monomeric GTPases. Different Rabs regulate many facets of membrane trafficking, including vesicle formation and movement and membrane fusion, and are localized to distinct endosomal compartments. Rab5 regulates the fusion and the tethering of the Early-Endosome (taken from Gwyn et al., 2009).

The regulatory principle of Rab proteins, as for other GTPases, lies in their ability to function as molecular switches that oscillate between GTP- and GDP-bound conformations. The GTP-bound form is considered the ‘active’ form. However, with respect to the physiology of the regulated process, the most important feature is the ability of GTPases to cycle regularly between GTP- and GDP-bound states. The Rab5-GTP bound state is promoted by its specific guanosine nucleotide exchange factor Rabex-5. The switch, Rab5-GTP Rab5-GDP, is mediated by the Rab5-specific GAP protein Rab-GAP5. Rab5 is localized mainly to the sorting endosome, though it is also present on the plasma membrane and on endocytotic vesicles. Its membrane association depends on a hydrophobic isoprenoid moiety close to its C-terminus domain, but is also regulated by a GTPase cycle.

Thus, in its GTP-bound state Rab5 is membrane-associated, while GDP-bound Rab5 is found in a cytosolic complex with the Rab guanine nucleotide dissociation inhibitor (GDI). Rab-GDI serves to release Rab5-GDP from membranes, to maintain cytosolic Rab5 in a soluble state and to recruit Rab5 efficiently to the endosomal

membrane in a reaction accompanied by nucleotide exchange (Ullrich, Horiuchi, Bucci, & Zerial, 1994). Rab5-GTP promotes endosome fusion by recruiting cytosolic components of the fusion apparatus. The first effector identified was Rabaptin-5 α , a homodimer with an extended structure consistent with a role in membrane docking. Rab5 binds close to the C-terminus domain of Rabaptin-5, in order to expose the bulk of Rabaptin-5 α to other binding partners (Stenmark, Vitale, Ullrich, & Zerial, 1995). In fact Rabaptin-5 α binds also Rab4, through its N-terminal domain, implicated in the recycling of membrane from the sorting endosome to the cell surface. Rabaptin-5 α is also directly involved in the GTP-GDP cycle of Rab5, it inhibits RabGAP1 and activates, through interaction, Rabex-5 (Zhang et al., 2014). In this way the Rab5/Rabaptin5 α interaction creates a positive feedback loop in order to have a local area of the membrane rich in active Rab5 (Woodman, 2000). Rabaptin5 α is also bound by the AP-1 γ 1-adaptin 'ear'-domain and this interaction is able to control Rabaptin5 α functions in early endosome membrane dynamics (Deneka et al., 2003).

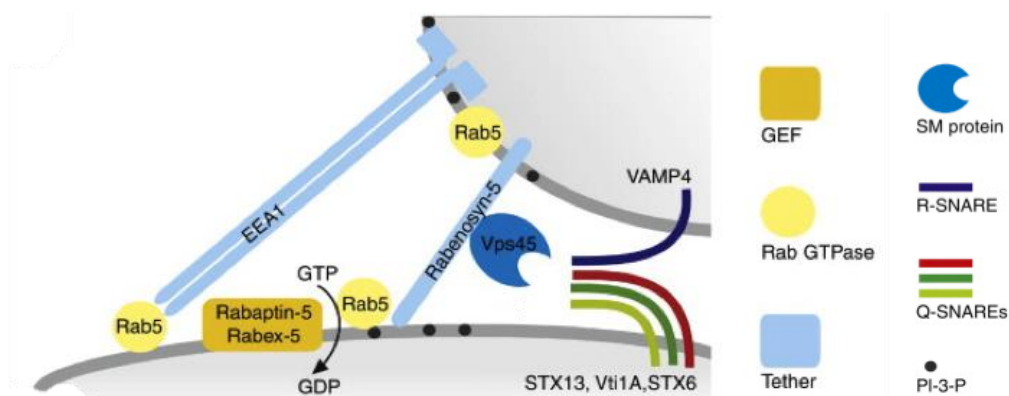


Fig.16 Models representing the essential components of the Rab and SNARE machineries involved in homotypic fusion of early endosomes. (Kümmel and Ungermann Current Opinion in Cell Biology, 2014)

However the EEA1 ability to bind simultaneously the two Rab5s, one from the donor compartment and the other one from the acceptor compartment, is essential for the tethering (fig.x) and the fusion. The accumulation of early-endosomes in “ko” synapses could be the consequence of an altered CCVs cycle caused in turn by the AP1/ σ 1B “ko”, as alteration in the CCVs composition and regulation could leads a

delay in the SV reformation mediated by Early-endosomes. On the other side the early-endosomal accumulation could be the reason of CCV cycle alteration: the $\sigma 1B$ “ko” could effect the Rab5/endosomal cycle leading changes in shape, size and release of clathrin vesicles, in turn this could cause the SV-proteins redistribution. Nothing is known about the apical role, in synapses, of endosome and AP1 CCV, however all the data coming from the $\sigma 1B$ “ko” revealed that early endosomes mediate synaptic vesicle biogenesis and that the AP-1 CCV cycle and the AP-2 SV re-uptake are somehow interdependently regulated.

Aim of the study

The adaptor complex AP-1 participates in the clathrin vesicles formation mediated by Early-endosome. Although nothing is known about the apical role of AP-1 complex in synapse, AP-1/ $\sigma 1B$ deficient mice showed mental retardation and an impaired spatial learning. This phenotype reflects alterations in the synaptic vesicles cycle: biogenesis and reuptake. The “ko” synapses is characterized, mainly, by an accumulation in Early-endosome and CCV. iswild type have to

First of all, we wanted to characterize the accumulated CCV in the “ko” synapse in order to understand the reason of this accumulation.

These accumulated CCV, have proved to be AP-2 CCV thus the next goal is to understand what kind of AP-2 CCV accumulate in the $\sigma 1B$ “ko” synapse and what are the differences from the “canonical” AP-2 CCV.

Furthermore we want to understand the molecular mechanism linking the AP-1/endosomal sorting and the rearrangement of the CCV in the other SV pools like the SV recycling, were AP-2 CCV are involved.

Another important goal of the project is to clarify how and why the AP-1/ σ 1B “ko” leads alterations in the Early-endosomal cycle

2. Materials and Methods

2.1.1 Specific laboratory equipment

Confocal Scanner Scanning Microscope	Leica, Bensheim
Sonicator 220F	Heat System Ultrasonic, QC Canada
Intelligent Dark Box II, LAS-1000	Fujifilm, Japan
Gradient Station IP	Biocomp, NB Canada

All solutions used were, except as otherwise specified, with Ultrapuredeionized water applied. This was made using the ultrapure water GenPure Recovered (TKM Niederelbert)

2.1.2 Buffers

PBS

(phosphate-buffered saline):	140 mM NaCl	(AppliChem, Darmstadt)
	2.5 mM KCl	(Carl Roth GmbH, Karlsruhe)
	6.5 mM Na ₂ HPO ₄	(Carl Roth GmbH, Karlsruhe)
	1.5 mM KH ₂ PO ₄	(Carl Roth GmbH, Karlsruhe)
	pH 7.5	
TBS		
(tris-buffered saline):	100 mM Tris/HCl	(Carl Roth GmbH, Karlsruhe)
	100 mM NaCl	(AppliChem, Darmstadt)
	pH 7.5	
TBS-T:	100 mM Tris/HCl	(Carl Roth GmbH, Karlsruhe)
	100 mM NaCl	(AppliChem, Darmstadt)
	0.05 % Tween 20	(AppliChem, Darmstadt)
	pH 7.5	
CCV Buffer:	10 mM MES	(SERVA GmbH, Heidelberg)/ (AppliChem, Darmstadt)
	0.5 mM EGTA	(Sigma, Steinheim)
	0.5 mM MgCl ₂	(Merck, Darmstadt)
	320 mM Sucrose	(Carl Roth GmbH, Karlsruhe)
	1 mM Na ₃ VO ₄	(Sigma, St. Louis, USA)
	10 mM NaF	(Sigma, St. Louis, USA)
	10 nM Calyculin A	(Axxora, Lörrach)

2.2 Cellular Culture Methods

Tab. 2-1: Cell lines used, deriving from WT, AP-1 / σ 1B-deficient mice and AP-1 / μ 1A-deficient mice

Cell line	Description	Reference
S1B111 D5	MEF, σ 1B +/+	Baltes 2008
S1B111 E8	MEF, σ 1B -/-	Baltes 2008
24 A	MEF, μ 1A +/+	Meyer 2000
24	MEF, μ 1A -/-	Meyer 2000

Solutions and Media:

PBS:	150 mM NaCl 120 mM KCl 10 mM Na ₂ HPO ₄ /KH ₂ PO ₄ 0.1 g Phenol red pH 7,4	(AppliChem, Darmstadt) (Carl Roth GmbH, Karlsruhe) (Carl Roth GmbH, Karlsruhe) (Carl Roth GmbH, Karlsruhe)
Trypsin-EDTA Solution:	0.5 g/L Trypsin 0.2 g/L EDTA	(Gibco Invitrogen, Karlsruhe)
Medium:	4.5 g/L Dulbecco's Modified Eagle Medium, (DMEM) 10% (v/v) Fetal Calf Serum (FKS) 1% (v/v) Penicillin/Streptomycin (100x Stock solution) 1% (v/v) Glutamine (200 mM, 100x Stocksolution)	(Gibco Invitrogen, Karlsruhe) (PAN, Aidenbach) (Gibco Invitrogen, Karlsruhe) (Gibco Invitrogen, Karlsruhe)
Freezing Medium:	4.5 g/L DME 10% (v/v) FCS 5% (v/v) Dimethylsulfoxide 1% (v/v) Penicillin/Streptomycin(100x Stocksolution) 1% (v/v) Glutamine (200 mM, 100x Stocksolution)	(Gibco Invitrogen, Karlsruhe) (PAN, Aidenbach) (Fluka, Schweiz) (Gibco Invitrogen, Karlsruhe) (Gibco Invitrogen, Karlsruhe)

2.2.1 Mouse embryonic fibroblast's culture

Mouse embryonic fibroblast (MEF) were incubated under a water-saturated atmosphere at 37°C and with a 5%(v/v) CO₂ concentration, in plastic flasks (25 cm²). After reaching confluence the cells were split under sterile conditions; washed with

PBS and then treated with trypsin-EDTA solution (0.5 mL), 5 minutes at RT in order to detach from the bottom of the flask. The cells were resuspended in 4.5 mL of fresh medium, thus the total volume was 5 ml. Only 500 μ l of the newly resuspended cells were placed in the flask with 4.5 ml of new medium in order to have a 1:10 split ratio (250 μ l in 4.75 ml for 1:10 split ratio). Cells reached again the confluence after 3-4 days.

2.2.2 Freezing and thawing of cells

For long-term storage, the cells were stored in liquid nitrogen. For this purpose, the cells were detached from the bottom of the cell culture flasks as described in 2.2.1.

The cells were centrifuged at room temperature for 5 min at 300g. The supernatant was removed; the cells were resuspended in freezing medium (1mL). Aliquots of 150-200 μ l were transferred in 1mL cryotubes and stored at -20 for 3 hours and then in liquid nitrogen for long-term storage. Dimethyl sulfoxide in the freezing medium is used to avoid the formation of deleterious ice crystals.

To avoid cell damage during thawing, is necessary to work speedily. The cells were thawed in a water bath at 37°C and 10 mL of pre-warmed medium was added. The cells were centrifuged at 300g for 10 min. The pellet was dissolved in fresh medium and the cells were plated in a cell culture flask and incubated as in 2.2.1

2.3 Molecular biology

2.3.1 Cloning Procedures

Bacterial strains

The following bacterial strains were used:

Strain	Application	Source
DH5 α	Plasmid amplification	Invitrogen
BL21D3	High level expression of recombinant proteins	Stratagene

Vectors

The following vectors were used:

Plasmid	Description	Tag	Resistance	Source
pGEX4T1	Bacterial expression vector	GST	Ampicillin	GE Healthcare
pKM260	Bacterial expression vector	6HIS	Ampicillin	GE Healthcare
pEGFP	Mammalian expression vector	GFP	Kanamycin	Invitrogen

Costrcuts

The following contruts were used:

Construct	Amino acids	Mutation	Vector	Origin
Arf-GAP1 Ubiquitous	Full length		pKM260	D. Cassel
Arf-GAP1 Brain iso.	Full length		pKM260	D. Cassel
GFP-Arf-GAP1 Ubiqu.			pEGFP	D. Cassel
GFP-Arf-GAP1 Brain			pEGFP	D. Cassel
Rab-GAP1	578-760		pGEX4T1	
Rabex5	396-491		pGEX4T1	
Rabex5 I	396-491	402 <E/A	pGEX4T1	
Rabex5 II	396-491	484 <L/A	pGEX4T1	

DNA Restriction Digest

DNA fragments were digested, from original vectors, using Fast Digestion Enzymes from Thermo Scientific with the relative buffers. 1-4 μ g of plasmid DNA was digested in a mix containing 10x Fast Digest buffer and 1 unit of restriction enzymes per 1 μ g of DNA, in a final volume of 30 μ l. After 1 μ incubation at 37°C, the DNA fragments were loaded in an agarose gel for analysis or for extraction and digestion.

Fragments digestion from agarose gel

Fragments digestion from agarose gel was performed using the Wizard® SV Gel and PCR Clean-Up System kit from Promega and following the relative instructions

Ligation

Ligation reaction was performed using the RapidDNA Ligation Kit from Thermo Scientific and following the relative instructions

Vector:	100ng
Construct:	5:1 molar excess over vector
T4 DNA Ligase:	1µl per reaction
5X Rapid Ligation Buffer:	4µl
Water, nuclease-free:	in order to have a 10µl final volume

Bacteria transformation

Luria Bertani (Wang et al.) medium:	0.5% yeast extract, 1% trypton, 0.5% NaCl
LB plates:	LB medium, 1,5% Agar

For heat shock transformation aliquots of chemically competent *E.coli* were thawed on ice. 40-70 ng of plasmid DNA, or 6-7 µl of the ligation reaction were added to the cells, incubated on ice for 30 min. For the heat shock, cells were incubated at 42°C for 1 min and immediately afterwards 1 ml of LB medium was added and they were incubated for 60 min at 37°C to induce antibiotic resistance. Afterwards, cells were pelleted (few seconds, 13000 rpm) and plated on LB-agar plates supplemented with the corresponding antibiotic. The plates were incubated overnight at 37°C. The next day, colonies were picked and inoculated into LB medium with corresponding antibiotic for further proceedings.

Plasmid DNA Preparation

For small scale purification of plasmid DNA, *E.coli* cells were grown overnight in 3 ml LB medium plus the antibiotic (3 µL from 100 µg/µL stock solution) at 37°C and purified using the Wizard® SV Genomic DNA Purification System kit (Promega) following the manufacturer's instructions.

2.4 Biochemical Methods

2.4.1 Overexpression of recombinant proteins in E.Coli

LB medium

Expression of recombinant proteins were induced in BL21D3 E. coli strain with 0.5 mM IPTG for 4 hours at 37°C. Cells were then harvested and washed with ice-cold PBS buffer (140 mM NaCl, 2.5 mM KCl, 6.5 mM NaHPO₄, 1.5 mM KH₂PO, 1 mM. PMSF, pH 7.4). Cells were incubated on ice 30 minutes with lysing buffer (PBS pH 7.4, Lysozime 0.1%, Proteinase Inhibitors) and sonicated 3 minutes at 4°C. After lysis, cells proteins were collected by centrifugation at 4,000 rpm for 25 minutes at 4°C. Pellet was resuspended in PBS with 7.2 M Urea and sonicated 3 minutes at 4°C to dissolve inclusion bodies. The recombinant proteins were then purified by Gluthation Sepharose Beads (GST-tagged recombinant proteins) or by Ni-NTA beads (6-His-Tagged recombinant proteins)

2.4.2 GST-tagged protein purification

Gluthatione Sepharose Beads: (Amershem, Freiburg)

60 µl of Gluthatione Sepharose Beads were washed with PBS Buffer in order to equilibrate the beads and remove the ethanol beads are 75% of the total volume, 25% left is ethanol). GST-tagged-recombinant proteins were incubated, for purification, with 45 µl of Gluthatione-sepharose beads over night at 4°C with up-down gentle rotation. The resin was harvested by 500 x g centrifugation for 20 min at RT, and washed with 10 volumes PBS buffer 5 times.

2.4.3 6-His-Tagged protein purification

Ni-NTA-beads: (Qiagen, Düren)

The 6-His-Tagged protein purification was performed exactly as the GST-tagged protein purification; the only difference is the beads incubation. In this case Ni-NTA-agarose beads were used to bind the 6-His tag.

2.4.4 Pulldown of proteins from brain cytosol by recombinant proteins

Brain cytosol preparation

$\sigma 1B^{-/-}$ and wt brains were sliced with a scalpel in 1.5 mL of lysing buffer (PBS pH 7.4 with Proteinase Inhibitors), the cut cortex was placed in a glass potter and homogenized by 20 strokes (up-and-down) with a “loose” piston and subsequently with a “tight” piston (40 strokes). The homogenate cortex was centrifuged at 1000 x g for 10 min. The supernatant (S1) was decanted in a new tube, the pellet (P1) was washed with lysing buffer and centrifuged again at 1000 g for 10 min; the supernatant (S2) was added to S1 and centrifuged at 9200 g for 15 min. The supernatant (S3) was discarded and the pellet (P3) resuspended in 1,5 mL of lysing buffer and centrifuged at 10200 g for 15 min. According to the size, the pellet (P10), containing the synaptosome was resuspended in 500-600 μ L of lysing buffer and homogenized with a ball homogenizer with a clearance of 12 μ m (Isobiotec, Heidelberg, Germany) through 40 passages. The homogenized synaptosome was centrifuged at 25000 x g for 20 min and the supernatant containing the synaptic cytosol was stored. The protein concentration was determined by Bradford assay.

2.4.4.1 Incubation of the synaptic cytosol with beads binding the recombinant proteins ‘Pull-down’ experiments

Beads with the purified recombinant proteins (6His-tagged or GST-tagged) were harvested, after the overnight incubation, and washed with lysi buffer 5 times. Subsequently the beads were incubated with the synaptic cytosol for 4 hours at RT.

The resin containing the recombinant protein bound to the cytosolic protein, was washed with lysis buffer 5 times, resuspended in 45-50 μ l (the same volume of the beads) of 3x SDS loading buffer and loaded into polyacrylamide gel for western blot analyses.

2.4.5 Transient transfection

MATra Transient Transfection

DMEM:	(Gibco Invitrogen, Karlsruhe)
MATra Beads: Magnetic Beads	(iba, GmbH, Goettingen)
Mounting Glass Slide:	(Roth GmbH Karlsruhe)

Cells have been were plated on a 24 multi-well plate, 24-36 hours before the transient transfection, in order to have a final confluence of 40-50%. Cells were incubated at 37°C in a 5% CO₂ in 500 μ l (each well) of growth medium.

The transfection was performed with the MATra magnetic beads:

0.6 μ g of GFP-tagged plasmid was incubated for 20 min at RT with 0.6 μ l of MATra reagent and with DMEM to an end volume of 50 μ l per cells slide (growth medium change was performed before the transfection). The solution containing the MATra reagent and the plasmid was added to the cells and the multi-well plate was placed immediately on a suitable Magnet Plate for 15 min at RT. Cells were incubated at 37°C in a 5%CO₂ incubator for at least 48 hours before the immunofluorescence assay.

2.4.6 Protein extraction from MEF

Proteinase-Inhibitor-Cocktail (PIC):	Roche, Mannheim
--------------------------------------	-----------------

MEF were incubated in 150 mm tissue culture dishes and after reaching confluence were washed with PBS, they were detached with a cell scraper and transferred in a 2 mL tubes; the cells were centrifuged at 200 g 4 C°, the pellet was washed with PBS and centrifuged again at 500g 4 C°. The pellet was resuspended and homogenized through a 22G needle.

2.4.7 Differential centrifugation for Clathrin Coated Vesicles isolation, from brain cortex.

Membrane-bound and soluble proteins from cell disruption are separated through differential centrifugation. Mouse cortex from wt and “ko” were sliced with a scalpel in 1.5 mL of CCV Buffer, the cut cortex was placed in a glass potter and homogenized by 10 strokes with a “loose” piston and subsequently with a “tight” piston. The homogenate cortex was centrifuged at 1000 g for 10 min. The supernatant (S1) was decanted in a new tube, the pellet (P1) was washed with CCV buffer and centrifuged again at 1000 g for 10 min; the supernatant (S2) was added to S1 and centrifuged at 9200 g for 15 min. The supernatant (S3) was discarded and the pellet (P3) resuspended in 1,5 mL of CCV buffer and centrifuged at 10200 g for 15 min. According to the size, the pellet (P10) was resuspended in 500-600 µL. The solution containing the synaptosome was lysed by 40 passages through a ball homogenizer (Isobiotec, Heidelberg, Germany) with a clearance of 12 µm. This extract was centrifuged at 25000 g for 20 min. The pellet (P20) was resuspended in 500 µL of CCV buffer, the protein concentration was determined by Bradford assay and wt and “ko” concentration were normalized; the solution was layered over 20-50% Sucrose gradient (3.5 mL) and centrifuged at 145000 g for 1.5 hours. The gradient (in total 4 mL) was fractionated in 10 fractions of 400 µL. CCV distribution was identified through Western Blots.

2.4.8 Hsc-70 Immunoprecipitation

Protein G Sepharose 4 Fast Flow

(GE Healthcare, Uppsala Sweden)

Hsc70 Antibody Mouse Monoclonal (SY SY, Göttingen)

Fractions containing the purified CCV were pooled together, for a 1 mL final volume, and incubated with 50 μ l of protein G sepharose bead slurry (previously washed x3 with CCV buffer to remove ethanol and equilibrate the beads) for a pre-clear procedure, and incubated at 4°C for 1 hour with upside down gentle rotation. The beads were spun out with a 30 sec centrifugation at 2000 rpm and flow through containing the CCV was saved. 5 μ g of Hsc70 antibody were added to the pre-cleared CCV and incubated overnight. The protein G sepharose beads were washed 3 times with CCV buffer and added to the Hsc70-conjugated CCV and incubated with gentle upside down rotation at 4°C for 4 hours. The beads were collected through 2000 rpm centrifugation and washed 5 times with 1 mL of CCV buffer. Finally the beads were resuspended in 60 μ l of 3X SDS loading buffer and incubated at 90°C for 5 minutes, the supernatant was stored as Elution1, then the beads were resuspended again in 60 μ l of 3X SDS loading buffer for a second elution cycle and thus incubated at 90°C for 5 minutes, the supernatant was stored as Elution2. The beads were resuspended in 40 μ l of 3X SDS loading buffer and stored. Elution 1, Elution2, and beads were loaded in a polyacrylamide gel for western-blot analyses or submitted for mass spectrometry analyses.

2.4.8.1 Immunoprecipitation with 4G10® Platinum-Anti-Phosphotyrosine-Agarose Conjugated-beads

As for the Hsc70 immunoprecipitation, fractions containing CCV were pooled and 250 μ g were incubated with 10 μ l of 4G10® Platinum-Anti-Phosphotyrosine-Agarose Conjugated-beads, overnight at 4°C. The beads were collected and eluted exactly as in 2.4.8 and analyzed by western-blots and mass spectrometry analyses

2.4.9 Protein Concentration Determination by Bradford Assay

To determine the protein concentration of cell lysates or purified protein a

Bradford assay was performed. 200 μ l of 5x Bradford solution was added to 1- 5 μ l of protein solution in 800 μ l water. After 3 min incubation at room temperature the absorption at 595 nm was measured. 1x Bradford solution served as a blank. The protein concentration from samples was calculated from a reference curve generated using BSA as standard.

2.4.10 Semi-quantitative Western blot Analyses

Polyacrylamide gel electrophoresis (SDS-PAGE)

The SDS-PAGE (sodium dodecyl sulfate polyacrylamide gel electrophoresis) is a biochemical method widely used for the separation of proteins according to their electrophoretic mobility; the technique is based upon the principle that a charged molecule will migrate in an electric field towards an electrode with opposite sign. Mobility is a function of the length, conformation and charge of the protein. SDS is a chemical anionic detergent added to linearize proteins and to impart an overall negative charge, thereby resulting in a fractionation solely by approximate size during electrophoresis. Samples were boiled in the presence of a reducing agent as dithiothreitol (DTT) or 2-mercaptoethanol (BME), which further denatures the proteins by reducing disulfide linkages of the tertiary protein folding.

Proteins samples run in a polyacrylamide matrix with N, N'-Methylenebisacrylamide. The polymerization of acrylamide and methylene bisacrylamide proceeds via a free-radical mechanism. The most common system of catalytic initiation involves the production of free oxygen radicals by ammonium persulfate (APS) in the presence of the tertiary aliphatic amine N,N,N',N'-tetramethylethylenediamine (TEMED). Tris-HCl buffer (containing also SDS) is added for pH adjustment. The gel used is divided in two parts, an upper "stacking" gel and a lower "running" gel. The stacking gel has a low percentage of acrylamide (with large pore size) and low pH (6.8), so that the proteins get squeezed down in a thin layer at the interface between the "stacking" and the "running" gel. The running gel has a pH 8.8 and the acrylamide percentage is set to 5%-12.5% according to the size range of the proteins to be detected.

Tab. 2-2: Compositions of gels of different acrylamide concentrations

The amounts are related to a minigel (55mm x 85mm)

Acrylamide %	Stacking gel	Running gel				
	4.5	5	7.5	10	12.5	15
Rotiphorese®-Gel30/mL	0.45	1.3	1.8	2.7	3.3	4
Tris/SDS Buffer/mL	0.75	2	2	2	2	2
H ₂ O/mL	1.75	4.6	3.9	3.2	2.6	1.9
TEMED/ μ L	3	8	8	8	8	8
10% APS/ μ L	30	80	80	80	80	80

Rotiphorese®-Gel30:	Acrylamide-/Bisacrylamide	(Carl Roth GmbH, Karlsruhe)
Stacking gel Buffer:	0,5 M Tris/HCl	(Carl Roth GmbH, Karlsruhe)
	0,4% (μ /v) Sodiumdodecylsulfate	(SERVA GmbH, Heidelberg)
	pH 6,8	
Running gel Buffer:	1,5 M Tris/HCl	(Carl Roth GmbH, Karlsruhe)
	0,4% (μ /v) Sodiumdodecylsulfate	(SERVA GmbH, Heidelberg)
	pH 8,8	
10% APS:	10% (μ /v) Ammonium persulfate	(Merck, Darmstadt)
TEMED:	N,N,N',N'- Tetramethylethylene- 1,2-diamine	(SERVA GmbH, Heidelberg)
Running Buffer:	50 mM Tris	(Carl Roth GmbH, Karlsruhe)
	400 mM Glycin	(Carl Roth GmbH, Karlsruhe)
	0,1%(μ /v) Sodiumdodecylsulfate	(SERVA GmbH, Heidelberg)
	pH 8,6	
6x reducing sample buffer:	750 mM Tris/HCl	(Carl Roth GmbH, Karlsruhe)
	9% (μ /v) Sodiumdodecylsulfate	(SERVA GmbH, Heidelberg)
	1% (v/v) Bromophenol blue	(Merck, Darmstadt)
	60% (v/v) Glycerol	(Sigma-Aldrich, Steinheim)
	300 mM DTT	(AppliChem, Darmstadt)
	pH 6,8	

Protein molecular

weight marker: Precision Plus Protein Standard (Bio-Rad, München)
All Blue

Protein samples were boiled at 95 C° with 6x reducing buffer (6:1) and fresh DTT (50mM) for 5 min. After loading the samples in the gel pockets (minigel), was applied a constant current of 15mA. Subsequently, when the samples reached the running part, the current was increased at 30mA.

2.4.11 WesternBlot & Immunostaining

After the electrophoretic separation in the SDS-polyacrylamide gel, the proteins were transferred to a support membrane of nitrocellulose or polyvinyl-nylidenfluorid (PVDF). The proteins have a negative charge (treated with SDS) and migrate in the electric field to the anode. The PVDF membrane has been activated in methanol (1 min) and then equilibrated in anode buffer. The “transfer sandwich” was assembled as shown in the Fig. 2.1.



Fig. 2.1. Schematic representation of a semi-dry Western Blot “sandwich”. The Anode, positively charged, is in the lower part, the Cathode, negatively charged, in the upper part: the proteins, negatively charged, migrate downwards, from the gel to the transfer membrane

The three lower filter papers, the gel and the supporting membrane were wetted in anode buffer, the 3 upper filter papers with cathode buffer. An electric field of 1mA x mm² was applied for 0.5-2 hours according to the size of the proteins to detect.

Non-specific binding sites on the membrane were saturated by incubation with blocking buffer (1 μ), subsequently the primary antibody was incubated over-night (4 C°). Membrane was washed with blocking solution, three times 10-15 min and incubated with secondary antibody (1 μ) at RT. Then membrane was incubated with horse radish peroxidase(HRP)-coupled secondary antibody, diluted 1:10000 in

blocking buffer, for one hour at room temperature.

The blot was washed three times 10-15 min with TBS-T and incubated with chemiluminescence substrate solution. Intelligent Dark Box II Camera was used for signal detection.

Anode Buffer:	75 mM Tris/HCl	(Carl Roth GmbH, Karlsruhe)
	20 % Methanol	(AppliChem, Darmstadt)
	pH 7,4	
Cathode Buffer:	40 mM Aminocaproic Acid	(Carl Roth GmbH, Karlsruhe)
	20 mM Tris/HCl	(Carl Roth GmbH, Karlsruhe)
	20 % Methanol	(AppliChem, Darmstadt)
	pH 9,0	
PVDF-Membrane:		(Millipore, Billerica, USA)
Nitrocellulose membrane:		(Whatman GmbH, Dassel)
Filter paper, 330 g/m ² :		(Satorius Stedim Biotech GmbH, Göttingen)

2.4.12 Stripping of transfer membranes.

Removal of antibodies from a blot was done under mild conditions, if it should serve to reduce the background for incubation with another primary antibody, either from a different species or for a protein of clearly distinct size than in the first decoration. After washing the membrane in TBST, it was incubated 5-20 min in glycine stripping solution. The solution was neutralised with 1 M Tris-Cl pH 8.5, followed by several washes in TBST.

2.4.13 Mass spectrometry

All the mass spectrometric measurements were performed by Dr. Olaf Jahn, MPI for experimental Medicine, Göttingen (iTRAQ labelling) and by the Dr. Bernhard Schmidt Group in our institut (peptide detection and quantification).

Washing solution:	25mM Ammonium carbonate	(Sigma, Steinheim)
Acetonitrile 50:	50%(v/v) Acetonitrile	(Merck, Darmstadt)
	25mM Ammonium carbonate	(Sigma, Steinheim)

Reducing reagent:	10mM DTT	(Applichem, Darmstadt)
	25mM Ammonium carbonate	(Sigma, Steinheim)
Carbamidomethyl reagents:	25mM Iodacetamide	(Sigma, Steinheim)
	25mM Ammonium carbonate	(Sigma, Steinheim)
Trypsin solution:	20ng/μl trypsin	(Promega, Mannheim)
Extraction solution:	1% trifluoroacetic acid	(Fluck, Buchs)
Releasing buffer:	0.1% trifluoroacetic acid	(Fluck, Buchs)

In order to reduce the number of proteins that were simultaneously processed and then measured for mass spectrometry, the samples containing the proteins were separated electrophoretically. Subsequently there was the gel digestion (Rose et al. 1992). It essentially consists of the following four steps: destaining of the gel pieces; reduction and alkylation of Cysteines to irreversible cleavage of disulfide bonds; obtain an optimal unfolding of the proteins; proteolytic cleavage and extraction of the resulting peptides. Proteolysis was performed using Trypsin, a Serine-protease, which specifically cleaves the peptide bonds at the carboxyl terminus of the basic amino acids arginine and lysine.

Each gel slice was incubated in 100 μl of wash solution for 15 min at 37°C with gentle shaking, the supernatant was discarded and incubated twice for 30 min at 37°C with gentle shaking in acetonitrile solution 50. The supernatant was removed and incubated for 10 min at 37°C with gentle shaking in 100% acetonitrile, the supernatant was removed and dried for 5 min at room temperature in an open reaction-chamber. To break the disulfide bridges the gel slice was incubated with reducing reagent for 1 hour at 56°C, cooled on ice and the supernatant was removed. For the alkylation of cysteines the gel slices were incubated in 10μl of Carbamidomethyl reagents for 30 min at room temperature, in the dark with gentle shaking. The supernatant was incubated at 37°C for 10min with gentle shaking with reducing reagent.

The gel slices were resuspended in 100μl of acetonitrile 50 solution and incubated for 30 minutes at room temperature, subsequently were incubated with 100μl of acetonitrile 100% for 10 min at 37°C with gentle shaking and the supernatant was removed. The slice was dried for 5 min at room temperature.

The digestion started adding 6μl of trypsin solution and incubating 15 min on ice and subsequently incubating at least 4 hours at 37°C. The supernatant was removed and

the gel incubated with 20µl of extraction solution for 20 min at 37°C with gentle shaking. The extraction solution was removed and combined with the supernatant of the digestion. The extracted peptides were dried in a vacuum centrifuge and resuspended in 10µl of dissolving buffer by vortexing and treating with ultra-sounds. Peptide were dissolved and measured for mass spectrometry or stored at -20°C.

Mass spectrometry of the trypsin-digested peptides

Peptides were either directly applied onto a MALDI Anchor chip target (Bruker Daltonics GmbH, Bremen) or separated via a NANO-LC, EASY-nLC II (Proxeon, Thermo Fisher Scientific, Dreieich) and fractionated on an LC-MALDI Fraction Collector, PROTEINEER fc II (Bruker Daltonics GmbH, Bremen, Germany) was applied to a MALDI Anchor chip target. MALDI mass spectrometry experiments in which the peptide mixtures were pre-fractionated in this manner are hereinafter referred to as LC-MALDI.

All steps were performed according to protocols of Bruker Daltonics GmbH (Bremen) and Proxeon, Thermo Fisher Scientific (Dreieich).

2.4.14 iTRAQ™- Mass spectrometry

SDS loading buffer:

(O. Jahn, Göttingen):	106 mM Tris HCl
	141 mM Tris base
	2% Lithium lauryl sulfate
	10% Glycerol
	0,51 mM EDTA
	0,22 mM Coomassie G250
	0,175 mM Phenol red
	50 mM 1,4-Dithiothreitol
	pH = 8,5

Gel digestion:

Ultrapure water	(LiChrosolv ®).
Acetonitrile	(ACN, LiChrosolv ®).

50 mM triethylammonium bicarbonate TEAB, (Sigma-Aldrich,
pH 8.0, prepared fresh Steinheim, Germany)

10 mM (m/v) dithiothreitol in 50 mM TEAB.
prepared fresh

55 mM (m/v) iodoacetamide in 50 mM TEAB.
prepared fresh

5% (v/v) formic acid (FA, p.a.)
prepared fresh

Trypsin, sequencing grade, 0.1 µg/µL. (Roche)

Buffer 1: 50 µL H₂O, 50 µL 50 mM TEAB,
15 µL trypsin. Prepared fresh

Buffer 2: 50 µL H₂O, 50 µL 50 mM TEAB.
Prepared fresh

iTRAQ-Labeling:

100mM TEAB, pH_≥8.0 prepared fresh

iTRAQ-reagents: iTRAQ™ Reagent Multi-Plex Kit (Applied Biosystems,
Foster City USA)

Samples were quantified by iTRAQ (Isobaric tags for relative and Absolute Quantitation). 15 µg of Wt and “ko” samples were loaded for a SDS1D PAGE separation and subsequent gel digestion. The following workflow has been used:

1. Separation of purified protein complexes by 1D PAGE on pre-cast gels (8 x 8 cm x 1 mm);
2. Cutting the entire sample lanes into pieces of exactly the same size;
3. Digestion of proteins with the endoproteinase trypsin;
4. iTRAQ labeling of extracted peptides;
5. Pooling of the differentially labeled samples and subsequent LC-MS/MS analysis (ESI MS);

Wt and “ko” samples have been marked separately to obtain a relative-difference information about the quantity of all the proteins and peptides. The iTRAQ method involves protein reduction and alkylation, enzymatic digestion, labeling up to four

different samples (or nowadays eight samples) with heavy and light isotope-labeled reagents, sample pooling, HPLC (high performance liquid chromatography) separation, and finally detection and quantification by tandem MS. The iTRAQ reagent is an amine-specific reagent that labels peptide amino termini and lysine side chains with multiplex (4-plex or 8-plex) mass tags: i.e., tags with identical masses. These tags are isobaric (i.e., they have the same mass of 144.1 Da), but their fragmentation patterns differ, allowing species bearing them to be distinguished after fragmentation. Upon fragmentation, every isobaric tag produces a specific marker ion (114.1, 115.1, 116.1, and 117.1 Da, respectively) and a corresponding neutral fragment, which is not detectable (28, 29, 30, and 31 Da, respectively).

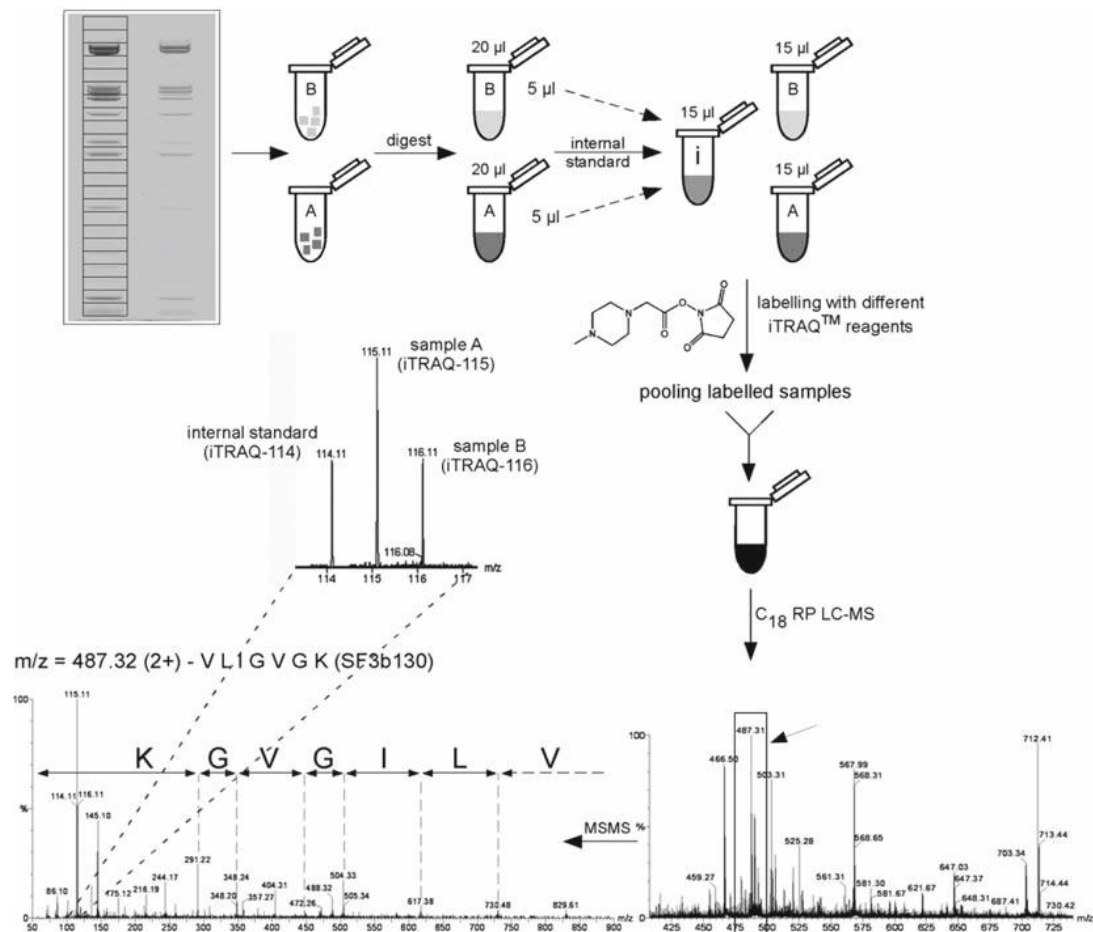


Fig. 2.2. Overall workflow of in-gel digestion and subsequent labeling with iTRAQ™ reagents. Entire gel lanes of different samples to be analyzed and quantified are cut into gel slices of equal size resulting in X samples per lane. Each gel slice further manually cut into small pieces and proteins within gel pieces are digested with trypsin. Extracted peptides are re-dissolved in 20 µL 100 mM TEAB and an internal standard is prepared by pooling 5 µL of each sample. Samples and internal standard are labeled with iTRAQ™ reagents 114, 115, 116, respectively. After pooling, the samples are analyzed by LC-MS/MS and quantitation is done by calculating the peak areas of individual reporter ions (114, 115, 116, and 117) in MS/MS.

2.4.15 Immunofluorescence

MEF cells were plated in a 24 multi-well plate (on 10mm coverslip) and incubated with growth medium at 37 C°, 24-36 hours before the experiment in order to reach a 70% confluence.

Cells were washed with PBS and fixed in fresh 4%-paraformaldehyde (PFA) for 10-15 min at RT. PFA was removed by aspiration and the cells were washed with PBS. The unreacted PFA was blocked adding 50 mM NH₄Cl for 10 min at RT. NH₄Cl was removed by aspiration and the cells were washed with PBS. Cells were permeabilised by adding 0.5% saponin in PBS, 3x 5 min (prepared fresh). Primary antibody was added diluted in 0.5% saponin and incubated for 45min-1h. Cells were washed and the appropriate secondary antibody was added diluted in 0.5% saponin, and incubated for 45min-1h. Cells were washed 3x 5min with 0.5% saponin, 3x 5min with PBS and once with ddH₂O. Drops of water were dried off and the slides were mounted upside-down on a microscope glass slide adding a drop of mounting medium (used at RT). The mounted slides were left at RT in the dark 4h-overnight until the mounting medium has set and analyzed at the confocal microscope.

PBS:	150 mM NaCl	(AppliChem, Darmstadt)
	120 mM KCl	(Carl Roth GmbH, Karlsruhe)
	10 mM Na ₂ HPO ₄ /KH ₂ PO ₄	(Carl Roth GmbH, Karlsruhe)
	0.1 g Phenol red	(Carl Roth GmbH, Karlsruhe)
	pH 7,4	

Paraformaldahyde:

Saponin: (Sigma, St. Louis, USA)

NH₄Cl: (Merck, Darmstadt)

24 multi-well plate (Greiner Bioone)

12 mm round coverslips (Marienfeld)

Mounting medium: Fluorescent Mounting Medium (DAKO, Hamburg)

Mounting Glass Slide: (Roth GmbH Karlsruhe)

2.4.16 Proximity Ligation Assay

Cells have been plated, fixed and permeabilised as in the Immunofluorescence assay. The antibodies of interest have been diluted in 0.5% saponin at optimized concentration. Samples were washed x2 with saponin. The two *PLA probes*, *Plus and Minus* (mouse and rabbit respectively), were diluted 1:5 in 0.5% saponin and applied to samples; samples were incubated for 60min at 37°C and washed with BufferA 2 x 5 min.

Ligation solution was prepared as follows: 5X ligation Buffer + Ligase (40:1 dilution) + ddH₂O; ligase was added in the end just before the incubation. Samples were incubated with Ligase solution 30 min at RT and then washed x2 with BufferA.

Amplification solution was prepared as follows: 5X Amplification Buffer + Polymerase + ddH₂O; samples were incubated at 37°C for 100 min and washed 2 x 10min with Wash Buffer B and with 0.01x Wash Buffer B 2 min. samples were mounted upside-down on a microscope glass slide adding fluorescence mounting medium (DAKO) and sited overnight in the dark at RT.

PBS:	150 mM NaCl	(AppliChem, Darmstadt)
	120 mM KCl	(Carl Roth GmbH, Karlsruhe)
	10 mM Na ₂ HPO ₄ /KH ₂ PO ₄	(Carl Roth GmbH, Karlsruhe)
	0.1 g Phenol red	(Carl Roth GmbH, Karlsruhe)
	pH 7,4	
Saponin:		(Sigma, St. Louis, USA)
NH ₄ Cl:		(Merck, Darmstadt)
Buffer A:	10 mM Tris/HCl	(Carl Roth GmbH, Karlsruhe)
	500 mM NaCl	(AppliChem, Darmstadt)
	50 mM Tween 20	(AppliChem, Darmstadt)
Buffer B:	100 mM NaCl	(AppliChem, Darmstadt)
	200 mM Tris/HCl	(Carl Roth GmbH, Karlsruhe)
PLA Probes;	Plus and Minus	(Sigma, St. Louis, USA)
Ligation solution:	ligase, oligonucleotides	(Sigma, St. Louis, USA)
Amplification solution:	polymerase, fluorescent dNTPs	(Sigma, St. Louis, USA)

2.4.17 Primary antibody:

Antibody	Epitope	Species	Source	Dilution
AAK1	C-term aa 724-863	Rabbit	Santa Cruz	1:100 WB
ACK1/TNK2	peptide	Rabbit	Proteintech	1:200 WB
Arf1	peptide	Rabbit	Felix Wieland	1:2500 WB
Arf-GAP1	peptide	Rabbit	Felix Wieland	1:3000 WB
Arf-GAP1 brain	peptide	rabbit	Dan Cassel	1:3000 WB
Arf-GEF2	C-Term	Rabbit	Sigma	1:500 WB
α -adaptin	aa 38-255	Mouse	BD	1:2000 WB 1:100 IF
γ 1-adaptin	C-term/ear-domain	Mouse	BD	1:2000 WB 1:75 IF
μ 1A-adaptin	peptide	Rabbit	AG Schu	1:1000 WB
μ 2-adaptin	Thr-156	Rabbit	S. Höning	1:500 WB
μ 2-adaptin-P	Thr-156	Rabbit	S.Höning	1:500 WB
σ 1A-adaptin	aa SCHVLE	Rabbit	Davids	1:100 WB
σ 1A-adaptin-P	aa SCHLQE	Rabbit	Davids	1:100 WB
γ 2-adaptin	peptide	Mouse	AG Schu	1:500 WB
Amphiphysin	aa 258-414	Mouse	BD	1:5000 WB
Amphiphysin	aa 2-15	Rabbit	SY SY	1:1000 WB
Anti-PhosphoTyr	Tyr-phosphorylated	Mouse	Millipore	1:500 WB
AP180	258-414	Mouse	BD	1:5000 WB
Auxilin 1	peptide	Rabbit	Camilli	1:1000 WB
Auxilin 1	peptide	Rabbit	Protein Tech	1:600 WB
CaMKII- α	peptide	Mouse	Millipore	1:1000 WB
CaMKII- δ	peptide	Mouse	Santa Cruz	1:1000 WB
CHC	aa 4:171	Mouse	BD	1:2000 WB
CLC	aa 156-173	Mouse	SYSY	1:5000 WB
Calmodulin	aa 128-148	Mouse	Millipore	1:1000 WB
CSP a	aa 182-198	Rabbit	SYSY	1:1000 WB
Dynamin 1 (2,3)	aa 2-17	Rabbit	SYSY	1:1000 WB

EAA1	C-term domain	Goat	Santa Cruz	1:100 WB
EAAT1	aa 1-50	Rabbit	Santa Cruz	1:200 WB
Endophilin1	aa 256-276	Rabbit	SYSY	1:1000 WB
Epsin-2	peptide	Rabbit	Camilli	1:1000 WB
Epsin-1	peptide	Rabbit	Abcam	1:500 WB
GAK/Auxilin 2	aa 1-360	Rabbit	Santa Cruz	1:200 WB
GST	GST-tag	Goat	Santa Cruz	1:200 WB
6His	Poly-his-tag	Rabbit	Santa Cruz	1:200 WB
Hsc70	peptide	Rat	GeneTex	1:100 WB
Hsc70	aa 391-546	Mouse	SYSY	1:500 WB 5 μ g IP
Hsp90	peptide	Rabbit	Bioss	1:100 WB
NECAP1	peptide	Rabbit	Prteintech	1:200 WB
PACS1	aa 300-350	Rabbit	Proteintech	1:200 WB
Pacsin1-P	Ser-346-P	Rabbit	Millipore	1:2000 WB
PICALM-CALM	C-term	Goat	Santa Cruz	1:100 WB
PPP2R2C	peptide	Rabbit	Proteintech	1:200 WB
PPP2R2C	peptide	Rabbit	Proteintech	1:200 WB
Rab 5	PKNEPQNPGANSA	Rabbit	Abcam	1:2000 WB 1:80 IP
Rabex-5	peptide	Rabbit	Proteintech	1:200 WB 1:35 IP
Rab-GAP5	peptide	Rabbit	Proteintech	1:1000 WB 1:30 IP
Rabaptin 5 α	aa 812-862	Rabbit	NBP1	1:2000 WB
SMAP2	peptide	Rabbit	Novus	1:1000 WB
Stonin 2	peptide	Rabbit	Haucke	1:500 WB
Synaptotagmin1	aa 120-131	Rabbit	SYSY	1:1000 WB
Synaptotagmin2	aa 406-422	Rabbit	SYSY	1:500 WB
Synaptogyrin-1	aa 220-234	Rabbit	SYSY	1:1000 WB
VAMP2	aa 2-17	Mouse	SYSY	1:100 WB

2.4.18 Secondary antibody:

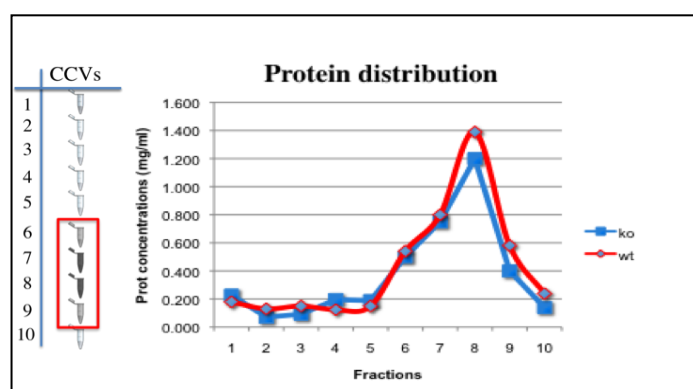
Antibody	Specification	Purchased from	Dilution
----------	---------------	----------------	----------

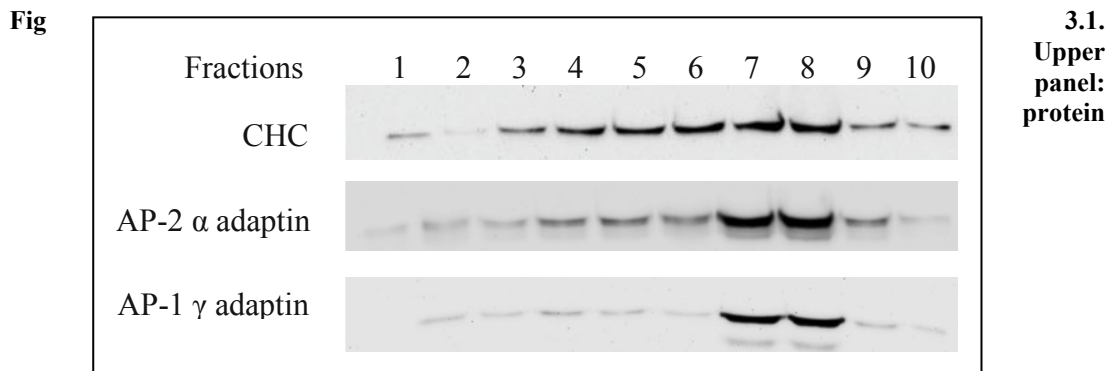
anti-rabbit Alexa Fluor [®] 488	Goat polyclonal	Invitrogen	1:400 IP
anti-mouse Alexa Fluor [®] 596	Goat polyclonal	Invitrogen	1:400 IP
anti-mouse Alexa Fluor [®] 633	Goat polyclonal	Invitrogen	1:400 IP
Anti-rabbit HRP conjugated	Goat polyclonal	Jackson ImmunoResarch	1:10000 WB
Anti-mouse HRP conjugated	Goat polyclonal	Jackson ImmunoResarch	1:10000 WB
Anti-rat HRP conjugated	Goat polyclonal	Jackson ImmunoResarch	1:10000 WB
Anti-goat HRP conjugated	Donkey polyclonal	Jackson ImmunoResarch	1:10000 WB

3. Results

3.1.1 The synaptic AP-1 and AP-2 Clathrin-Coated-Vesicles (CCV)

AP-1/ σ 1B deficient mice have impaired spatial memory, and σ 1B-deficient humans have a severe mental retardation. The phenotype reflects the alterations in the synaptic vesicle cycle. AP-1/ σ 1B $-/-$ synapses have fewer synaptic vesicles under resting conditions and this SV pool is further reduced after stimulation of SV exocytosis and recycling. This reduction in the SV is accompanied with an accumulation of endosomes and of clathrin-coated-vesicles (CCV) (Glyvuk et al. 2010). In order to define these σ 1B $-/-$ “bulk” endosomes and to classify them as well as to determine their functions in SV recycling, we had developed, in a previous study of our group, a protocol to separate them from the majority of the neuronal endosomes. The σ 1B $-/-$ ‘bulk’ endosomes proved to be classic early endosomes with an increase in the phospholipid phosphatidylinositol 3-phosphate (PI-3-P) and a second population as late endosomes (Kratzke et al. 2014). AP1/ σ 1B $-/-$ synapses showed also a totally unexpected accumulation of CCV. This was unexpected firstly, because there is one AP-1 complex missing forming CCV and secondly, SV protein recycling is reduced and thus SV protein endocytosis via CME should be decreased as well. Therefore, the most likely explanation for the increase in CCV was that they are functionally impaired AP-1/ σ 1A CCV due to the loss of the AP-1/ σ 1B complex. In order to clarify their origin and whether they are AP-1, AP-2 or entirely aberrant CCV and to identify the molecular mechanisms, leading to their accumulation, these synaptic CCV were isolated from wt and mutant mice synapses, separated on sucrose-density gradients, as described in 2.4.7 Material and Methods (McPherson et al 2010, Borner et al 2010, *modified*) and the protein compositions of CCV isolated from wt and ‘ko’ synapses were compared.





distribution in the gradient fractions. Most proteins are concentrated in fractions 6 to 9 in wt and ‘ko’ extracts. Lower panel: representative Western-Blots of CCV proteins from the sucrose-gradient centrifugation fractions.

First of all, to verify normal CCV formation, the CCV distribution over all the fractions of the sucrose-density gradient centrifugation was analyzed by semi-quantitative Western-Blots. The distribution of AP-1 CCV was detected by the distribution of its γ 1-adaptin and of AP-2 by the α -adaptin subunit. Clathrin-heavy-chain (CHC) distribution served as the marker for clathrin-cages. The distribution of AP-1/ γ 1, AP-2/ α and CHC revealed the presence of the CCV mainly within fractions 6 to 9, as shown in Fig 3.1 (lower panel). CHC has a broader distribution than both adaptins, because CHC tends to aggregate and to form also empty clathrin cages without a vesicle membrane and adaptor-protein complexes. In cells, these cages are rapidly disassembled by Hsc70 and its co-chaperones auxilin-1 and -2. There were no differences in the CCV distribution on the gradients between CCV isolated from wt and ‘ko’ synapses. Although the gradient does not have a high resolution, this indicates that σ 1B-deficiency does not induce the formation of aberrant CCV.

3.1.2 iTRAQTM analyses

In order to compare the protein content of CCV fractions isolated from wt and ‘ko’

mice, they were analyzed by isobaric iTRAQ mass spectrometry first. The iTRAQ analyses identified 668 proteins from the CCV. 470 of them were valid for quantitative analyses. As summarized in Tab. 3.1, 32% of the proteins are SVs proteins, including vesicle cargo proteins and coat-proteins like the subunits of the adaptor-protein complexes. 26% are cargo proteins like channel and receptors, eg the glutamate receptor NMDA or the voltage-gated potassium channel. Reorganization of the cytoskeleton is also a key factor in the CCV cycle, in fact 23% of the identified proteins are cytoskeleton factors like spectrin (both subunits), myosin, or the nerve terminal-specific protein Bassoon.

PScape approved	SV, Adaptin	Receptors, Channels	Cytoskeleton	Kinases, P'ases	Chaperones (Hsp; 14-3-3 etc)	Protein turnover
470	149	120	107	37	29	28
	32%	26%	23%	8%	6%	5%

Table 3.1 proteins identified by iTRAQ analyses: on average 10% in each group are changed in the “ko” CCV

The remaining 20% consists of regulatory proteins like kinases and phosphatases (8%), 14-3-3 proteins and Hsp chaperone proteins (6%), and finally turnover protein factors (5%). This indicates that the pool of CCV isolated from ‘ko’ mice is mainly formed at the plasma membrane and next to active zones, retrieving SV proteins and membrane like the majority of the CCV from wt synapses.

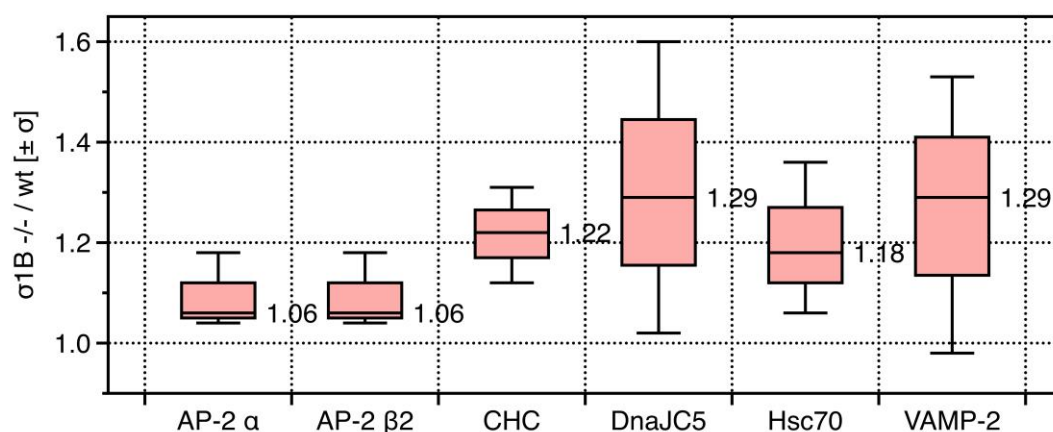


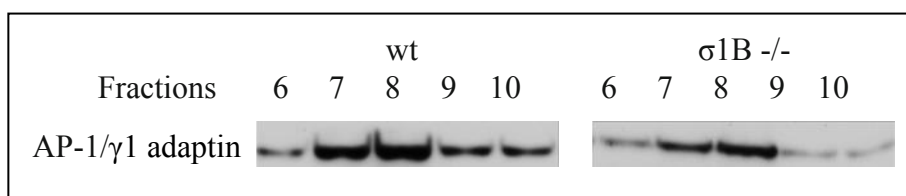
Fig. 3.2. Box plots of ko/wt ratio for AP-2 subunits α and $\beta 2$, clathrin (CHC), chaperon proteins DnaJC5, Hsc70 and cargo protein VAMP-2. Statistical calculation were performed on results coming from iTRAQ quantitative spectrometry mass analyses

The iTRAQ analyses revealed significant increases of several proteins in “ko” CCV. The data of some of them are presented in the Fig. 3.2. Two subunits of the AP-2

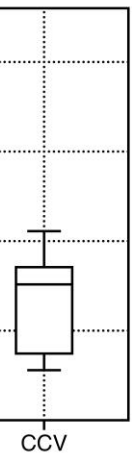
complex are increased in “ko” CCV and they show exactly the same increase, thus the ratio is unaltered confirming the validity of the analyses. Clathrin-Heavy-Chain (CHC) is also increased as are the uncoating proteins DnaJC5 (CSP) and Hsc70. The data did not indicate clear and significant changes in AP-1 proteins. These data strongly indicate that the AP-1/ σ 1B deficiency significantly leads alterations in the synaptic CCV pool and an increase in the amount of endocytotic AP-2 CCV. These proteins listed here, were the first ones whose content in CCV fractions were analysed by semi-quantitative Western-blot analyses (shown in the following paragraphs). All these changes indicated by the iTRAQ analysis of CCV isolated from just one wt and one ‘ko’ mouse brain had to be verified. Thus we can assume that the changes in the CCV pool composition as indicated by iTRAQ are correct. Firstly, we determined changes in the content of AP-1 and AP-2 in CCV fractions isolated from multiple wt and ‘ko’ mice and the respective co-adaptor and accessory proteins by semi-quantitative Western-blot to characterize changes in the CCV in ‘ko’ mice in greater detail.

3.1.3 AP-1 CCV levels and AP-1 distribution in σ 1B $-/-$ synapses

First, I determined the total level of AP-1/ γ 1 CCV in wt and σ 1B $-/-$ synapses. This was done by semi-quantitative western-blot and iTRAQ quantitative mass spectrometry (for details see Material and methods 2.4.13). In σ 1B $-/-$ synapses the AP-1 CCV showed a significant reduction by 20% compared to the wt. Western-blot of sucrose-density gradient fractions and their quantifications are shown in figure 3.2. This reduction was expected due to the absence of AP-1/ σ 1B complexes, but it also indicates that the deficiency in this AP-1 complex, does not induce an accumulation of functionally impaired AP-1 CCV formed by the ubiquitous AP-1 complex. Several attempts in the past to generate σ 1-isoform specific antibodies to quantify their relative expression levels failed and thus these data are used to estimate the σ 1A/ σ 1B ratio in synapses. The reduction of AP-1 CCV by 20 % indicates a 4:1 ratio of AP-1/ σ 1A to AP-1/ σ 1B complexes. Although CCV and synapses have a clear reduction of AP-1 complexes, AP-1 association with the accumulating endosomes is increased, indicating that AP-1/ σ 1A is enriched on these



membranes (endosomal characterization performed by Dr. M Kratzke(, (Kratzke et al. 2014))).



7 7 7 4 8

Fig. 3.3. Upper panel: representative semi-quantitative Western-blot of AP-1/ γ 1 adaptin. Lower panel: statistical analyses: boxplots of ko/wt ratio for AP-1/ γ 1 adaptin expression (cortex), distribution (Synapse) and association with early (ld low-density) and late (hd high-density) endosomes. Wt levels were set as 100%, numbers above the boxes indicate the numbers of quantifications performed with wt/ko animal pairs.

This accumulation on endosomes is in line with microscopic data, which showed enhanced co-localization of AP-1 with the SV protein synaptotagmin-1 upon stimulation of SV exocytosis and recycling (Glyvuk et al. 2010). AP-1 binding is increased despite the fact that the amount of endosomal PI-4-P, required for high affinity AP-1 membrane binding, is decreased. On the other hand, the amount of ArfGAP1, which induces GTP hydrolysis of Arf1 and thus weakens AP-1 membrane binding, is reduced. Accumulating cargo proteins could contribute to the Arf1-dependent stable AP-1 membrane binding. Thus the molecular mechanisms leading to the endosomal accumulation of AP-1/ σ 1A is not known and has to be analyzed in greater detail. As we are detecting signals of purified CCV we can not use canonical quantitative controls in the Western-analyses, however in order to have a statistical validity, at least 4 different proteins were detected from the same blot.

3.1.4 AP-2 CCV levels and AP-2 distribution in σ 1B^{-/-} synapses

The amount of AP-2 CCV is with 200 % strongly increased in “ko” synapses (fig

3.4). AP-2 concentration is also increased in these synapses.

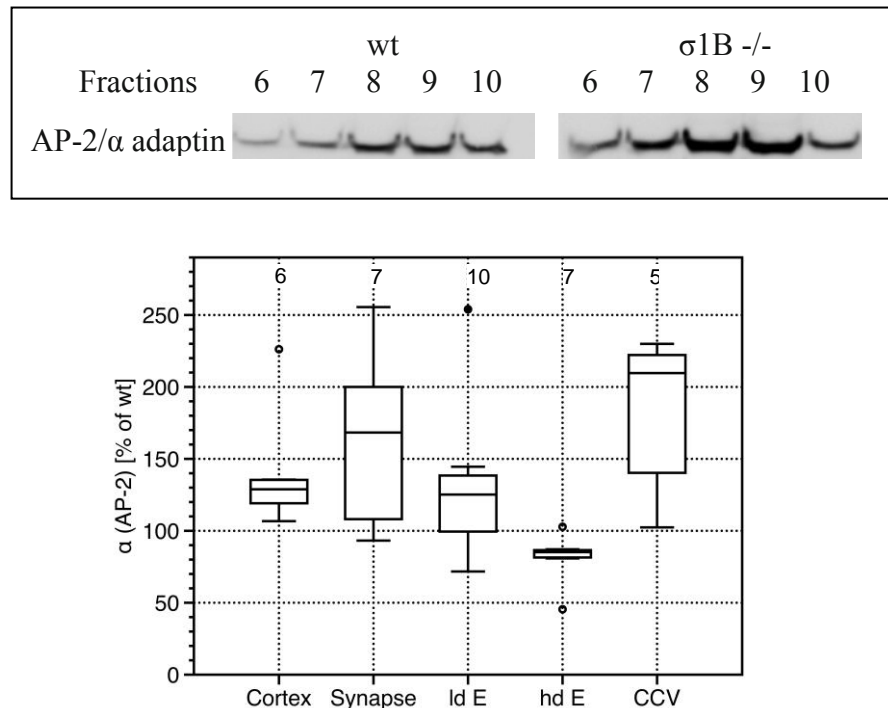


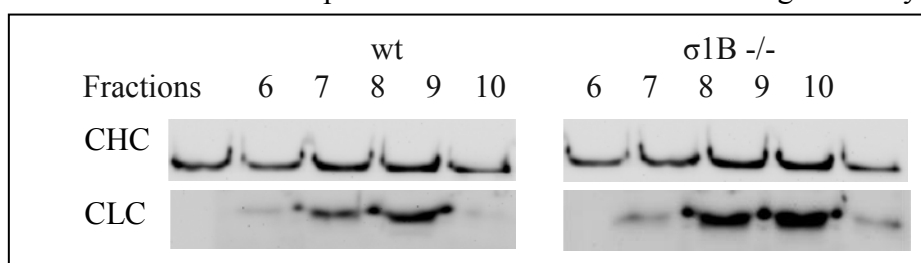
Fig. 3.4. Upper panel: representative semi-quantitative Western-blot of AP-2/ α adaptin. Lower panel: statistical analyses: box-plots of ko/wt ratio for AP-2/ α adaptin expression (cortex), distribution (Synapse) and association with early (ld low-density) and late (hd high-density) endosomes. Wt levels were set as 100%, numbers above the boxes indicate the numbers of quantifications performed with wt/ko animal pairs.

This increase is very surprising because in the “ko” synapse the SV recycling is reduced, and thus, also the AP-2 CCV mediating SV protein endocytosis should be reduced as well. However the double amount in the “ko” synapse could be due to an enhanced Clathrin mediated endocytosis (CME) independent of SV recycling, or to an altered regulation of AP-2 CCV uncoating, these two possibility are not mutually exclusive.

3.1.5 AP-2 CCV coat-protein composition and CCV stability

3.1.5.1 The clathrin cage

We determined an accumulation of endocytotic AP-2 CCV and thus the next question to answer is the reason for their accumulation. In order to test for the model of delayed AP-2 CCV un-coating as the reason for this accumulation, first I characterized their content in proteins known to affect clathrin cage stability.



First, I

determined the ratio of the clathrin subunits, the clathrin-light-chain (CLC) and clathrin-heavy-chain (CHC).

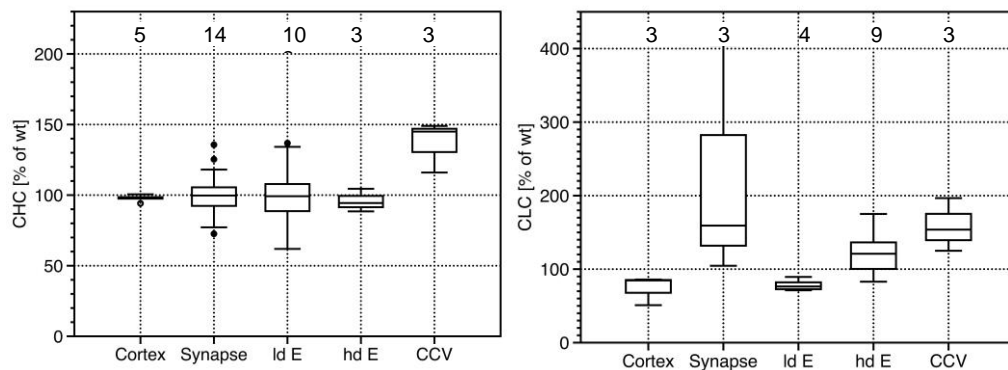


Fig. 3.5. Upper panel: Representative semi-quantitative Western blot of CHC and CLC. Lower panel: Statistical analyses; box plot of ko/wt ratio for CHC and CLC in the different “compartments”: Cortex, Synapses, Late endosome (Gravotta et al.), Early endosome (hdE)

CLC regulates several steps in CCV formation as well as the stabilization of the clathrin basket. Furthermore the CHC:CLC ratio is 1:1 only in the brain, whereas CLC expression is lower in other tissues, indicating a crucial role especially in the cycle of brain CCVAs shown in the Fig. 3.5 (confirmed by iTRAQ analyses), the amount of CHC in “ko” extracts is increased by 50%. The CLC is increased as well by 60%, meaning that their ratio is not changed, and their increase is in line with the increase of the CCV in the “ko” synapse. Therefore, from this analysis, it seems that the relative clathrin cage composition is not altered and thus does not account for the CCV accumulation.

3.1.5.2 Association of clathrin cage disassembly proteins

Another reason for a delayed AP-2 CCV disassembly in “ko” synapses could be a reduction in proteins of the cage disassembly machinery. Three proteins have been demonstrated to take part in the uncoating reaction. Hsc70 and the two co-chaperones auxilin-1 and auxilin-2 also known as GAK (G-protein receptor associated kinase), its kinase activity appears to be dispensable for clathrin cage

disassembly. First I compared the levels of Hsc70 in the cortex and in the synaptosome between wt and ‘ko’ brains. As shown in the Fig 3.6 (a), the Hsc70 levels are not changed in the cortex and in the synaptosome as well, indicating that expression and distribution of the protein are not altered in “ko” synapse. However, there is a strong increase in the “ko” CCV pool, indicating that the targeting of the protein to the CCV pool is not impaired and is even increased in line with the increase in CCV.

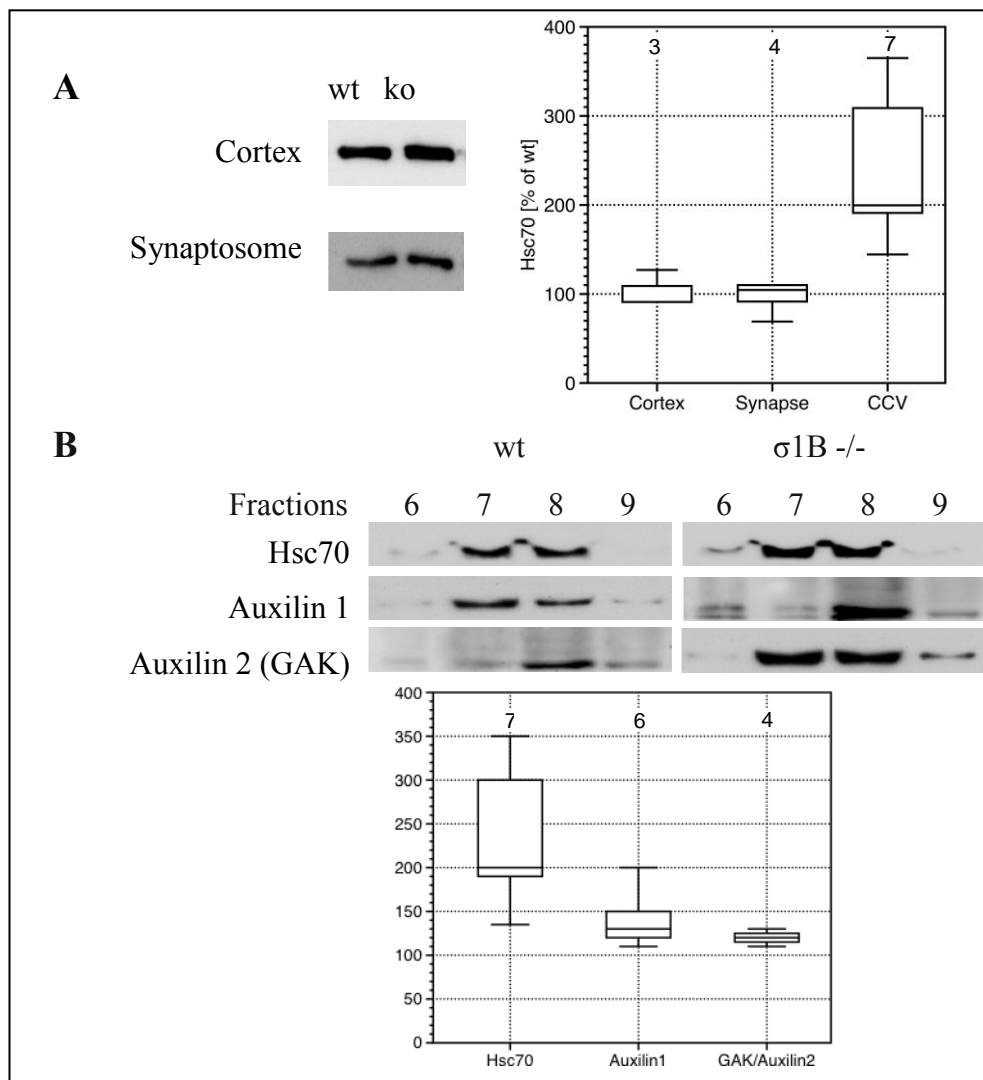


Fig 3.6. (A) left: representative Semi-quantitative Western-blot of Hsc70 in wt and “ko” cortex, synaptosome; right: box plot of ko/wt ratio for Hsc70 expression (cortex), distribution (synaptosome) and association with CCV. (B) Upper panel: representative semi-quantitative Western-blot of Hsc70, Auxilin1 Auxilin2 (GAK). Lower panel: “ko”/wt ratio in CCV for Hsc70, Auxilin, GAK1.

The increased targeting of Hsc70 in the “ko” CCV pool could be caused by a hypothetical altered coat composition of the AP-2 CCV that requests higher level of Hsc70 for the uncoating of the clathrin cage. The level of Hsc70 is doubled in the “ko” CCV and the co-chaperons auxilin1 and auxilin2 (GAK1) are increased as well, indicating that the level of the uncoating proteins are not limiting the reaction. Thus, if delayed uncoating contributes to the accumulation of AP-2 CCV, the activities of the uncoating proteins could be inhibited, eg by modifications like phosphorylation.

3.1.6 AP-2 CCV coadaptor proteint composition

The CCV coat is mainly formed by the heterotetrameric AP-complexes, but it also contains numerous monomeric co-adaptor proteins, which recognize cargo proteins not efficiently bound by the AP-complexes. In addition, the coat contains so called ‘auxillary’ or ‘accessory’ proteins, which play a role in the regulation of transport vesicle formation. Many of these proteins are bound by the so called ‘ear’-domains of γ 1- (AP-1) and α -adaptins (AP-2), which have different structures and thus AP-1 and AP-2 CCV have specific sets of coat proteins. Next Therefore, I investigated the CCV coat composition because also an altered composition of the coat could be responsible for an eventual slower CCV uncoating to characterize the accumulated AP-2 CCV pool in greater detail. I tested for AP180, epsin1/2, NECAP1 and stonin 2 expression and distribution, because they are the major co-adaptors of AP-2. In addition, AP180 is a pre-synapse-specific AP-2 co-adaptor, that binds CHC with an even higher affinity than AP-2 and also binds PIP₂, like AP-2. It contributes to VAMP/synaptobrevin-2 sorting and possibly takes part in the regulation of SNARE protein complex assembly. Due to the near doubling of AP-2 CCV, the AP180 content in the “ko” CCV fraction should be increased as well and an increase could even contribute to increased clathrin cage stability. Surprisingly, I found AP180 to be reduced not only in CCV, but also its expression level (cortex) and its amount in

synapses (fig 3.7). I and its reduction could make the clathrin cage even less stable. Its ubiquitously expressed isoform PICALM (also known as CALM), which is 10 times less abundant in the brain than AP180, is not increased in the CCV and thus does not compensate for the reduced amount in AP180. Stonin 2 is also a cargo co-adaptor, which has a μ -adaptin homology domain, which binds synaptotagmin-1 mediating its sorting. In a stonin 2 “ko” mouse, AP-1 CCV and SV numbers are increased in pre-synapses, presumably due to enhanced CCV formation from ‘bulk’ endosomes (Kononenko et al., 2013). Thus, the decrease in AP-1 CCV in the ‘ko’ synapses should lead to an increase in stonin 2, if the same molecular mechanisms are altered. However, also stonin 2 is decreased in cortices, in synaptosomes and in CCV, just like AP180 (Fig3.5).

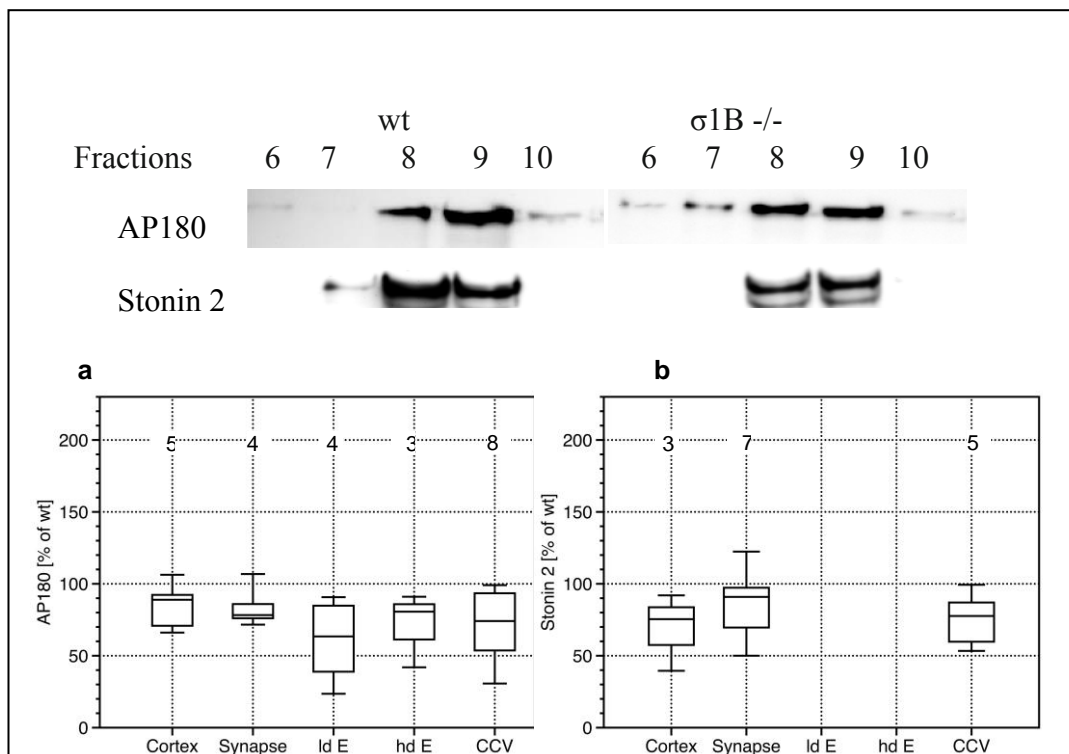


Fig. 3.7. Upper panel: representative western blots of wt and “ko” fractions containing CCV. Lower panel: ko/wt ratio of cargo-specific co-adaptors. a) AP180 expression and distribution in synapse, endosomes and CCV. b) Stonin2 expression (cortex) and distribution in synapse and CCV.

The co-adaptors epsin1/2, which fulfill redundant functions in CCV protein sorting,

are, unlike AP180 and stonin 2, not reduced in ‘ko’ cortices and are even enriched in synaptosomes. However, their association with CCVs from ‘ko’ synapses is nevertheless reduced by 45% (Fig. 3.8). Currently, we can not explain this distribution, but it indicates differences in the recycling of epsin1/2 between CCV and the cytoplasmic pool (notice that their association with endosomes is not increased as well). Thus its distribution differs from that of the AP-1/ σ 1A complexes in the ‘ko’ synapses.

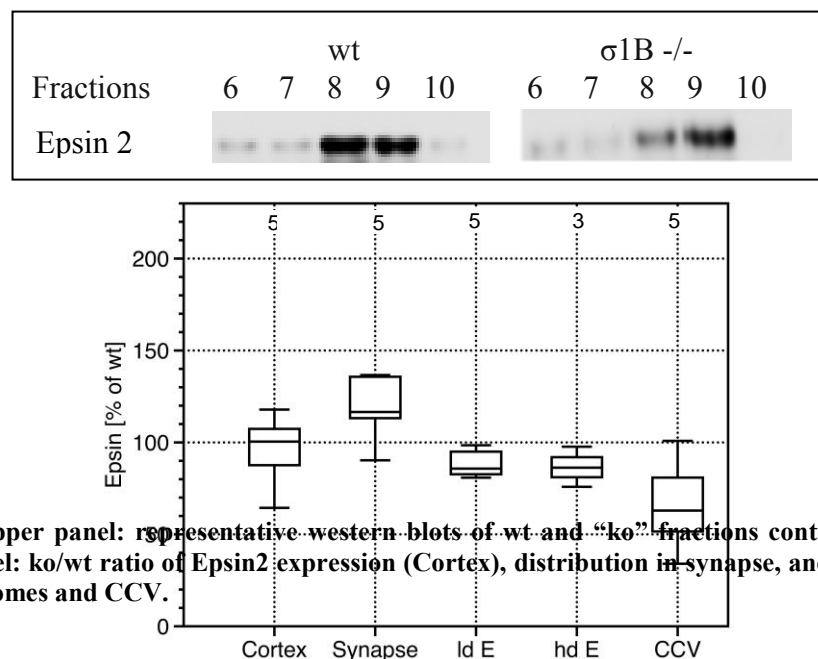


Fig. 3.8. Upper panel: representative western blots of wt and “ko” fractions containing CCV. Lower panel: ko/wt ratio of Epsin2 expression (Cortex), distribution in synapse, and association with endosomes and CCV.

The only AP-2 specific co-factor that follows the AP-2 “behavior” is NECAP1 (Fig. 3.9). NECAP1, binding the α -ear of AP-2 competes with clathrin for access to the AP-2 β 2-linker, in this way, NECAP1 mediates the coordination of accessory protein recruitment and clathrin polymerization at sites of vesicle formation, representing a organizational control vesicle size, number and cargo recruitment. Thus NECAP1 increase indicates proper quality control of the AP-2 CCV.

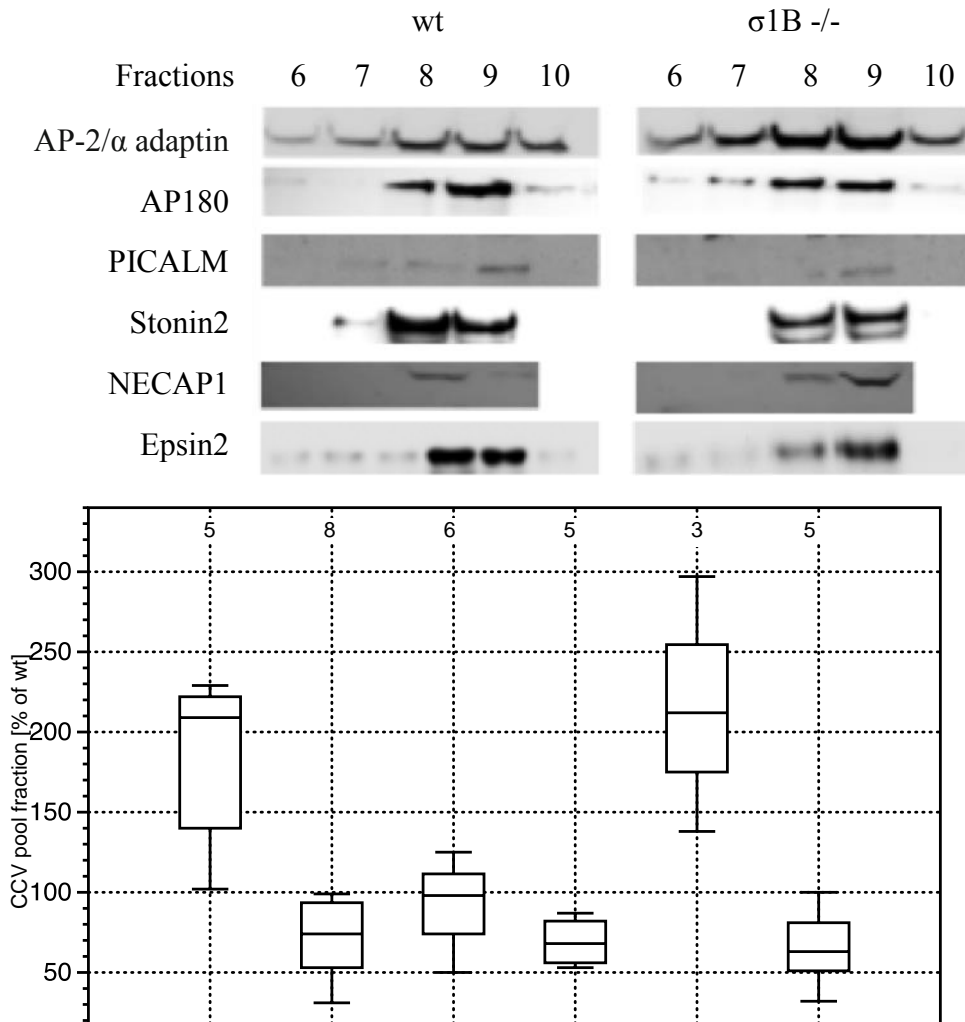


Fig. 3.9 Upper panel: representative Western blots: stonin2, NECAP1 and epsin2 are represented only from 6th to 10th fractions as the signal is totally blank in the 10th fraction. The distribution of CCV on the sucrose-density gradient is variable ± 1 fraction from experiment to experiment. Lower panel: “o”/wt ratio comparison, between AP2/a adaptin and its specific co-adaptors, AP-2/a adaptin is reported again for a clear comparison with the other proteins. NECAP1 is the only co-adaptor that follows the AP-2 “behavior”

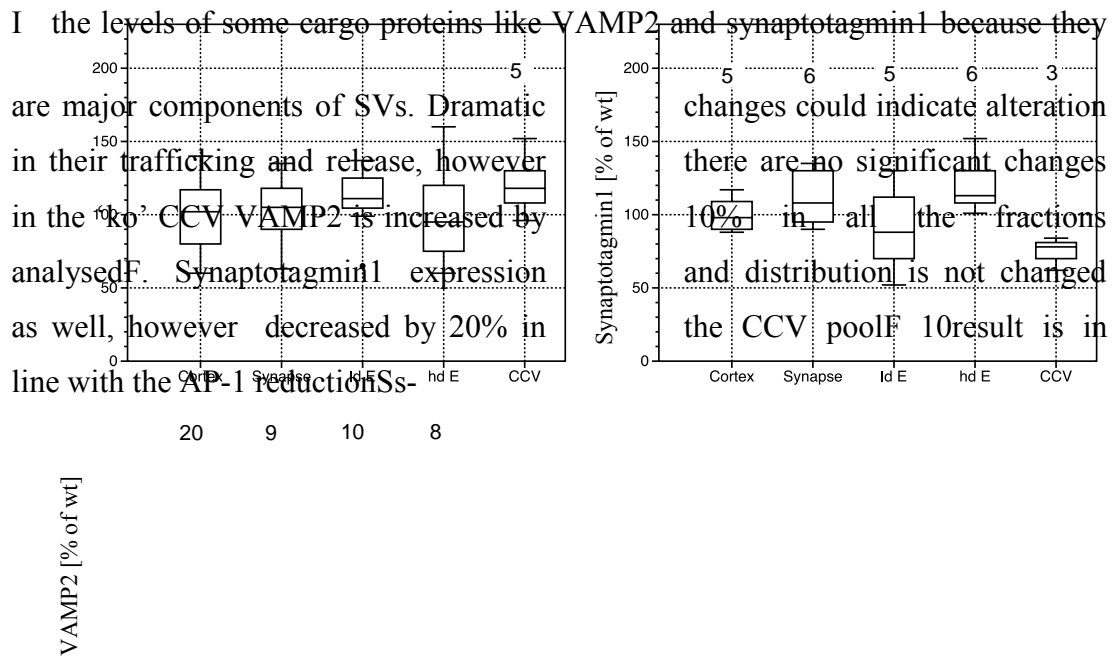


Fig. 3.10. Left panel, “ko”/wt ratio of cargo proteins; VAMP2 (left panel) and synaptotagmin-1 (right panel)

Synaptotagmin1 might thus be stranded in the plasma membrane or other synaptic membrane compartments, which we will have to identify. It is in fact slightly increased in the high-density endosome fraction, which is enriched in late endosomes. There it might be bound by AP-1 and colocalize with AP-1 as already discussed. AP-1 binding could even prevent its sorting into the endolysosomal pathway and its degradation

3.1.7 Dynamin recruitment to CCV

Dynamin is a large GTPase and mechanoenzyme essential for plasma membrane endocytosis. It mediates the narrowing of the budding vesicle neck through a GTP hydrolysis induced conformational change. It is recruited late in the CCV budding reaction to the neck. This binding is facilitated by BAR domain proteins like Endophilin and Amphiphysin, but also remains associated with the CCV. I investigated the levels of all these proteins to see if there are alterations, in the vesicle scission process, in “ko” CCV.

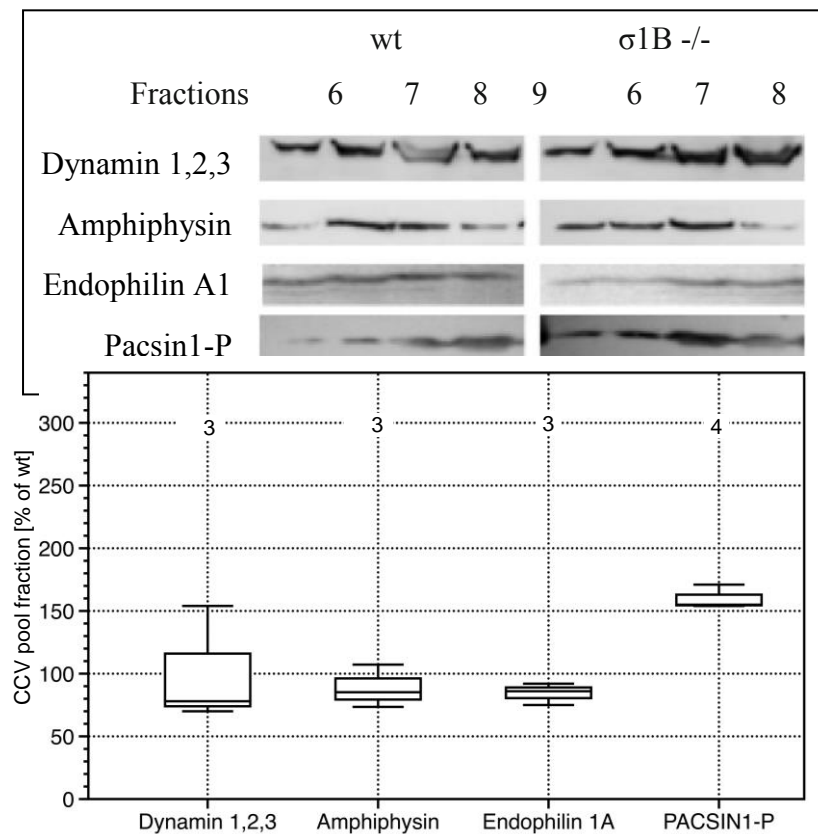


Fig. 3.11. Upper panel: representative Western blots of CCV fractions. Lower panel: “Ko”/wt ratio of vesicle scission effector proteins in CCV

The amount of dynamin was not changed in the “ko” CCV and also the amounts of amphiphysin and endophilin were not altered, suggesting that the neck scission pathway is not modified for AP-2 CCV in the “ko” synapse. Endophilin is also important for the CCV un-coating. endophilin deficient cells accumulate CCV, because endophilin binds synaptojanin, which turns PI-4,5-P₂ into PI-4-P. AP-2 requires PIP₂ for high affinity membrane binding and thus synaptojanin is required for fast and efficient AP-2 CCV uncoating. Thus another CCV uncoating factor is present in normal amounts. However, phospho-PACSIN1/Syndapin was increased by 50% in “ko” CCV. This protein binds simultaneously synaptojanin, and dynamin and at the same time the Wiscott-Aldrich syndrome protein (WASP), which promotes actin-depolymerization. Actin reorganization is involved in CCV formation and thus the phospho-PACSIN1 increase supports the model of enhanced and faster CME (Qualmann et al. 1999).

3.1.8 Stability of AP-2 CCV and μ 2-adaptin phosphorylation

Phosphorylation of the AP-2 complex on its μ 2-adaptin on Thr156 occurs in the linker domain of its N-terminal β 2-adaptin-anchor domain and the C-terminal cargo binding domain. This phosphorylation stabilizes the open, cargo binding conformation of the AP-2 complex. The induced conformational change of μ 2 brings the cargo binding motif and the second PIP₂ membrane-binding motif (the other one is in α -adaptin) close to the membrane and thus increases the stability of AP-2 membrane binding by two binding modes. Thus one reason for the AP-2 CCV accumulation could be a hyper-phosphorylation of μ 2 mediated by the AAK1 kinase. I determined the level of the phosphorylated μ 2 by semi-quantitative western-blot (Fig. 3.12) using a phospho-site specific antibody that specifically recognizes the phosphorylation in Thr165 (Miller et al.). However, the increase of AP-2 CCV is higher than the increase in phosphorylated μ 2, indicating that the accumulation of AP-2 CCV is not caused by a hyper-phosphorylation leading an increased stability of the AP-2 coat. Also the binding of the modifying kinase AAK1 to the CCV is not increased, but even slightly decreased.

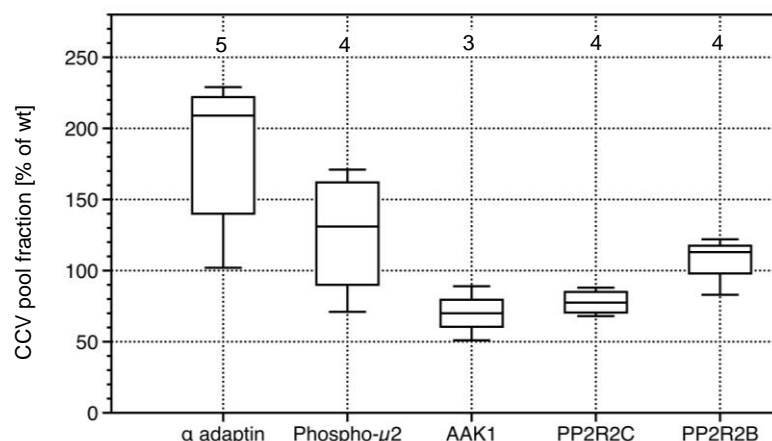
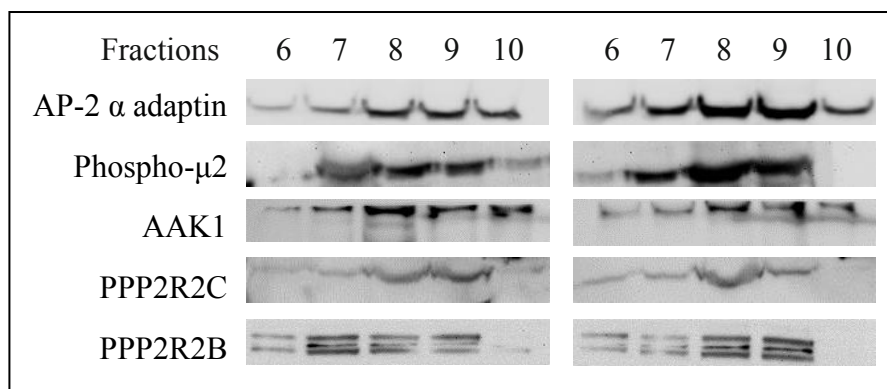


Fig. 3.12. Upper panel, representative semi-quantitative Western-blot of fractions containing CCV. Lower panel, “Ko”/wt ratio of phosphoporylated μ 2 adaptin and its specific kinase AAK1

and phosphatases subunits of PP2A, PPP2R2C and PPP2R2B

Although the amount of the catalytic and the regulatory subunit of the de-phosphorylating phosphatase PP2A, PPP2R2C and PPP2R2B, were not altered, excluding a reduced de-phosphorylation rate of $\mu 2$.

3.1.9 Arf-GAP1 distribution in the synapse and synaptic CCV and redistribution also in the other pools (Both isoforms)

Arf-GAP1 is the GTPase-activating protein for the small Arf1 G-protein, which is required for high affinity membrane binding of AP-1. Arf-GAP1 activity induces membrane dissociation of AP-1. Arf-GAP1 is however also found in AP-2 CCV although its GAP-activity is not required for the AP-2 CCV cycle. Overexpression of Arf-GAP1 even induces AP-2 CME, but the molecular mechanism for this effect is not known (Bai et al. Nature Cell Biology 2011). They proposed that it is a co-adaptor for the transferrin-receptor in CME. Arf-GAP1 consists of the N-terminal GAP-domain and a C-terminal tail with two lipid-sensor motifs (ALPS1 and 2), which adopt a helical conformation upon membrane lipid contact. In brain, a splice-variant is expressed with a deletion-insertion modification changing the ALPS2 motif. Functional consequences of this modification are not known. Arf-GAP1 has been shown to bind via its GAP-domain the ‘ear’-domains of AP-1 $\gamma 1$ and of AP-2 α and additional motifs have been identified in the tail sequence, but whether these interactions have an in-vivo function is not known. The first important results came from the distribution analyses of the ubiquitous Arf-GAP1 (Fig. 3.13). The expression (cortex) of either isoform is not drastically changed, however their concentration in the synapse is increased by 30% in “ko” mice. On the other side, their association with early and late endosomes is dramatically reduced. As explained before, the “ko” synapse showed the presence of enlarged endosomes, and as the ALPS domains of Arf-GAP1 are curvature sensing, these endosomal rearrangements in shape and size could affect their binding to the endosomal membrane.

Both, the Arf-GAP1 increase in the “ko” synapse and the reduced association with the endosomes would explain the strong and surprising increase of Arf-GAP1 in the “ko” CCV or better their increased formation, if membrane pool dynamics alone determine their functions.

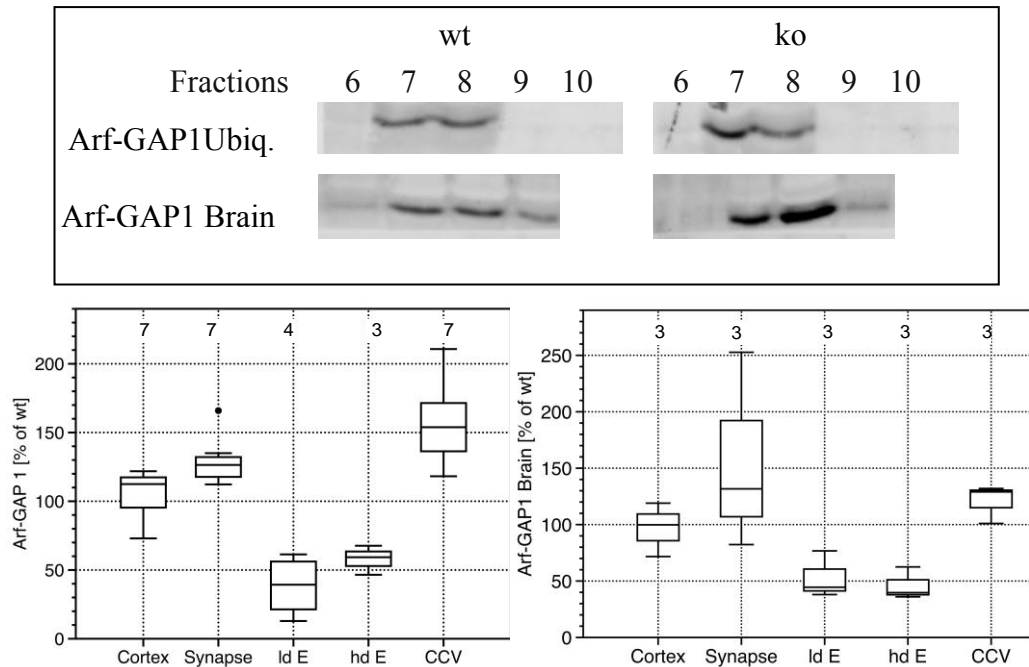


Fig. 3.13. Upper panel, representative semi-quantitative Western-blot of fractions containing CCV. Lower panel, “Ko”/wt ratio of Arf-GAP1 ubiquitous isoform(left) and brain isoform (Poupon et al.), expression (cortex), distribution (synapse), endosomes association (Id E, hd E), CCV association.

The only significant difference found between the two Arf-GAP1 isoforms is a lower increase of the brain isoform in the CCV pool from ‘ko’ synapses. The induction of CME should be mediated by functions of the C-terminal domain, because the GAP-activity is dispensable for this function. Thus the altered tail sequence of the brain isoform could be responsible for this difference.

These data all-together make Arf-GAP1 one of the potential candidates as molecular mechanism linking the AP-1/ σ 1B-dependent SV exocytotic route and the AP-2-dependent endocytotic pathway.

3.2 AP-2 CME up-regulation and CCV stability

These results indicated that CME is indeed up-regulated, but this can not account for the doubling in synaptic AP-2 CCV. SV protein CME is by far the most active synaptic pathway and it is difficult to imagine that CME of non-SV proteins could be up-regulated to a level well above that of SV protein CME. Thus both, up-regulation of CME and also a delayed CCV un-coating should contribute to the increase in synaptic AP-2 CCV. We reasoned that an increased stability of CCV might be associated with alterations in Hsc70 binding to these CCV, because its uncoating activity appears to be blocked. Stable CCV might bind less Hsc70, but might also bind it more stable, because it does not disassemble the clathrin-cage by binding-dissociation cycles. In addition, it could be modified by phosphorylation impairing ATP-binding or hydrolysis. We thus tested, whether anti-Hsc70 immunoprecipitation of the density-gradient purified CCV fractions is able to isolate a CCV subfraction with specific properties and whether such a CCV pool from $\sigma 1B$ -/- synapses differs from the respective CCV pool from wt synapses.

3.2.1 Hsc70 and co-chaperonines distributions in the CCV pools

The anti-Hsc70 antibody was indeed able to isolate CCV from the pooled sucrose-density fractions derived from 'ko' as well as from wt synapses. First, I looked for differences in the levels of the uncoating machinery proteins. Hsc70 is doubled in the total "ko" CCV pool relative to the total CCV pool from wt synapses (par. 3.1.4.2), but its amount does not differ between the Hsc70-isolated CCV pools of 'ko' and wt synapses (Fig. 3.14). Comparison of CHC input and isolate indicates that the anti-Hsc70 CCV pool represents 20% of the total pool. However, the immunoprecipitation may not isolate 100% of this sub-fraction and thus this number can only be a rough estimate. Interestingly, the amounts of the two co-chaperons auxilin1 and auxilin 2 (GAK1), which are also increased in the total CCV pool from 'ko' synapses, are even further increased in this pool. This questioned the theory that this is in fact a more stable CCV pool. The SV and CCV chaperone CSP α , which is

also increased in the total ‘ko’ CCV pool is only slightly further increased in the “ko” Hsc70-pooled CCV.

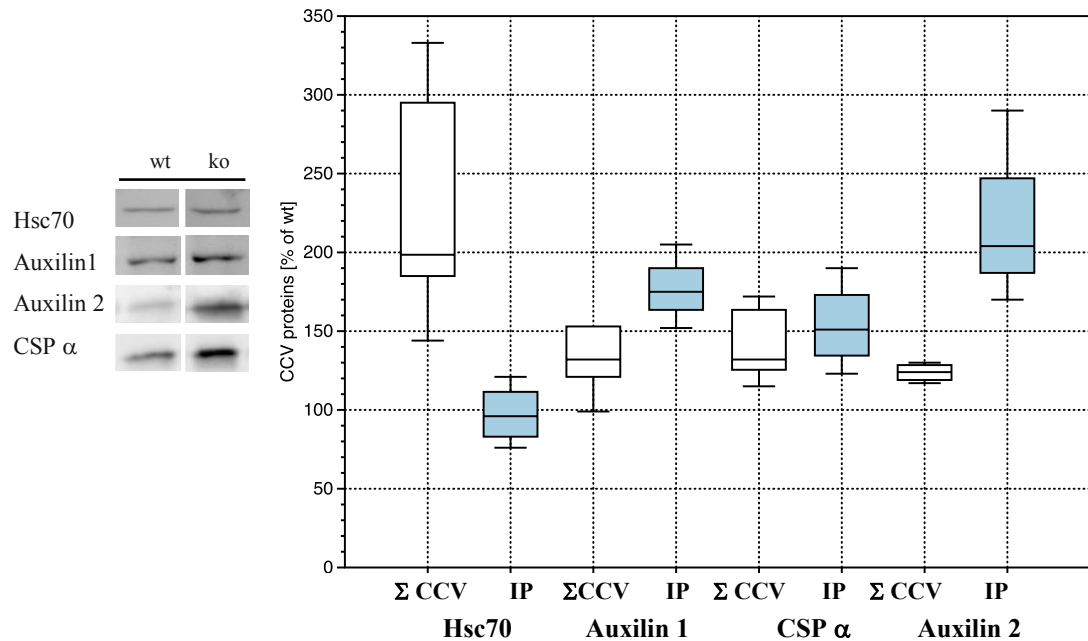


Fig. 3.14. Left, representative semi-quantitative Western-blot of wt and “ko” Hsc70-pooled CCV. Right, comparison of “ko”/wt ratios between total-CCV pool (white) and Hsc70-IP CCV (blue). All the experiments, for a statistical validity, have been performed at least 3 times, the representative western-blot of different proteins are from one membrane

These data strongly indicated that “ko” synapse differ from wt synapses in their two AP-2 CCV populations. The fact that the Hsc70 ‘ko’/wt ratios differ between the total CCV pool and the anti-Hsc70 enriched CCV pool supports the model of a “stable” AP-2 CCV population. However, these data do not clearly show, whether this pool is the less or the more stable CCV pool. The same amount in Hsc70 indicates that it might be the ‘normal’ CCV pool, which is not changed in the ‘ko’ synapse, but the alterations in the co-chaperones indicate the opposite. Hsc70 is hidden or however not properly bound and activated, in fact the ratio should not change. This could be the principle reason of a delayed uncoating of the AP-2 CCV in the “ko” synapse

3.2.2 Clathrin cage proteins in the CCV pools

As already discussed, the amount of CLC bound to CHC influences the stability of the clathrin cage and therefore I determined whether CHC/CLC ratios differ between the total and the isolated CCV pools (par 3.1.4.1). As shown in the Fig 3.15, the CHC is increased in the Hsc70-IP CCV by 35% compared to wt, in line with the increase observed in the total CCV pool (by 50%). CLC increase, instead, is much stronger in the Hsc70-IP CCV pool (by 230%), compared to the increase observed in the total synaptic CCV total pool (by 50 %) (Fig. 3.15).

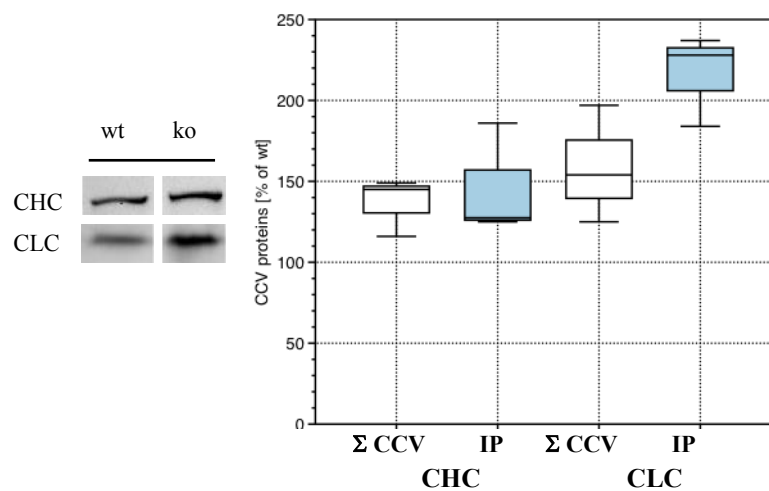


Fig. 3.15. Left, representative semi-quantitative Western-blot of wt and “ko” Hsc70-pooled CCV. Right, comparison of “ko”/wt ratios between total-CCV pool (white) and Hsc70-IP CCV (blue).

This dramatic change in the CHC:CLC ratio strongly indicates that the anti-Hsc70 CCV pool indeed is a “stable” AP-2 CCV pool. Hsc70 binding to these vesicles obviously makes it more accessible to the antibody and in addition it might be bound more tightly, allowing the isolation of Hsc70-antibody complexes and the attached CCV.

3.2.3 AP-2 and μ 2 phosphorylation

To obtain additional data allowing to determine, whether this second AP-2 CCV pool is indeed a pool with an increased stability, I looked for differences in the amount of μ 2-adaptin phosphorylation (Thr156). This was increased by 50%, while AP-2 α adaptin was doubled, thus the μ 2-phospho: α adaptin ratio was 0.5 meaning that there

were no hyper-phosphorylation of the AP-2 complex. First, I investigated the levels of the kinase AAK1 and then the levels of its reaction product μ 2-phospho adaptin in the Hsc70-IP CCV. AAK1, which was slightly reduced in the total “ko” CCV, is doubled in the “ko” Hsc70-IP CCV (Fig. 3.16), compared to the anti-Hsc70 isolated CCV from wt. Also the μ 2-phospho adaptin is increased by 200%. The level of the AP-2 α subunit is increased, as in the total pool, by 100%, thus the AP-2 amount is not changed. Therefore the μ 2-phospho: α adaptin ratio is 1.5 demonstrating hyper-phosphorylation of the AP-2 μ 2-adaptin in this CCV pool increased. Therefore, the anti-Hsc70 isolated CCV represents a more stable CCV pool supporting the model about a delayed AP-2 CCV uncoating as a mode to couple SV protein exo- and endocytotic pathways.

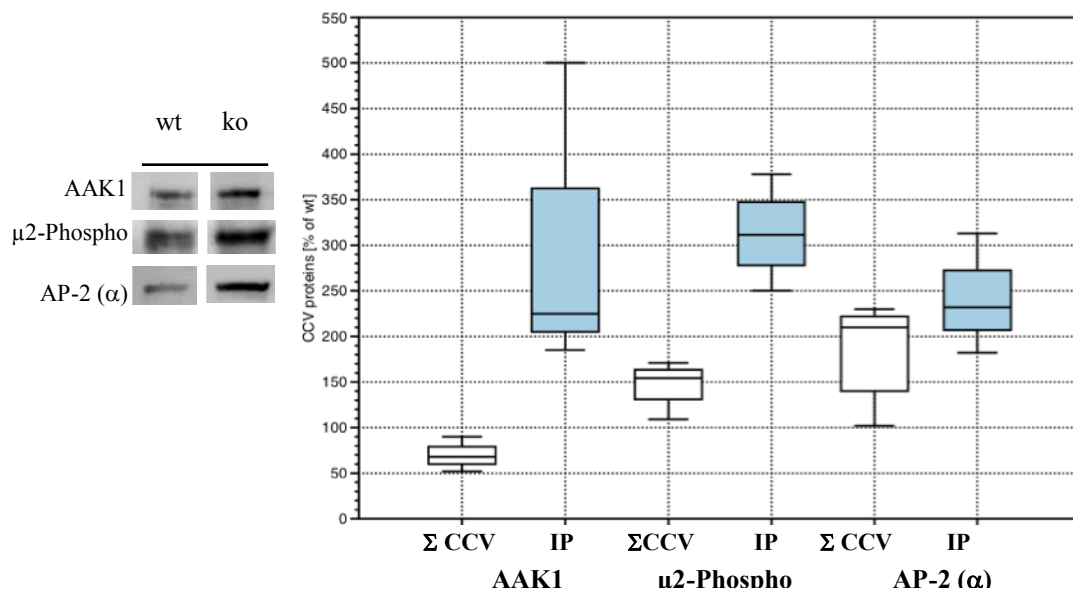


Fig. 3.16. Left, representative semi-quantitative Western-blot of wt and “ko” Hsc70-pooled CCV. Right, comparison of “ko”/wt ratios between total-CCV pool (white) and Hsc70-IP CCV (blue).

3.2.4. ‘Accessory’ coat proteins in the CCV pools

As shown in the paragraph 3.1.5, “ko” CCV have significant alterations in coat protein composition that could of course, effect the dynamics of coat assembly and disassembly. In the total CCV pool AP180 and stonin2 were decreased in “ko”

versus wt CCV, despite they are very specific AP-2 co-adaptors. The only cofactor that followed the AP-2 “behaviour” was NECAP1. Therefore I looked for differences in the association of these AP-2 co-adaptors and ‘accessory’ proteins between “ko” and wt Hsc70-IP CCV. AP-2 ratios are not changed as shown above.

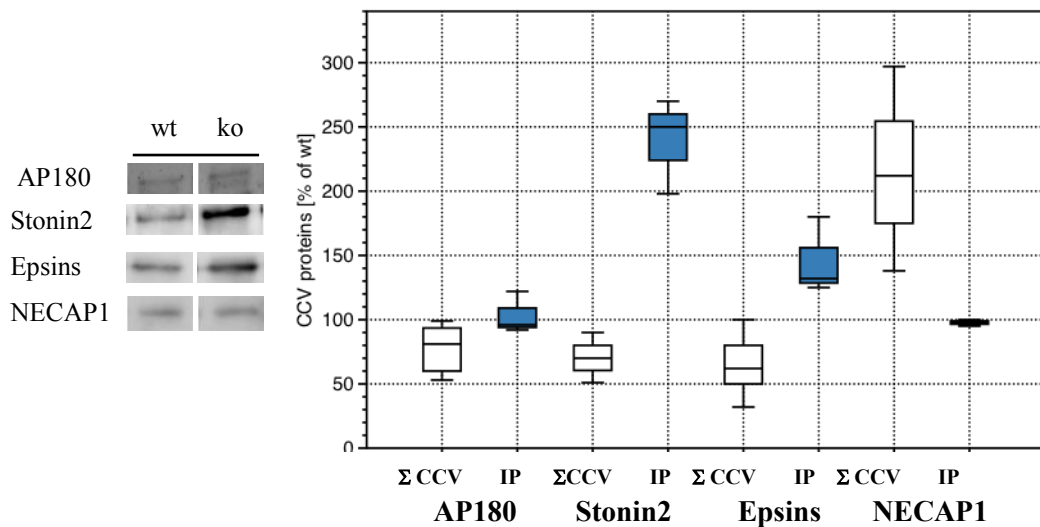


Fig. 3.17. Left, representative semi-quantitative Western-blot of wt and “ko” Hsc70-pooled CCV. Right, comparison of “ko”/wt ratios between total-CCV pool (white) and Hsc70-IP CCV (blue).

First, is important to specify that AP-2 increase in the “ko” Hsc-70 pooled down CCV is the same observed in the total CCV pool (Fig 3.16). AP180 was slightly reduced in the “ko” CCV pool, but ‘ko’/wt ratios are unaltered also in the Hsc70-pooled CCV, (Fig. 3.17 blue plot). On the other hand Stonin2 that was also reduced in the total “ko” CCV pool is drastically increased (250%) in the “ko” Hsc70-pooled CCV compared to wt. Epsin that was also decreased in the “ko” CCV (by 40%) and it is increased by 30% in Hsc70 pooled “ko” CCV. NECAP1 showed the opposite “behavior”. In the total CCV pool, it was doubled in ‘ko’ CCV. In the Hsc-70 pooled CCV there are no differences between wt and ‘ko’ CCV. The AP-2:NECAP1 ratio in the “ko” total CCV pool was ≈ 1 indicating a proper cargo and size quality control mediated by NECAP1. In the “ko” Hsc70-pooled CCV the ratio is dramatically reduced, suggesting a reduced “quality control” by NECAP1. There are no data about co-adaptors and coat stability in the literature besides AP180 binding affinities for clathrin and thus these changes can not be discussed. However, they show again that the Hsc70 IP CCV pool represents a specialized AP-2 CCV pool, whose

formation is induced by the σ 1B-deficiency.

3.2.5 Arf-GAP1 protein distributions in the CCV pools

Arf-GAP1 redistribution in “ko” remains one of the most striking data of this analysis. Both isoforms, brain and ubiquitous, are significantly increased in the synapse and at the same time drastically reduced in the early and late endosomes and increased in the total CCV pool; this strongly suggested a redistribution to the plasma membrane and in the CCV. The ubiquitous expressed Arf-GAP1 is increased to the same level in “ko” Hsc70-IP CCV as in the total CCV pool. Interestingly, the brain isoform has an even higher increase in the Hsc70-IP “ko” CCV compared to the increase observed in the total CCV pool (Fig. 3.18). These data strongly suggest that the increased association of Arf-GAP1 with the CCV in ko, is not CCV pool specific. This is exciting as it suggests that CME of the stable CCV pool as well as CME of a normal CCV pool is upregulated by the σ 1B-deficiency, supporting the model of delayed AP-2 CCV uncoating and upregulation of CME of non-SV proteins as mechanisms for the increase in synaptic AP-2 CCV. How Arf-GAP1 proteins fulfill their specific role in AP-2 CME and whether the isoforms really differ in this respect has to be addressed in the future.

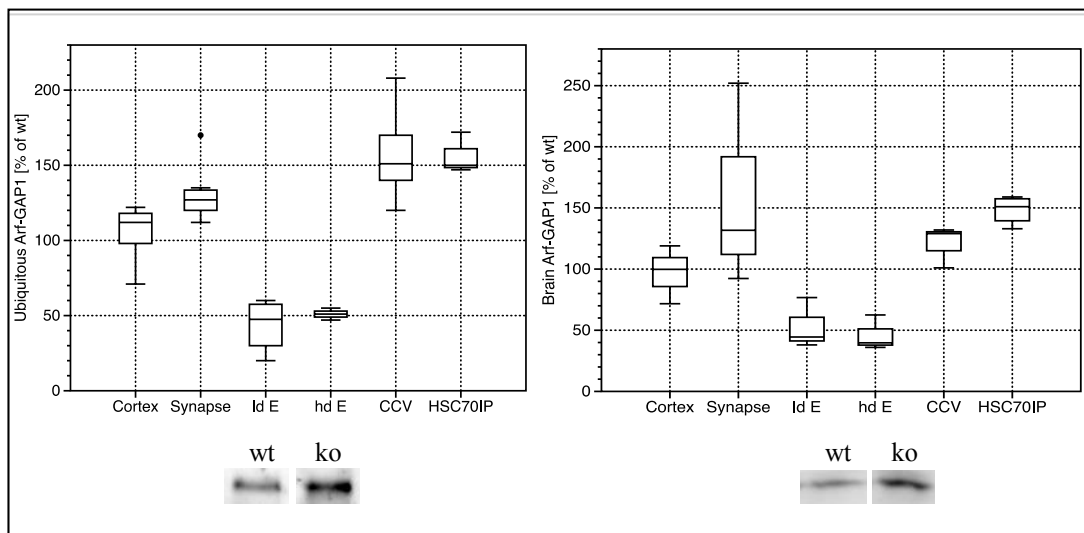


Fig. 3.18. “ko”/wt ratio box plots representing the Arf-GAP1 ubiquitous (left) and brain(Poupon et al.) isoforms expression e distribution. Lower panel, representative semi-quantitative western blot of Hsc70-pulled CCV for Arf-GAP1 ubiquitous (left) and brain (right) isoforms.

3.3. Analyses of the CCV Phosphoproteome

Isolation and characterization of the stable pool revealed important alterations in the phosphorylation state of the AP-2 complex. Furthermore, it is known for a subset of coat proteins that their phosphorylation status differs between their cytoplasmic and membrane bound pools. Thus, the activation and inactivation of the regulatory proteins and co-adaptors is most likely controlled through phosphorylation/dephosphorylation cycles. Therefore, we decided to determine differences in the phosphorylation/dephosphorylation status between ‘ko’ and wt CCV proteins. This is currently being done by phospho-peptide proteomics that yielded promising results, which however have to be confirmed and verified by different methods.

This time we tried to isolate the CCV with a phosphorylated-tyrosine IP. Fractions containing the CCV were incubated with 4G10 platinum Anti-Phosphotyrosine beads and then we compared the tyrosine-phosphorylation status through semi-quantitative western blot, using anti-phosphotyrosine antibody. As shown in the Fig.3.19,, the strongest signal is at 50 kDa which correspond to the μ 2 adaptin size. There is a significant increase in the “ko” P-tyr isolate signal, indicating regulation of CCV coat dynamics by tyrosine-phosphorylation in addition to the already established Ser/Thr phosphorylation of several AP-adaptins and other coat proteins (the same amount of proteins was incubated with the p-tyr-conjugated beads, see M&M paragraph 2.4.8.1).

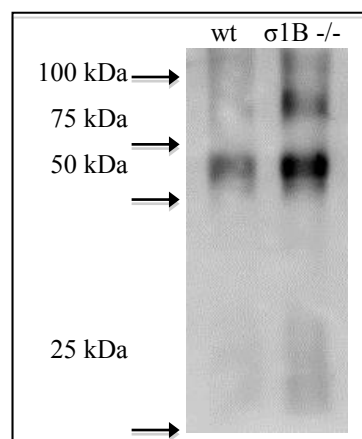


Fig 3.19. Semi-quantitative western-blot of 4G10 platinum Anti-Phosphotyrosine immunoprecipitated CCV. 250 μ g of pooled CCV from wt and “ko” were incubated with 4G10 platinum Anti-Phosphotyrosine beads.

Furthermore the intensity is much higher in “ko” compared to wt by 200%. A clear

signal is also present at 75 kDa that is the size of the bigger subunits of the APs complexes, γ 1 and α adaptin, and there is a smearing signal in the CLC range size. Thus we decided to analyze the phospho-tyrosine-immunoprecipitated pool through Mass-Spec analyses and Semi-quantitative western blot

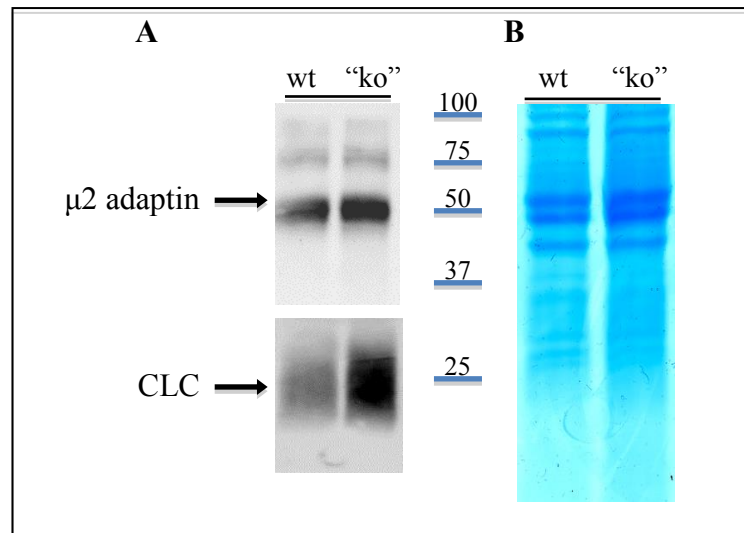


Fig 3.20. Phospho-tyr-immunoprecipitated CCV. (A) Semi-quantitative western-blot of μ 2 adaptin and CLC. (B) Blue coomassie gel used for Mass-Spec analyses (Performed by Olaf Reinhard).

Very surprisingly the “ko” phospho-tyrosine-immunoprecipitated CCV have higher level of μ 2 at the very same position than the anti-phospho-tyrosine blots. This is surprising as, the phosphorylation of μ 2 adaptin on Thr156 has been well characterized, but nothing is known about tyrosine-phosphorylation. Furthermore the smear observed at 25 kDa, with the phosphotyrosine staining (Fig.3.19) appears again with the CLC staining and is much stronger in “ko”. As already explained the stability of the clathrin cage is regulated by phosphorylation/dephosphorylation of the CLC.

Proteins contained in the three intense protein bands at 50 kDa were also analyzed by Mass-spectrometry. Besides μ 2 this analysis identified also Pacsin1 as a presumably tyrosine-phosphorylated protein and which is increased in “ko”. This is in line with the identified increase of phospho-Pacsin in the “ko” total pool (paragraph 3.1.6). Pacsin1/Syndapin negatively regulates endocytosis by binding dynamin (Modregger et al 2000), in line with the decreased CME in “ko” synapse. RabGDI β is, on the other hand, decreased in “ko”; GDI proteins inhibit the activation of Rab proteins.

The decrease of GDI in “ko” reinforces and confirms the model of an accelerated Rab5 cycle in “ko” synapse (for further details see also paragraphs 1.3.1 and 3.4). β and δ isoforms of the CaMK-II kinase, showed different behavior in wt and “ko” phospho-tyr-immunoprecipitated CCV. The β isoform showed a significant shift in the migration, indicating additional post-translation modifications. The δ isoform is found only in “ko” CCV. They are both ser/thr kinases with autophosphorylation/de-phosphorylation activity and nothing is known about their regulation and activity by tyrosine-phosphorylation or their functions in the CCV cycle. However, as these kinases have a central role in the long-term potentiation (LTP) by the Ca^{2+} influx, it is important to investigate in detail the molecular mechanism leading to these differences between wt and “ko” CCV. Finally and most importantly, Arf-GAP1 was detected in the mass-spec analyses of the tyrosine-phosphorylated CCV. One of the reported Arf-GAP1 tyrosine-phosphorylation sites is exactly in the middle of the ALPS1 domain, Tyr208. As already explained (in the paragraph 3.1.9.1), the ALPS1 domain forms a helix upon membrane lipid contact and thus mediates the binding to membranes. In concert with the ALPS2, membrane binding is also influenced by membrane curvature. We found decreased levels of Tyr-phosphorylated-Arf-GAP1 in “ko” CCV. Nothing is known, so far, about the link between the phosphorylation in Tyr208 of Arf-GAP1 and its membrane binding, however the phosphorylation of the residue could affect it by blocking either lipid binding or APLS1 helix formation (Bigay et al., 2005). Thus the tyrosine-phosphorylation in wt would indicate that Arf-GAP1 is associated with, but is not bound to the CCV membrane, while in the “ko” it is bound to AP-2 CCV membranes. However, this preliminary analysis has to be confirmed through different biochemical approaches to characterize it in greater detail.

3.4 Membrane dynamics of early endosomes and AP-1 complexes

In our previous study we characterized the endosomes accumulating in AP-1/ σ 1B $-/-$ synapses as PI-3-P positive early endosomes and showed that proteins accumulating in these endosomes either enter endolysosomal, multi-vesicular-body (MVB) pathways or that they are being stored in them for further use. Other PI-3-P dependent protein sorting pathways are not up-regulated. Endosomal PI-3-P is mainly generated by the class III PI3-kinase Vps34p (PI3KC3), the only member of this class, and a minor fraction is formed by the de-phosphorylation of PI-3,4-P₂ (J. M. Backer, *Biochem J* 410, 1 (2008)). The increase in PI-3-P and the endosomal accumulation of AP-1/ σ 1A complexes suggested that the regulation of neuronal Vps34p-activity might involve also AP-1/ σ 1B and thus both AP-1 complexes. M. Kratzke thus measured whether these endosomes also contain more Vps34p, but this is not the case (Kratzke & Schu, unpublished). This indicated that Vps34p activity is stimulated on these endosomes. Vps34p catalytic activity is highest in a complex with Vps15p (Schu et al. 1991, Stack et al. 1992). The Vps34p C-terminal domain blocks the active center and Vps15p binds to this Vps34p domain releasing this block. In non-neuronal cells both proteins recycle between the cytoplasm and endosomes regulating PI-3-P synthesis. In neurons, Vps34p/Vps15p complexes appear to be stably bound to endosomes and their activity is regulated by Rab5, which activates Vps34p activity via an unknown molecular mechanism. Thus we reasoned that σ 1B might bind the complex inhibiting its activity or that it regulates effector proteins of the Rab5 cycle. We demonstrate a novel molecular mechanism by which AP-1 regulates protein sorting, besides its well known function in CCV pathways.

3.4.1 AP-1 adaptin binding of Rab5 effector proteins

We tested whether σ 1B binds the Rab5 effectors Rabex-5 (GDP-GTP exchanger) and RabGAP5 (GTPase activator) using the Yeast-3-Hybrid System in which protein binding to γ 1/ σ 1 hemi-AP complexes can be tested (performed by S. Zafar). Rabex-5 has a Vps9-GEF domain and it binds ubiquitinated proteins and also has E3-ligase activity (Mattera et al. 2008, Zhu et al. 2007, Pagano et al. 2004, Esters et al 2001, Lippe et al 2001, Lee et al 2006). We tested specifically for σ 1B-binding to the Rabex-5 C-terminal domain of aa 396-491, which was shown to mediate binding to early endosomes independent of the linker protein Rabaptin-5 α (Mattera et al. 2008, Zhu et al. 2007, Lee et al- 2006). We detected binding of Rabex-5 to σ 1B, but not to σ 1A (Fig. 3.18). RabGAP5 consists of the catalytic TBC domain, a SH3-domain and a C-terminal RUN-domain, present in several proteins linked to the functions of GTPases. Therefore, we tested the RUN-domain (aa 578-760) for specific γ 1/ σ 1 binding. Also RabGAP5 bound to σ 1B, but not to σ 1A (Fig.3.21). We reasoned that both proteins might use similar motifs for σ 1B binding and sequence alignment revealed two conserved motifs in both: **P_E_A:E_C:L_L** and **P_L_Q:K_P:E_Q:G_V**. After exchange of the E and L residues following the P's in both sequences by A in Rabex-5, binding to γ 1/ σ 1B was abolished, confirming the specificity of σ 1B binding (Fig. 3.21). This result also indicates that one of the motifs stabilizes the second one enabling σ 1B binding.

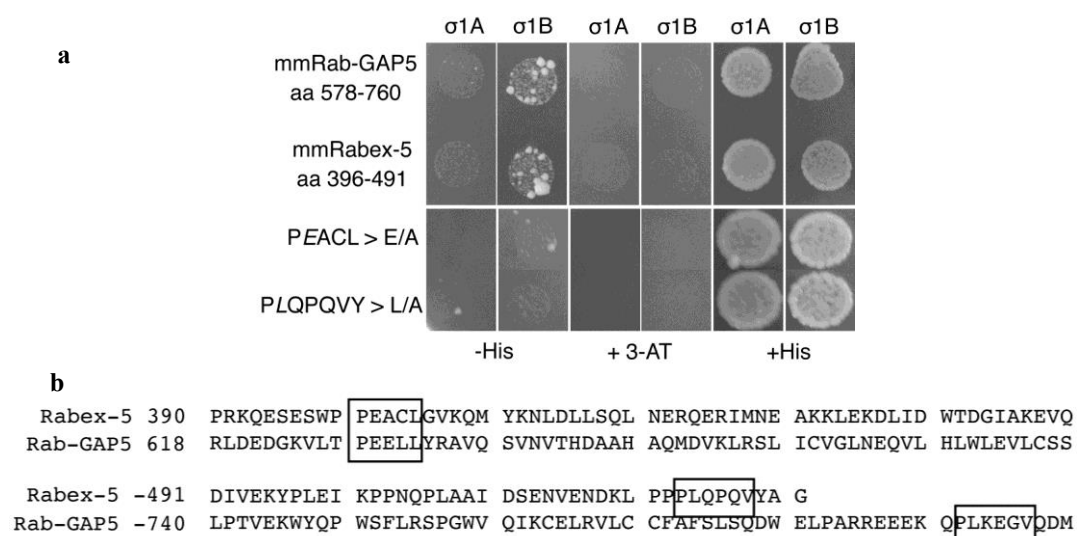


Fig 3.21 a) Yeast-3-hybrid (Y3H) assays (performed by S. Zafar). $\gamma 1$ was cloned into pGADT7, $\sigma 1$ -adaptins were cloned in the MSC-II and proteins to be tested for binding into the MSC-I site of pBridge (InVitrogen). Plasmids were transformed for interaction assays into the yeast strain AH109. Upper panel, Rabex-5 and RabGAP binding to AP-1/ $\sigma 1B$ complexes from wt and to the AP-1/ $\sigma 1A$ complex from $\sigma 1B^{-/-}$ brain. Central panel, 3-AT was added for negative control. Right panel, histidine was added for positive control. Lower panel, mutated Rabex5 binding to AP-1/ $\sigma 1B$ and AP-1/ $\sigma 1A$; point mutation in PEACL > E/A and in PLQPQVY > L/A. b) Sequence alignment of Rabex-5 and RabGAP

Next, I tested if the $\sigma 1B$ binding specificity occurs also in the brain and by pull-down experiments. Thus I expressed the protein fragments in *E. coli* as GST-tagged proteins: the mmRabex-5 fragment (aa 396-491) wt and the mutated forms, PEACL > E/A (named Rabex5 I) and PLQPQVY > L/A (named Rabex5 II), and the mmRabGAP5 (aa 578-760) (see details in mat & meth x. μ .z). Rabex-5 recombinant protein and the RabGAP5 protein were incubated with synaptic cytosol from wt and $\sigma 1B^{-/-}$ mice. Very surprisingly the $\sigma 1B$ binding specificity is reverted in these experiments. Rabex-5 pull down experiments of AP-1 revealed an higher affinity for the AP-1 complex in 'ko' extracts, meaning that the Rabex-5 affinity for AP-1/ $\sigma 1A$ is higher than the affinity for AP-1/ $\sigma 1B$ present in wt extracts (Fig.3.22). RabGAP5 binding affinity for the AP-1 complex was also increased, but to a much lesser degree, indicating that the GAP binds the AP-1/ $\sigma 1A$ complex with the lower affinity (Fig. 3.19). These data are in conflict with the Y3H experiments, indicating that $\sigma 1$ modifications are involved or that a third protein is involved binding both proteins simultaneously.

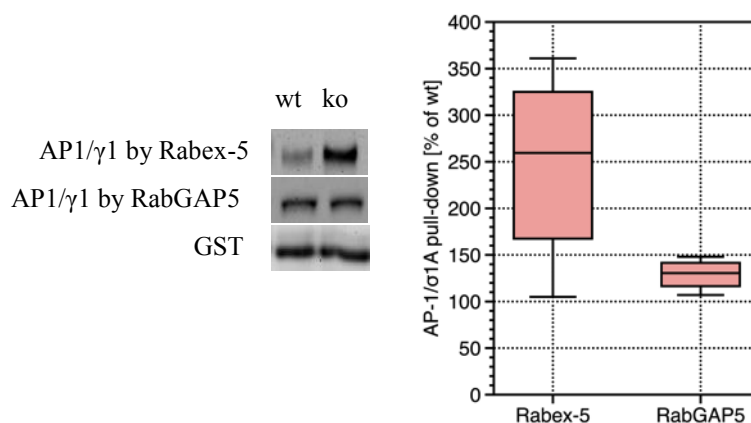


Fig. 3.22. Left, representative Western-blot of AP1- $\gamma 1$ pulled down by Rabex-5 and RabGAP5. In the lower panel GST as control. Right, ko/wt ratio of the binding specificity of Rabex-5 and RabGAP5, experiments have been repeated at least 3 times for statistic validity.

This dramatic difference between the Y3H results and the pool-down results would

be explained by the presence of a binding-mediating effector, meaning that Rabex-5 binds not directly the AP-1 complex. Mutated forms, Rabex-5 I and Rabex-5 II, that in the Y3H showed no binding activity to AP-1/ σ 1A and AP-1/ σ 1B, showed in the pulldown experiments no reliable binding activity, suggesting that the mutations decrease the stability of the protein conformations. This is actually in line with the Y3H-data, which showed that mutation of either motif abolishes σ 1-binding. The most plausible candidate for a third protein was Rabaptin-5 α . Rabaptin-5 α is an important effector of the Rab5 cycle, it activates, by interaction, the GEF activity of Rabex-5. Rabaptin-5 α binds Rabex-5 through its CC2-1 domain (551-656), and binds the AP-1 γ 1-adaptin ‘ear’ domain through its FGPLV motif (aa 301-449) (Fig.3.23).

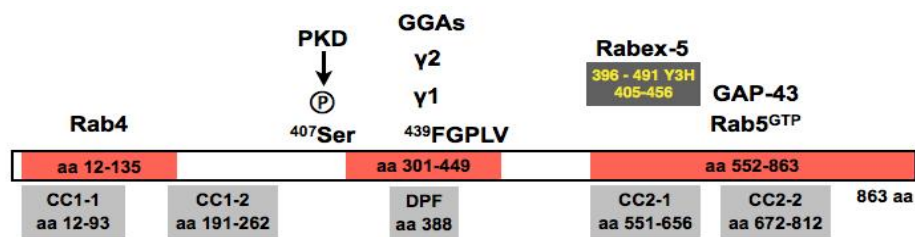


Fig. 3.23. Rabaptin 5 α domains.

However, Rabex-5 did not isolate more Rabaptin-5 α , but even slightly less, from ‘ko’ brain extracts, excluding Rabaptin-5 α as linker for Rabex-5 and AP-1. Thus analysis of the protein composition of the pulldown fractions has to reveal the identity of the linker protein.

We thought that a promising candidate could be ArfGAP-1: it is an endosomal protein, which also binds to the C-terminal “ear”-domain of γ 1 of AP-1 and it exists like σ 1 in a brain specific isoform, allowing tissue-specific regulations; furthermore Arf-GAP1 showed a very significant redistribution in the different compartments, synapse, endosomes, CCV and Hsc70-IP CCV, last not least Arf-GAP1 has also regulatory activity, independent of its GAP activity, is interesting to see first of all if it binds Rabex-5 and then if there are differences in wt and “ko”. As shown in the fig 3.21 Rabex-5 binds Arf-GAP1, this was very exciting as we found the interactions between the two proteins for the first time. Even more exciting is the difference

between wt and “ko”; as shown in the box plot of the fig. 3.21 the binding activity is much stronger in “ko”, and exactly correspond to the binding activity of AP-1 with Rabex-5, strongly suggesting that Arf-GAP1 could be the candidate mediating the binding between Rabex-5 and AP-1 complex.

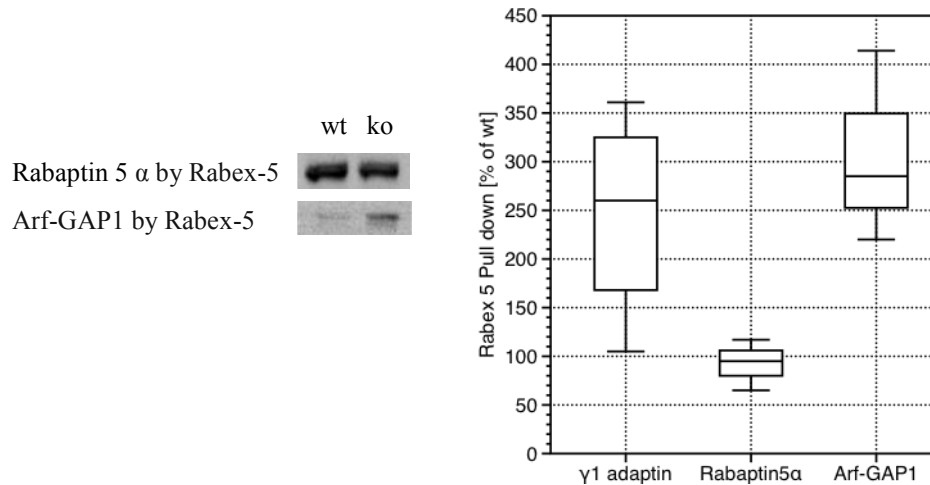


Fig 3.21. Left, representative Western-blot of Rabaptin 5 α and Arf-GAP1 pulled down by Rabex-5. Right, ko/wt ratio of the binding specificity of Rabex-5 to AP-1 γ 1 (showed again for easy comparison), Rabaptin 5 α and Arf-GAP1. For statistic validity experiments have been repeated at least 3 times.

3.4.2 Membrane distributions of Rab5-effector proteins and co-localization with AP-1

As the pull-down results seemed to contradict the Y3H data we tested for co-localization of the Rab5-effector proteins and AP-1 complexes on membranes in vivo with the Proximity-Ligation-Assay (PLA), whose details are described in Mat2.4.16.

Briefly, two proteins are being labeled in fixed cells with their respective primary antibodies. These are derived from two different species. These complexes are labeled with specie-specific secondary antibodies and in turn conjugated with oligonucleotides. If these complexes are in close proximity, primers can use the oligonucleotides as templates allow the PCR amplification of DNA. The incorporation of fluorescently labeled nucleotides demonstrates DNA synthesis. Due

to the PCR amplification and the incorporation of many fluorescent molecules, this is a highly sensitive method to determine protein-protein complexes in fixed cells by microscopy. We used MEF cell lines for these experiments, because their endosomes are larger than synaptic endosomes providing a higher spatial resolution. We used wt and $\sigma 1B^{-/-}$ MEF cell lines and their endogenous Rab5/Rab5 effectors and AP-1 proteins. Primary antibodies detected AP-1/ $\gamma 1$ -adaptin and Rab5, Rabex-5 and Rab-GAP5, respectively.

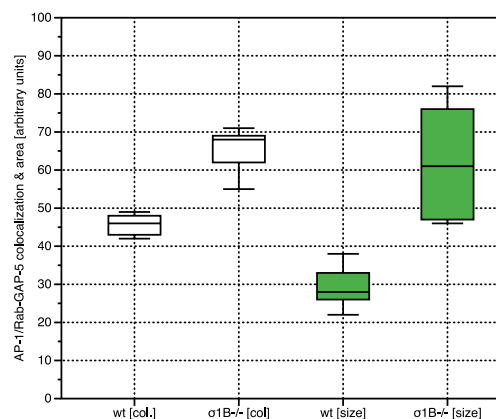
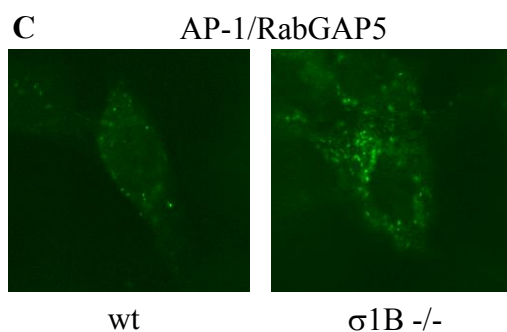
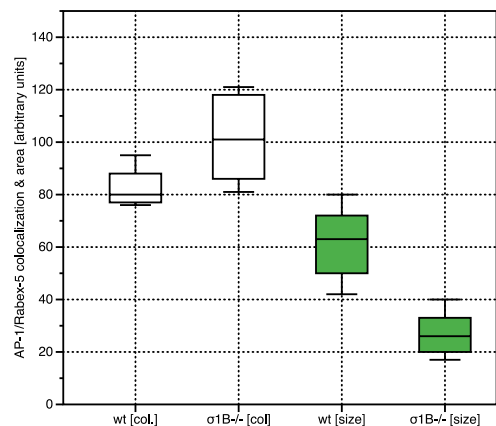
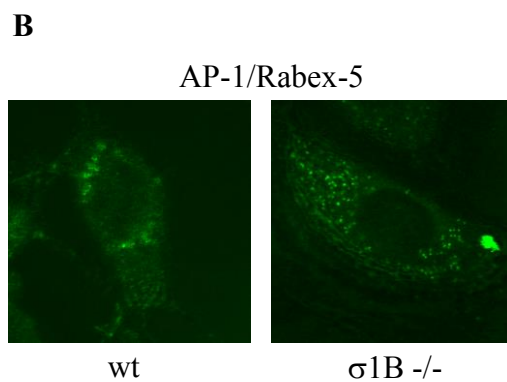
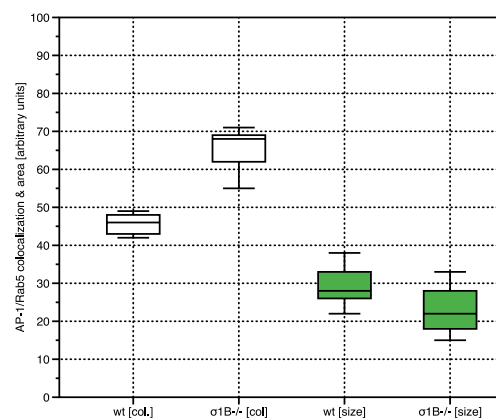
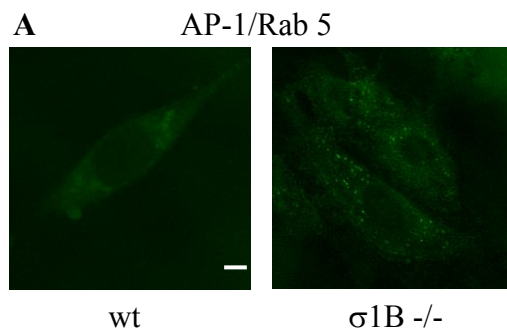


Fig. 3.24. Co-localization of AP-1/ γ 1 adaptin with Rab5, Rabex-5 and RabGAP5 was detected by in situ PLA. Scale bar 50 μ m. Wt and σ 1B^{-/-}MEF cells were stained with anti-AP-1/ γ 1 adaptin and anti-Rab5(A), Rabex-5 (B), Rab-GAP5 (C). Left, representative confocal microscopy images: the fluorescent spot signals are generated when the stained proteins are in proximity (<40 nm). Right, statistical analyses of the co-localization (white plots) and area size (green plots)

As shown in the Fig. 3.24, in σ 1B^{-/-} cells more AP-1/Rabex-5 and more AP-1/Rab5 complexes are formed confirming the Rabex-5 pull-down results and indicating an accelerated Rab5 activation, which would also activate the Vps34p-activity. The area of the co-localization is reduced in σ 1B^{-/-} cells for AP-1/Rab5 and also for AP-1/Rabex5 indicating a specific co-localization and concentration of Rabex5 with Rab5. I found also more RabGAP5 to be co-localized with AP-1, which is also in line with the pulldown experiments. However, those complexes were not confined to small areas, indicating reduced co-localization with Rab5 and thus reduced inhibition of Rab5-activity. These data are also in line with our biochemical analysis of σ 1B^{-/-} neurons, which showed increased Rabex-5 association with early endosomes (Kratzke et al 2014). As negative control cells were treated with only the γ 1 adaptin primary antibody and then stained with both the secondary antibodies to confirm that the observed spots are exclusively generated when AP-1 co-localizes with Rab5 effectors. Thus AP-1/ σ 1A stimulates Rab5 and thus Vps34p activation, whereas it appears to be less efficient in the presence of the AP-1/ σ 1B complex. Therefore, Rab5-effector protein binding by σ 1B, as demonstrated by the Y3H experiments, appears to prevent AP-1/ σ 1A plus protein-X mediated Rabex-5 and Rab5 concentration in endosomal microdomains This model is close to be verified as we are going to identify the AP-1/ σ 1A Rabex-5 linker protein.

4 Discussion

Thus far, three mouse AP-1 adaptin ‘knock-out’ models have been established in our group. However, only the σ 1B ‘knock-out’ mouse is viable and fertile, whereas ‘knock-outs’ of the ubiquitously expressed γ 1 and μ 1A isoforms are embryonic lethal at early stages. Viability of σ 1B-deficient mice and the tissue-dependent σ 1B expression pattern demonstrate that σ 1B adaptin is not required for ubiquitous “house-keeping” AP-1 functions, but is expected to mediate tissue-specific and due to its highest expression in brain, especially brain-specific AP-1 functions.

The σ 1B deficient mice are hypoactive, display deficits in neuromotor learning and spatial learning and memory tasks. These data support a genetic screen in humans for analyzing X-chromosome-based diseases that link the σ 1B locus to severe mental retardation. Patients with pre-mature STOP-codons in the σ 1B adaptin gene develop X-linked mental retardation (XLMR) and they showed also hypotonia and delay in walking and lipodystrophy. The hypotonia is infrequent in XLMR patients with an unaltered σ 1B gene (Glyvuk et al. 2010, Tarpey et al. 2007). A lipodystrophy has been detected also in σ 1B deficient mice, with a reduction of adipose tissue mass on average by 20% and of epididymal adipose tissue by 50% (Baltes et al. 2014). This phenotype is caused by the overexpression of the adipogenesis inhibiting receptor DLK1, which is not sorted directly by AP-1/ σ 1B complexes but by sortilin, a neurotrophin and receptor binding receptor. Previous analyses of sorting motifs did not reveal σ 1-isoform specific cargo proteins. Sortilin is the first cargo protein identified to be specific for σ 1B and is overexpressed in σ 1B-deficient adipocytes, thereby preventing DLK1 downregulation. However sortilin and DLK1 are not overexpressed in these brains, indicating that σ 1B sorting functions in the trans-Golgi network - endosomal pathways appear to be tissue specific (Baltes et al. 2014). The previous analysis of the brains of AP-1/ σ 1B $-/-$ mice revealed reduced numbers of synaptic vesicles under resting condition, but also after stimulation of SV exocytosis and recycling. The delayed synaptic vesicle recycling is accompanied by the accumulation of membrane enclosed organelles as endosomes and Clathrin-Coated-Vesicles (CCV) in hippocampal synapses.

4.1 AP-1 CCV reduction and AP-2 CCV accumulation in the σ 1B $-/-$ synapse

We isolated the synaptic CCV from wt and “ko” brains by differential and density-gradient centrifugations. There are no differences in the migration behavior of the CCVs in the density-gradient centrifugation, indicating that CCV size and physical properties are not altered in the CCV isolated from AP-1/ σ 1B $-/-$ synapses. The main goal of this study was to characterize the accumulated CCV pool and thus to understand the reason for their accumulation and the molecular link to the defects in SV recycling and the animals phenotypes and the human disease.

Firstly, we looked for differences between wt and ‘ko’ brains in the adaptor protein complex AP-1 CCVs, because its σ 1B subunit is “knocked out”. As expected, there is a significant reduction by 20% in “ko” synapse AP-1 CCV. The AP-1 CCV reduction confirms the impaired endosome-mediated SV biogenesis and the AP-1 function in an apical endosome-plasma membrane recycling pathway, which was the first apical AP-1 pathway to be reported (Glyvuk et al. 2010). However, it also demonstrates that the accumulating CCV are not functionally impaired AP-1 CCV and thus this result does not explain why there is an CCV accumulation in the σ 1B $-/-$ synapse. The further analysis of the synaptic CCVs revealed with 200% a very strong increase in AP-2 CCV in “ko” synapses. This is surprising, because due to the reduced SV recycling in the “ko”, one would expect that fewer AP-2 CCV are formed because of the reduced AP-2 clathrin-mediated-endocytosis (CME). We reasoned that their accumulation could be due to an enhanced CME, independent of SV protein recycling or to an altered and delayed AP-2 CCV uncoating. We decided to study their composition in terms of coat proteins, clathrin cage proteins, regulatory proteins and all the cofactors having a role in the AP-2 CCV cycle, in order to obtain data pointing to the molecular mechanisms that link the σ 1B $-/-$ and SV recycling alterations, with the AP-2 CCV accumulation.

4.1.1 Accumulating AP-2 CCV have an altered coat composition

One reason for the accumulation could be the alteration of the clathrin cage itself. The ratio between the two clathrin subunits forming the basket, CLC and CHC, is only in the brain 1:1, while it is lower in other tissues. As CLC regulates many aspects of the formation and stabilization of the clathrin basket, its functions might

be especially important in the brain and synaptic CCV. Both the subunits are increased by 50% in the “ko” CCV and thus the relative amount of the clathrin basket components is not changed and does not explain the increased AP-2 CCV pool.

The accumulation of the AP-2 CCV could also be caused by a delayed uncoating. However all the currently known proteins composing the uncoating machinery, the chaperon Hsc70 and its cochaperonins auxilin 1, auxilin 2 and CSP α are enriched in the CCV fractions meaning that at least their levels, are not limiting for the uncoating reaction.

Analyzing the inner coat layer, we found that “ko” CCV have a significant alteration in their coat composition. Although AP-2 is doubled in “ko” CCV, the very specific AP-2 co-adaptors are not increased, but are even slightly reduced. The reduction in AP180 is especially remarkable, because it is a pre-synapse-specific AP-2 CCV adaptor protein. Its binding affinity to the clathrin cage is higher than the affinity of AP-2 and thus its increase could have contributed to the increased stability of the vesicles. However, it is not only reduced in the “ko” CCV, but also in all other sub-fractions of “ko” brains, suggesting that AP180 might be a co-adaptor of AP-1 CCV as well. There are indeed some data in the literature, which link it to AP-1 (Maritzen et al., 2012, Petralia et al., 2013). Stonin2, which participates in synaptotagmin-1 sorting, is also slightly reduced. Its reduction in CCVs suggests a reduced requirement for SNARE sorting in line with reduced SV recycling. Interestingly, in Stonin2 “ko” synapses, SVs and AP-1 CCV are reduced as well, and synaptotagmin-1 distribution is not altered, although transport kinetics are, and thus the SV and CCV phenotypes in both model systems are based on different molecular mechanisms. The simplest explanation for the reduction in co-adaptors would be that they sort cargo proteins, which are also sorted by AP-1/ σ 1B into the SV recycling pool. Their absence would lead to a reduced recruitment of these co-adaptors to clathrin-coated pits at the PM. However, this does not explain the increase in AP-2 CCVs. If an SV recycling-independent CME would be up-regulated, those CCV should be enriched in the respective cargo proteins. We did not detect specific cargo proteins, which are dramatically enriched in the AP-2 CCV. The SV recycling-independent CME model is also supported by the increase of phospho-PACSIN1, that couples the vesicles scission machinery and the cytoskeleton reorganization

proteins. Although scission machinery proteins as dynamin, amphiphysin, endophilin are not increased, phospho-PACSIN1/syndapin was increased by 50% in “ko” CCV. This protein binds dynamin and at the same time the Wiscott-Aldrich syndrome protein (WASP), which promotes the actin-depolymerization. Actin reorganization is involved in CCV formation and thus the phospho-PACSIN1 increase supports the model of an enhanced CME pathway. The increase of NECAP1, a factor mediating the size and cargo recruitment “quality control”, is exactly in line with the AP-2 increase (also doubled in “ko”), indicating a proper control of the CCV formation. The accumulation could be caused also by an increased stability of the coat, in turn caused by a hyper-phosphorylation of the AP-2 complex. The phosphorylation on AP2/ μ 2 subunit leads an open conformation and thus the release of the second membrane-binding domain (Conner et al., 2003). The levels of the phosphorylated μ 2 adaptin are increased in “ko” CCV, however the AP-2 adaptin increase is much higher and the phospho- μ 2 adaptin/AP-2 ratio is 0.5, indicating that there is no hyper-phosphorylation of the AP-2 complex and thus the accumulation of AP-2 CCV is caused by some other molecular mechanism. However, there is one co-adaptor of AP-2 that is surprisingly enriched, ArfGAP1. Besides its function as an Arf1 GTPase activator, and thus a regulator of AP-1 membrane binding and CCV formation, ArfGAP1 is a co-adaptor of AP-2 CCVs for the transferrin receptor (Ren X et al., 2012, Bai et al., 2011). We did not detect this receptor in the CCVs, and other cargo proteins have not been described. ArfGAP1 is redistributed from endosomal membranes into AP-2 CCVs, and its enrichment in synaptosomes suggests that it is even trapped in these CCVs. Based on this first data set, we propose a model that AP-1/ σ 1B-dependent SV formation and AP-2 endocytosis are interdependently regulated, possibly via Arf-GAP1 or AP180.

4.1.2 Characterization of a ‘stable’ CCV pool in σ 1B^{-/-} synapses

The iTRAQ and the semi-quantitative western-blot analyses revealed an accumulation of AP-2 CCV and significant changes in the AP-2 CCV coat composition. However it is also possible that there are two different pools of AP-2 CCV, one “normal” and one with a more “stable” coat. The stable one might bind less Hsc70, but might also bind it more stable, because it does not disassemble the

clathrin-cage. Indeed, we were able to isolate this second stable pool of AP-2 CCV through a Hsc70 IP (see details in 3.2, and 2.4.8 paragraphs). This ‘stable’ CCV pool from $\sigma 1B^{-/-}$ differs in the Hsc70/co-chaperonins ratios from the total $\sigma 1B^{-/-}$ CCV pool. While auxilin 1 and 2 are even further increased, Hsc70 is not. In the total CCV pool from $\sigma 1B^{-/-}$ synapses there was more Hsc70 compared to wt CCV. The Hsc70-IP CCV contain however the same amount of Hsc70, than the IP CCV fraction from wt synapses. Importantly, only the Hsc70-IP CCV pool from $\sigma 1B$ synapse shows hyper-phosphorylation of $\mu 2$ adaptin Thr156, whereas the IP pool from wt does not. Also more of the responsible kinase, AAK1, is associated with this fraction. Phosphorylation of $\mu 2$ adaptin enhances cargo binding and PIP2 binding by the second PIP2 motif of AP-2 contained within $\mu 2$ subunit. This protects PIP2 from the phosphatases synaptojanin1 and thus stabilizes the CCV coat. Thus, only the Hsc70-IP CCV from $\sigma 1B$ synapses contains more stable CCV pool, whereas the corresponding fraction from wt is not stabilized, although both CCV have Hsc70 bound in a manner enabling their immunoprecipitation. The inability of co-chaperonines/Hsc70 interactions could be caused by a multitude of factors: first of all an altered composition of the clathrin cage. In the “ko” total CCV pool the CHC:CLC ratio was not changed as both are increased by 50% (Fig. 3.5). However in the “ko” Hsc70-IP CCV the ratio is dramatically changed and the CLC showed an increase compared to the increase in the total “ko” pool. Hsc70 is recruited by auxilin 1 to a CCV, where it has to bind, first of all, the QLMLT motif in the C-terminal domain of CHC. The strong increase of CLC in the “ko” stable pool could limit this interaction and thus the triggering of the uncoating. The coat composition of the stable CCV pool shows yet a different coat-composition than the majority of the $\sigma 1B^{-/-}$ synaptic CCV. AP180 and Stonin2 were decreased in the “ko” total CCV pool, despite they are very specific AP-2 co-adaptors. In the stable CCV pool the AP180 “ko”/wt ratio is unaltered, but stonin 2 is dramatically increased in the stable “ko” CCV. NECAP1, responsible for the cargo and size quality control, was increased in the “ko” total pool as is AP-2, but in the stable “ko” CCV pool the NECAP1/AP-2 ratio is dramatically reduced suggesting a reduced “quality control” by NECAP1. Nothing is known until now about the correlation of the co-adaptor/coat composition and the coat stability and this has to be analyzed in the future using this mouse model however Hsc70-pooled CCV represent a specialized AP-2 pool, whose composition

is influenced by the σ 1B-deficiency. Based on this set of data, we can develop a model, in which the increased stability of the ko “stable” CCV pool, and thus the delayed uncoating is caused by an hyper-phosphorylation of the AP-2 complex, that binds with higher affinity to the membrane, and by a dramatic alteration of the clathrin cage composition that in turn lead to a disturbed activation of Hsc70 mediated uncoating.

4.2 The phosphoproteome of CCV from σ 1B -/- synapses

Several CCV proteins and associated proteins, are activated/inactivated according to their phosphorylation/dephosphorylation status. Thus we are characterizing the phosphorylation status of proteins like the clathrin proteins, coat proteins and of the regulatory proteins. Our preliminary studies reveal in “ko” CCV, a general increase in tyrosine-phosphorylation. The first candidates, which were analyzed, were of course the adaptor complex adaptins. Interestingly, AP-2/ μ 2 adaptin showed an increased tyr-phosphorylation in “ko” CCV, but so far nothing is known about phospho-tyr regulation of μ 2 function. On the other hand, the phospho-tyr regulation of the CLC has been well characterized. The stability of the clathrin basket and the CLC-mediated regulation of endocytosis involve its tyrosine-phosphorylation. The strongly increased levels of CLC in “ko” CCV indicate significant alteration in the clathrin cage stability. CaMK-II isoforms shifted in the electrophoretic migration, between “ko” and wt CCV, suggesting that some post-translational modifications could be induced by the σ 1B deficiency. It is important to investigate these modifications and thus the regulation of kinase activities, because CaMK-II is involved in LTP, a key factor in memory formation. Finally and most importantly with respect to AP-1 and AP-2 CCV dynamics, less Arf-GAP1 is isolated by the anti-phospho-tyr antibody from “ko” CCV. One of the reported tyrosine phosphorylation occurs in the middle of the ALPS1 domain, which is a key structure of the geometrical-stoichiometric-binding to the membrane. Thus the phosphorylation could reduce the membrane binding; the binding to the CCV would be mediated by protein-protein interaction, like the already demonstrated binding to the γ 1 and α adaptins ‘ears’.

The tyrosine-phosphorylation of CCV coat and associated proteins has to be studied in more detail in the future, however it is already clear that the σ 1B-deficiency

induces alterations of the tyrosine phosphorylation of proteins, that in turn orchestrates the CCV cycle.

4.3 Reorganization of the Rab5 cycle by AP-1/ σ 1B deficiency

In AP-1/ σ 1B $-/-$ synapses endosomes accumulate and in our previous study, we characterized these endosomes as PI-3-P and Rab5 positive early endosomes. (Kratzke et al., 2014). Endosomal PI-3-P is mainly generated by the class III PI3-kinase Vps34p (PI3KC3), the only member of this class, and a minor fraction is formed by the de-phosphorylation of PI-3,4-P₂. The increase in PI-3-P and the endosomal accumulation of AP-1/ σ 1A complexes in the “ko” synapses, suggested that the regulation of neuronal Vps34p-activity might involve AP-1/ σ 1B and thus both AP-1 complexes. Vps34p activity is stimulated by complex formation with the Ser/Thr kinase Vps15p (p150). In neurons, Vps34p/Vps15p complexes appear to be stably bound to endosomes and the activity of the complex is regulated by Rab5, which activates Vps34p activity via an yet unknown molecular mechanism. Thus we reasoned that σ 1B might bind Vps34p inhibiting its activity or that it regulates effector proteins of the Rab5 cycle. Y3H assays revealed a specific binding activity of σ 1B adaptin with the Rab5 effectors, Rabex-5 and RabGAP5. The ubiquitous σ 1A is not able to bind both the effectors in this experiment (Fig. 3.21), however in “ko” brains the AP-1/ σ 1A complex showed a higher affinity for Rabex5, indicating that a protein(s) mediating complex formation is up-regulated or modified in “ko” brains. One potential candidate was Rabaptin-5 α as this protein is able to bind the γ 1-‘ear’ of the AP-1 complex and Rabex5, however, the Rabaptin-5 α levels are not increased in pull down fraction from “ko”. The protein/s mediating this binding is close to be identified.

4.4 Model of AP-1 functions in SV recycling

In this study we found that the AP1/ σ 1B deficiency strongly affects the endosomal protein sorting and the SV recycling mediated by CCV; the model is summarized in the Fig. 4.1. The alterations in the endosomal protein sorting are mediated by both synaptic AP-1 complexes and their binding to Rab5 effector proteins. In the absence of AP-1/ σ 1B, AP-1/ σ 1A activates the Rab5 cycle and thus the Rab5-dependent late endosome recycling. SV proteins accumulating in these endosomes are therefore readily transported into endolysosomes and are degraded.

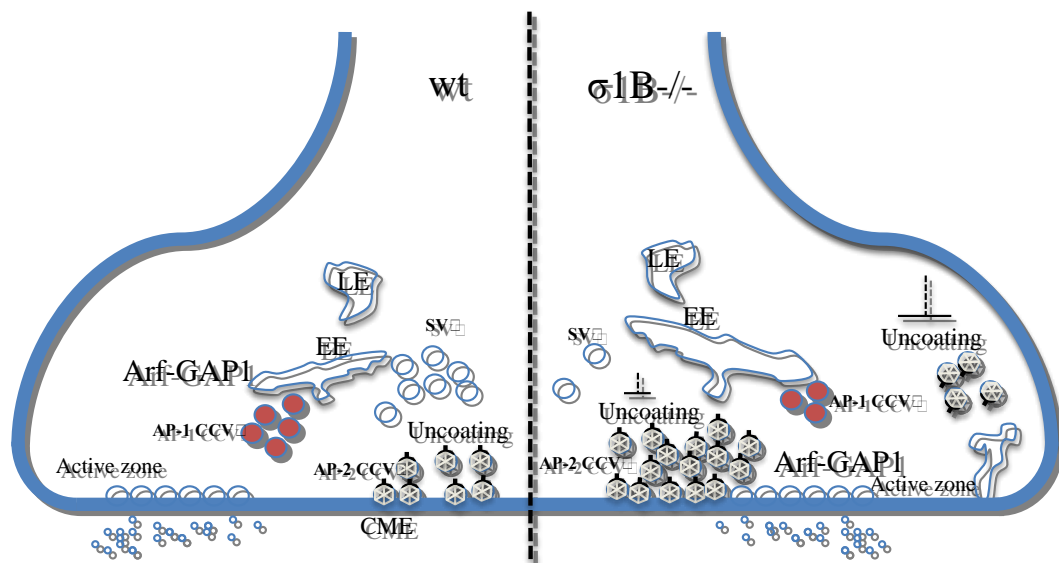


Fig. 4.1. Final model. Early endosomes (EE) with accelerated Rab5 and alterations in the shape and size accumulate in the σ 1B $-/-$ synapse. Several proteins, like Arf-GAP1 showed a drastic redistribution in the synaptic compartments. The redistribution effects the stability and the efficiency of the uncoating, leading an accumulation of the AP-2 CCV. This in turn leads less SV proteins available for the SV turnover and then a reduction of SV in the “ko” mice.

The synaptic AP-2 CCV pool is increased in σ 1B $-/-$ synapses. Analysis of two CCV pools indicate up-regulation of clathrin mediated endocytosis of non-SV proteins, which remain to be identified, and also an extended life time of AP-2 CCV due to their slower un-coating. Analysis of AP-2 μ 2-adaptin phosphorylation revealed its enhanced phosphorylation as one of the stabilizing mechanisms, mediated by an increased association of the respective kinase, AAK1. Also the family of co-adaptor proteins present in the CCVs differs between the two pools, suggesting that adaptor composition of the CCV determines the dynamics of the CCV cycle. Delayed AP-2 CCV uncoating limits protein transport to the endosomes and thus prevents sorting of the CCV cargo proteins into degradative pathways. Thus, these CCV might represent a buffer reservoir for SV proteins. Fewer proteins are degraded and a sufficient number of SV proteins are present in the synapse, enabling the synapse to rapidly

response to different signaling requirements. This model can explain why SV numbers are decreased in the $\sigma 1B^{-/-}$ synapses and why the pools of AP-2 CCV and endosomes are increased instead.

The identification of the regulatory molecular mechanisms operating in these pathways is under way and they will be identified in future studies.

Bibliography

- Baltes, J., Larse, J., Radhakrishnan, K., Geumann, C., Kratzke, M., Petersen, C., Schu, P., (2014) *J. Cell Sci.* σ 1B adaptin regulates adipogenesis by mediating the sorting of sortilin in adipose tissue.
- Bai, M., Gad, M., Turacchio, G., Cocucci, E., Yang, JS., Li, J., Beznoussenko, GV., Nie, Z., Luo, R., Fu, L., Collwn, JF., Kirschhausen, T., Luini, A., Hsu, VW. (2003) ARFGAP1 promotes AP-2-dependent endocytosis *Nat Cell Biology* 13(5), 559-567.
- Bigay, J., Gounon, P., Robineau, S., & Antonny, B. (2003). Lipid packing sensed by ArfGAP1 couples COPI coat disassembly to membrane bilayer curvature. *Nature*, 426(6966), 563-566. doi: 10.1038/nature02108
- Bigay J, Casella JF, Drin G, Mesmin B, Antonny B. ArfGAP1 responds to membrane curvature through the folding of a lipid packing sensor motif. *Embo J* 2005;24:2244–53.
- Bocking, T., Aguet, F., Harrison, S. C., & Kirchhausen, T. (2011). Single-molecule analysis of a molecular disassemblase reveals the mechanism of Hsc70-driven clathrin uncoating. *Nat Struct Mol Biol*, 18(3), 295-301. doi: 10.1038/nsmb.1985
- Bonifacino, J. S., & Glick, B. S. (2004). The mechanisms of vesicle budding and fusion. *Cell*, 116(2), 153-166.
- Boucrot, E., Saffarian, S., Zhang, R., & Kirchhausen, T. (2010). Roles of AP-2 in clathrin-mediated endocytosis. *PLoS One*, 5(5), e10597. doi: 10.1371/journal.pone.0010597
- Brett, T. J., Traub, L. M., & Fremont, D. M. (2002). Accessory protein recruitment motifs in clathrin-mediated endocytosis. *Structure*, 10(6), 797-809.
- Chen, M. J., Goldstein, J. L., & Brown, M. S. (1990). NPXY, a sequence often found in cytoplasmic tails, is required for coated pit-mediated internalization of the low density lipoprotein receptor. *J Biol Chem*, 265(6), 3116-3123.
- Christoforidis, S., Miaczynska, M., Ashman, K., Wilm, M., Zhao, L., Yip, S. C., . . . Zerial, M. (1999). Phosphatidylinositol-3-OH kinases are Rab5 effectors. *Nat Cell Biol*, 1(4), 249-252. doi: 10.1038/12075
- Collawn, J. F., Kuhn, L. A., Liu, L. F., Tainer, J. A., & Trowbridge, I. S. (1991). Transplanted LDL and mannose-6-phosphate receptor internalization signals promote high-efficiency endocytosis of the transferrin receptor. *EMBO J*, 10(11), 3247-3253.
- Collawn, J. F., Stangel, M., Kuhn, L. A., Esekogwu, V., Jing, S. Q., Trowbridge, I. S., & Tainer, J. A. (1990). Transferrin receptor internalization sequence YXRF implicates a tight turn as the structural recognition motif for endocytosis. *Cell*, 63(5), 1061-1072.
- Collins, B. M., McCoy, A. J., Kent, M. M., Evans, P. R., & Owen, D. J. (2002). Molecular architecture and functional model of the endocytic AP2 complex. *Cell*, 109(4), 523-535.
- Conner, S. D., Schroter, T., & Schmid, S. L. (2003). AAK1-mediated micro2 phosphorylation is stimulated by assembled clathrin. *Traffic*, 4(12), 885-890.
- Cremona, O., Di Paolo, G., Wenk, M. R., Luthi, A., Kim, M. T., Takei, K., . . . De Camilli, P. (1999). Essential role of phosphoinositide metabolism in synaptic vesicle recycling. *Cell*, 99(2), 179-188.
- Dell'Angelica, E. C. (2009). AP-3-dependent trafficking and disease: the first decade. *Curr Opin Cell Biol*, 21(4), 552-559. doi: 10.1016/j.ceb.2009.04.014

- Dell'Angelica, E. C., Klumperman, J., Stoorvogel, M., & Bonifacino, J. S. (1998). Association of the AP-3 adaptor complex with clathrin. *Science*, *280*(5362), 431-434.
- Deborde, S., Perret, E., Gravotta, D., Deora, A., Salvarezza, S., Schreiner, R., Rodriguez-Boulan, E. (2008) Clathrin is a key regulator of basolateral polarity. *Nature*, *452*(7188), 719-23.
- Deneka, M., Neeft, M., Popa, I., van Oort, M., Sprong, M., Oorschot, V., . . . van der Sluijs, P. (2003). Rabaptin-5/alpha/rabaptin-4 serves as a linker between rab4 and gamma(1)-adapin in membrane recycling from endosomes. *EMBO J*, *22*(11), 2645-2657. doi: 10.1093/emboj/cdg257
- Di Fiore, P. P., & von Zastrow, M. (2014). Endocytosis, signaling, and beyond. *Cold Spring Harb Perspect Biol*, *6*(8). doi: 10.1101/cshperspect.a016865
- Di Paolo, G., & De Camilli, P. (2006). Phosphoinositides in cell regulation and membrane dynamics. *Nature*, *443*(7112), 651-657. doi: 10.1038/nature05185
- Dickman, D. K., Horne, J. A., Meinertzhagen, I. A., & Schwarz, T. L. (2005). A slowed classical pathway rather than kiss-and-run mediates endocytosis at synapses lacking synaptojanin and endophilin. *Cell*, *123*(3), 521-533. doi: 10.1016/j.cell.2005.09.026
- Donaldson, J. G., & Jackson, C. L. (2011). ARF family G proteins and their regulators: roles in membrane transport, development and disease. *Nat Rev Mol Cell Biol*, *12*(6), 362-375. doi: 10.1038/nrm3117
- Doray, B., Lee, I., Knisely, J., Bu, G., & Kornfeld, S. (2007). The gamma/sigma1 and alpha/sigma2 hemicomplexes of clathrin adaptors AP-1 and AP-2 harbor the dileucine recognition site. *Mol Biol Cell*, *18*(5), 1887-1896. doi: 10.1091/mbc.E07-01-0012
- Drake, M. T., & Traub, L. M. (2001). Interaction of two structurally distinct sequence types with the clathrin terminal domain beta-propeller. *J Biol Chem*, *276*(31), 28700-28709. doi: 10.1074/jbc.M104226200
- Ferguson, S. S., Downey, M. E., 3rd, Colapietro, A. M., Barak, L. S., Menard, L., & Caron, M. G. (1996). Role of beta-arrestin in mediating agonist-promoted G protein-coupled receptor internalization. *Science*, *271*(5247), 363-366.
- Ferreira, C., & Veldhoen, M. (2012). Host and microbes date exclusively. *Cell*, *149*(7), 1428-1430. doi: 10.1016/j.cell.2012.06.005
- Ghosh, P., Dahms, N. M., & Kornfeld, S. (2003). Mannose 6-phosphate receptors: new twists in the tale. *Nat Rev Mol Cell Biol*, *4*(3), 202-212. doi: 10.1038/nrm1050
- Glyvuk, N., Tsytsyura, M., Geumann, C., D'Hooge, R., Huve, J., Kratzke, M., . . . Schu, P. (2010). AP-1/sigma1B-adapin mediates endosomal synaptic vesicle recycling, learning and memory. *EMBO J*, *29*(8), 1318-1330. doi: 10.1038/emboj.2010.15
- Gravotta, D., Carvajal-Gonzalez, J. M., Mattera, R., Deborde, S., Banfelder, J. R., Bonifacino, J. S., & Rodriguez-Boulan, E. (2012). The clathrin adaptor AP-1A mediates basolateral polarity. *Dev Cell*, *22*(4), 811-823. doi: 10.1016/j.devcel.2012.02.004
- Hayashi, M., Raimondi, A., O'Toole, E., Paradise, S., Collesi, C., Cremona, O., . . . De Camilli, P. (2008). Cell- and stimulus-dependent heterogeneity of synaptic vesicle endocytic recycling mechanisms revealed by studies of dynamin 1-null neurons. *Proc Natl Acad Sci U S A*, *105*(6), 2175-2180. doi: 10.1073/pnas.0712171105

- Heldwein, E. E., Macia, E., Wang, J., Yin, M. L., Kirchhausen, T., & Harrison, S. C. (2004). Crystal structure of the clathrin adaptor protein 1 core. *Proc Natl Acad Sci U S A*, *101*(39), 14108-14113. doi: 10.1073/pnas.0406102101
- Hicke, L., & Riezman, M. (1996). Ubiquitination of a yeast plasma membrane receptor signals its ligand-stimulated endocytosis. *Cell*, *84*(2), 277-287.
- Hirst, J., Irving, C., & Borner, G. M. (2013). Adaptor protein complexes AP-4 and AP-5: new players in endosomal trafficking and progressive spastic paraplegia. *Traffic*, *14*(2), 153-164. doi: 10.1111/tra.12028
- Hirst, J., Motley, A., Harasaki, K., Peak Chew, S. M., & Robinson, M. S. (2003). EpsinR: an ENTH domain-containing protein that interacts with AP-1. *Mol Biol Cell*, *14*(2), 625-641. doi: 10.1091/mbc.E02-09-0552
- Jadot, M., Canfield, M. M., Gregory, M., & Kornfeld, S. (1992). Characterization of the signal for rapid internalization of the bovine mannose 6-phosphate/insulin-like growth factor-II receptor. *J Biol Chem*, *267*(16), 11069-11077.
- Janvier, K., Kato, M., Boehm, M., Rose, J. R., Martina, J. A., Kim, B. M., . . . Bonifacino, J. S. (2003). Recognition of dileucine-based sorting signals from HIV-1 Nef and LIMP-II by the AP-1 gamma-sigma1 and AP-3 delta-sigma3 hemicomplexes. *J Cell Biol*, *163*(6), 1281-1290. doi: 10.1083/jcb.200307157
- Kirchhausen, T. (2000). Three ways to make a vesicle. *Nat Rev Mol Cell Biol*, *1*(3), 187-198. doi: 10.1038/35043117
- Kirchhausen, T., Owen, D., & Harrison, S. C. (2014). Molecular structure, function, and dynamics of clathrin-mediated membrane traffic. *Cold Spring Harb Perspect Biol*, *6*(5), a016725. doi: 10.1101/cshperspect.a016725
- Krauss, M., & Haucke, V. (2007). Phosphoinositides: regulators of membrane traffic and protein function. *FEBS Lett*, *581*(11), 2105-2111. doi: 10.1016/j.febslet.2007.01.089
- Lanoix, J., Ouwendijk, J., Lin, C. C., Stark, A., Love, M. D., Ostermann, J., & Nilsson, T. (1999). GTP hydrolysis by arf-1 mediates sorting and concentration of Golgi resident enzymes into functional COP I vesicles. *EMBO J*, *18*(18), 4935-4948. doi: 10.1093/emboj/18.18.4935
- Letourneur, F., & Klausner, R. D. (1992). A novel di-leucine motif and a tyrosine-based motif independently mediate lysosomal targeting and endocytosis of CD3 chains. *Cell*, *69*(7), 1143-1157.
- Mahon, M. Clathrin-Mediated Endocytosis. *Endocytosis.org*.
- Malsam, J., Gommel, D., Wieland, F. T., & Nickel, M. (1999). A role for ADP ribosylation factor in the control of cargo uptake during COPI-coated vesicle biogenesis. *FEBS Lett*, *462*(3), 267-272.
- Marityen, T., Koo, S.J., Haucke, V. (2012) Turning CALM into excitement: AP180 and CALM in endocytosis and disease. *Biol Cell*, *104*(10), 588-602
- Medigeshi, G. R., Krikunova, M., Radhakrishnan, K., Wenzel, D., Klingauf, J., & Schu, P. (2008). AP-1 membrane-cytoplasm recycling regulated by mu1A-adaptin. *Traffic*, *9*(1), 121-132. doi: 10.1111/j.1600-0854.2007.00672.x
- Meyer, C., Eskelinen, E. L., Guruprasad, M. R., von Figura, K., & Schu, P. (2001). Mu 1A deficiency induces a profound increase in MPR300/IGF-II receptor internalization rate. *J Cell Sci*, *114*(Pt 24), 4469-4476.
- Miller, S. E., Sahlender, D. A., Graham, S. C., Honing, S., Robinson, M. S., Peden, A. A., & Owen, D. J. (2011). The molecular basis for the endocytosis of

- small R-SNAREs by the clathrin adaptor CALM. *Cell*, 147(5), 1118-1131. doi: 10.1016/j.cell.2011.10.038
- Milosevic, I., Giovedi, S., Lou, X., Raimondi, A., Collesi, C., Shen, M., . . . De Camilli, P. (2011). Recruitment of endophilin to clathrin-coated pit necks is required for efficient vesicle uncoating after fission. *Neuron*, 72(4), 587-601. doi: 10.1016/j.neuron.2011.08.029
- Modregger, J., Ritter, B., Witter, B., Paulsson, M. and Plomann, M. (2000). All three PACSIN isoforms bind to endocytic proteins and inhibit endocytosis. *J. Cell Sci.* 113, 4511-4521
- Neumann, S., Schmid, S. (2013) Dual rol of BAR Domain-containing Proteins in Regulating Vesicle Release Catalyzed by the GTPas, Dynamin-2. *JBC* 288(28)25119-25128
- Nickel, M., Malsam, J., Gorgas, K., Ravazzola, M., Jenne, N., Helms, J. B., & Wieland, F. T. (1998). Uptake by COPI-coated vesicles of both anterograde and retrograde cargo is inhibited by GTPgammaS in vitro. *J Cell Sci*, 111 (Pt 20), 3081-3090.
- Pepperkok, R., Whitney, J. A., Gomez, M., & Kreis, T. E. (2000). COPI vesicles accumulating in the presence of a GTP restricted arf1 mutant are depleted of anterograde and retrograde cargo. *J Cell Sci*, 113 (Pt 1), 135-144.
- Petralia, RS., Ya-Xian, M., Indig, FE., Bushlin, I., Wu, F., Mattson, MP., Yao, PJ., (2013), Reduction of AP180 and Calm produces defects in synaptic vesicle size and density. *Neuromelcular med.* 15(1)
- Piper, R. C., Dikic, I., & Lukacs, G. L. (2014). Ubiquitin-dependent sorting in endocytosis. *Cold Spring Harb Perspect Biol*, 6(1). doi: 10.1101/cshperspect.a016808
- Pond, L., Kuhn, L. A., Teyton, L., Schutze, M. P., Tainer, J. A., Jackson, M. R., & Peterson, P. A. (1995). A role for acidic residues in di-leucine motif-based targeting to the endocytic pathway. *J Biol Chem*, 270(34), 19989-19997.
- Poupon, V., Girard, M., Legendre-Guillemain, V., Thomas, S., Bourbonniere, L., Philie, J., . . . McPherson, P. S. (2008). Clathrin light chains function in mannose phosphate receptor trafficking via regulation of actin assembly. *Proc Natl Acad Sci U S A*, 105(1), 168-173. doi: 10.1073/pnas.0707269105
- Pryor, P. R., Jackson, L., Gray, S. R., Edeling, M. A., Thompson, A., Sanderson, C. M., . . . Luzio, J. P. (2008). Molecular basis for the sorting of the SNARE VAMP7 into endocytic clathrin-coated vesicles by the ArfGAP Hrb. *Cell*, 134(5), 817-827. doi: 10.1016/j.cell.2008.07.023
- Qualmann, B. and Kelly, R. B. (2000). Syndapin isoforms participate in receptor-mediated endocytosis and actin organization. *J. Cell Biol.* 148, 1047-1062.
- Ren, X., Farias, G. G., Canagarajah, B. J., Bonifacino, J. S., & Hurley, J. M. (2013). Structural basis for recruitment and activation of the AP-1 clathrin adaptor complex by Arf1. *Cell*, 152(4), 755-767. doi: 10.1016/j.cell.2012.12.042
- Reusch, U., Bernhard, O., Koszinowski, U., & Schu, P. (2002). AP-1A and AP-3A lysosomal sorting functions. *Traffic*, 3(10), 752-761.
- Ricotta, D., Hansen, J., Preiss, C., Teichert, D., & Honing, S. (2008). Characterization of a protein phosphatase 2A holoenzyme that dephosphorylates the clathrin adaptors AP-1 and AP-2. *J Biol Chem*, 283(9), 5510-5517. doi: 10.1074/jbc.M707166200

- Rohde, G., Wenzel, D., & Haucke, V. (2002). A phosphatidylinositol (4,5)-bisphosphate binding site within mu2-adaptin regulates clathrin-mediated endocytosis. *J Cell Biol*, *158*(2), 209-214. doi: 10.1083/jcb.200203103
- Saheki, M., & De Camilli, P. (2012). Synaptic vesicle endocytosis. *Cold Spring Harb Perspect Biol*, *4*(9), a005645. doi: 10.1101/cshperspect.a005645
- Sato, K., Ernstrom, G. G., Watanabe, S., Weimer, R. M., Chen, C. M., Sato, M., . . . Grant, B. D. (2009). Differential requirements for clathrin in receptor-mediated endocytosis and maintenance of synaptic vesicle pools. *Proc Natl Acad Sci U S A*, *106*(4), 1139-1144. doi: 10.1073/pnas.0809541106
- Schu, P. V., Takegawa, K., Fry, M. J., Stack, J. M., Waterfield, M. D., & Emr, S. D. (1993). Phosphatidylinositol 3-kinase encoded by yeast VPS34 gene essential for protein sorting. *Science*, *260*(5104), 88-91.
- Schuske, K. R., Richmond, J. E., Matthies, D. S., Davis, M. S., Runz, S., Rube, D. A., . . . Jorgensen, E. M. (2003). Endophilin is required for synaptic vesicle endocytosis by localizing synaptojanin. *Neuron*, *40*(4), 749-762.
- Stack, J. M., DeWald, D. B., Takegawa, K., & Emr, S. D. (1995). Vesicle-mediated protein transport: regulatory interactions between the Vps15 protein kinase and the Vps34 PtdIns 3-kinase essential for protein sorting to the vacuole in yeast. *J Cell Biol*, *129*(2), 321-334.
- Stack, J.M., Herman, P. K. Schu, P.V. Emr, S.D. (1993). A membrane-associated complex containing the Vps15 protein kinase and the Vps34 PI 3-kinase is essential for protein sorting to the yeast lysosome-like vacuole. *EMBO J*, *12*(5), 2195-2204
- Stenmark, M., Vitale, G., Ullrich, O., & Zerial, M. (1995). Rabaptin-5 is a direct effector of the small GTPase Rab5 in endocytic membrane fusion. *Cell*, *83*(3), 423-432.
- Tarpey, P. S., Stevens, C., Teague, J., Edkins, S., O'Meara, S., Avis, T., . . . Raymond, F. L. (2006). Mutations in the gene encoding the Sigma 2 subunit of the adaptor protein 1 complex, AP1S2, cause X-linked mental retardation. *Am J Hum Genet*, *79*(6), 1119-1124. doi: 10.1086/510137
- Traub, L. M., & Bonifacino, J. S. (2013). Cargo recognition in clathrin-mediated endocytosis. *Cold Spring Harb Perspect Biol*, *5*(11), a016790. doi: 10.1101/cshperspect.a016790
- Ullrich, O., Horiuchi, M., Bucci, C., & Zerial, M. (1994). Membrane association of Rab5 mediated by GDP-dissociation inhibitor and accompanied by GDP/GTP exchange. *Nature*, *368*(6467), 157-160. doi: 10.1038/368157a0
- Ungewickell, E., & Ungewickell, M. (1991). Bovine brain clathrin light chains impede heavy chain assembly in vitro. *J Biol Chem*, *266*(19), 12710-12714.
- Venditti, R., Wilson, C., & De Matteis, M. A. (2014). Exiting the ER: what we know and what we don't. *Trends Cell Biol*, *24*(1), 9-18. doi: 10.1016/j.tcb.2013.08.005
- Verstreken, P., Koh, T. M., Schulze, K. L., Zhai, R. G., Hiesinger, P. R., Zhou, M., . . . Bellen, M. J. (2003). Synaptojanin is recruited by endophilin to promote synaptic vesicle uncoating. *Neuron*, *40*(4), 733-748.
- Wang, M. J., Wang, J., Sun, M. Q., Martinez, M., Sun, M. X., Macia, E., . . . Yin, M. L. (2003). Phosphatidylinositol 4 phosphate regulates targeting of clathrin adaptor AP-1 complexes to the Golgi. *Cell*, *114*(3), 299-310.

- Wieffer, M., Cibrian Uhalte, E., Posor, M., Otten, C., Branz, K., Schutz, I., . . . Haucke, V. (2013). PI4K2beta/AP-1-based TGN-endosomal sorting regulates Wnt signaling. *Curr Biol*, *23*(21), 2185-2190. doi: 10.1016/j.cub.2013.09.017
- Wilde, A., & Brodsky, F. M. (1996). In vivo phosphorylation of adaptors regulates their interaction with clathrin. *J Cell Biol*, *135*(3), 635-645.
- Woodman, P. G. (2000). Biogenesis of the sorting endosome: the role of Rab5. *Traffic*, *1*(9), 695-701.
- Xiong, M., Yuan, C., Chen, R., Dawson, T. M., & Dawson, V. L. (2012). ArfGAP1 is a GTPase activating protein for LRRK2: reciprocal regulation of ArfGAP1 by LRRK2. *J Neurosci*, *32*(11), 3877-3886. doi: 10.1523/JNEUROSCI.4566-11.2012
- Yu, A., Xing, M., Harrison, S. C., & Kirchhausen, T. (2010). Structural analysis of the interaction between Dishevelled2 and clathrin AP-2 adaptor, a critical step in noncanonical Wnt signaling. *Structure*, *18*(10), 1311-1320. doi: 10.1016/j.str.2010.07.010
- Zerial, M., & McBride, M. (2001). Rab proteins as membrane organizers. *Nat Rev Mol Cell Biol*, *2*(2), 107-117. doi: 10.1038/35052055
- Zhang, Z., Zhang, T., Wang, S., Gong, Z., Tang, C., Chen, J., & Ding, J. (2014). Molecular mechanism for Rabex-5 GEF activation by Rabaptin-5. *Elife*, *3*. doi: 10.7554/eLife.02687

Acknowledgments

At the end of this amazing crazy and instructive journey I have a lot of people to thank. First of all I want to thank my supervisor Prof Dr. Peter V. Schu: thank you for the opportunity to perform my PhD project in your group, thank you for your guidance and support during these intense years; thank you for being ALWAYS present during all my lab troubles and problems, your daily enthusiasm for our amazing project has been contagious till the end.

A special thanks to the former people of my group, Dr. Manuel Kratzke and Sarah Zafar, from the begin, they tried first of all to be good friends, good company and then good teachers.

Thank to the Schimdt Group for their brilliant contribution, a special thanks to Olaf Bernhard, every day kindly available for help, suggestions and tips.

I want to thanks the colleagues of the three departments, for help and advice, especially Dr. Ivan Manzini and the Nuno Raimundo's "crazy" group (of course specially John), thanks to them for creating a pleasant and fun atmosphere.

*A special thanks to my friends, they have **been** one of the big sources of my mental power and stability, especially in hard times; of course stand out among all Esther, Alfredo & Fabio. I will always be grateful to them for being so loyal friends across these years, thanks to them for having wiped out the boredom from our every day life. Thanks to my great friend Diego, always present and ready to share bad and good adventures even from afar.*

A loving thanks to the love of my life Roberta: Grazie per il tuo prezioso supporto, grazie per esserci sempre stata. Grazie per avermi fatto arrivare il tuo amore, sempre! Grazie per avermi salvato dall'abisso delle mie paranoie con un semplice sorriso, una semplice carezza, la nostra quotidianità ha reso la mia vita migliore. Tutto quello che mi aspetta, con te al mio canto, non può che essere meraviglioso.

*Grazie ai miei nonni, Umberto e Silvia, il percorso fatto finora, e quello che ne verrà
è stato possibile soprattutto grazie a loro.*

*Grazie alle persone più importanti della mia vita, mia madre Elisa e i miei fratelli
Emanuel e Omar. Anche se lontani mai così vicini e disposti al sacrificio per me.
Questo nuovo traguardo è Nostro, spero di riuscire sempre a ricambiare tutto il
vostro amore e rendervi orgogliosi di me.*

Curriculum vitae

Personal Information

Name: Ermes Candiello
Date of Birth: 28.05.1987
Place of Birth: Benevento
Gender: Male
Marital Status: Single
Nationality: Italian
Languages: Italian (native), English (fluent)
Email: ermes.candiello@med.uni-goettingen.de

University Education

12.2011 MSc in Genetic Sciences and Technologies
Faculty of Mathematical, Physical and Natural Sciences.
Università degli Studi Del Sannio, Benevento, Italy.
Graduation Mark: 110/110 *cum laude*.

09.2009 BSc in Botechnologies.
Faculty of Mathematical, Physical and Natural Sciences.
Università degli Studi del Sannio, Benevento, Italy.
Graduation Mark: 110/110 *cum laude*.

Research Experience

04.2012-present PhD Thesis “Synaptic vesicles dynamics in $\sigma 1B$ -/- mouse model” in the group of Prof. Dr. Peter V Schu.
Molecular Biology of Cells doctoral program of the Göttingen Graduate School for Neurosciences, Biophysics, and Molecular Biosciences (GGNB).

11.2009-12.2011 Master Thesis “Notch-1 mutational analyses in ovarian cancer” in the group of Prof. Giuseppe Viglietto, Molecular Oncology, Center of Genetic Research BIOGEM, Ariano

Irpino, Italy

Other Interests

Soccer, Music, Travelling, Creative Music Composer, Singer, Cinema, Art.

List of publications

Kratzke M, **Candiello E**, Schmidt B, Olaf J and Schu P (2014) AP-1/ σ 1B Dependent SV Protein Recycling is Regulated in Early Endosomes and is Coupled to AP-2 Endocytosis. *Molecular Neurobiology* DOI 10.1007/s12035-014-8852-0

Candiello E, Kratzke M, Wenzel D, Cassel D and Schu P (2015) Organisation of endosomal protein sorting by AP-1 complexes. (In preparation)